Section A

GENERAL MECHANICS

DISCRIMINANT SEPARABILITY AND SYSTEMS OF KOWALEVSKI TYPE

Vladimir Dragović (*) and Katarina Kukić (**)

(*) Mathematical Institute SANU
Kneza Mihaila 36, 11000 Belgrade, Serbia
Mathematical Physics Group, University of Lisbon
e-mail: vladad@mi.sanu.ac.rs
(**) Faculty for Traffic and Transport Engineering
Vojvode Stepe 305, 11000 Belgrade, Serbia
e-mail: k.mijailovic@sf.bg.ac.rs

Abstract

Abstract

The theory of discriminantly separable polynomials has been initiated in a recent work of one of the authors (V. Dragovic, Geometrization and generalizations of the Kowalevski top, Comm. Math. Phys, 298 (2010)) in the context of pencils of conics and it has been recognized there as one of the key features in integration procedure of the famous Kowalevski top. The main property of such polynomials is that all discriminants are expressed as products of polynomial in one variable each. Based on that characteristic, we develope different methods of obtaining new integrable systems of differential equations which we call the systems of the Kowalevski type. An integration procedure for such systems leading to explicit genus two theta-functions formulae is presented.

1 Introduction

1.1 Discriminantly separable polynomials-an overview

In a very recent paper [4] of one of the authors of the present paper, a new approach to the Kowalevski integration procedure has been suggested. It has been based on a new notion introduced therein of *discriminantly separable polynomials*. A family of such polynomials has been constructed there as pencil equations from the theory of conics

$$\mathscr{F}(w,x_1,x_2)=0,$$

where w, x_1, x_2 are the pencil parameter and the Darboux coordinates respectively. (For classical applications of the Darboux coordinates see Darboux's book [2], for modern applications see the book [5] and [3].) The key algebraic property of the pencil equation, as quadratic equation in each of three variables w, x_1, x_2 is: *all three of its discriminants are expressed as products of two polynomials in one variable each*:

$$\begin{aligned} \mathscr{D}_w(\mathscr{F})(x_1,x_2) &= P(x_1)P(x_2) \\ \mathscr{D}_{x_1}(\mathscr{F})(w,x_2) &= J(w)P(x_2) \\ \mathscr{D}_{x_2}(\mathscr{F})(w,x_1) &= P(x_1)J(w) \end{aligned} \tag{1}$$

where J, P are polynomials of degree 3 and 4 respectively, and the elliptic curves

$$\Gamma_1 : y^2 = P(x), \quad \Gamma_2 : y^2 = J(s)$$

are isomorphic (see Proposition 1 of [4]) .

Let us recall here the definitions from [4]: A polynomial $\mathscr{F}(x_1,\dots,x_n)$ is *discriminantly separable* if there exist polynomials $f_i(x_i)$ such that for every $i = 1,\dots,n$

$$\mathscr{D}_{x_i}F(x_1,\dots,\hat{x}_i,\dots,x_n) = \prod_{j\neq i} f_j(x_j).$$

It is *symmetrically discriminantly separable* if

$$f_2 = f_3 = \cdots = f_n,$$

while it is *strongly discriminantly separable* if

$$f_1 = f_2 = f_3 = \cdots = f_n.$$

It is *weakly discriminantly separable* if there exist polynomials $f_i^j(x_i)$ such that for every $i = 1,\dots,n$

$$\mathscr{D}_{x_i}F(x_1,\dots,\hat{x}_i,\dots,x_n) = \prod_{j\neq i} f_j^i(x_j).$$

1.2 Kowalevski case-basic lines

As the name says motivation for introducing new class of systems called *systems of Kowalevski type* gave us the famous Kowalevski top. Let us recall briefly that the Kowalevski top [10] is a heavy spinning top rotating about a fixed point, under the conditions $I_1 = I_2 = 2I_3, I_3 = 1$, $y_0 = z_0 = 0$. Here (I_1, I_2, I_3) denote the principal moments of inertia, (x_0, y_0, z_0) is the center of mass, $c = Mgx_0$, M is the mass of the top, (p,q,r) is the vector of angular velocity and $(\gamma_1, \gamma_2, \gamma_3)$ are cosines of the angles between z-axis of the fixed coordinate system and the axes of the coordinate system that is attached to the top and whose origin coincides with the fixed point.

Then the equations of motion take the following form, see [10], [7]:

$$\begin{aligned} 2\dot{p} &= qr \\ 2\dot{q} &= -pr - c\gamma_3 \\ \dot{r} &= c\gamma_2 \\ \dot{\gamma}_1 &= r\gamma_2 - q\gamma_3 \\ \dot{\gamma}_2 &= p\gamma_3 - r\gamma_1 \\ \dot{\gamma}_3 &= q\gamma_1 - p\gamma_2, \end{aligned} \tag{2}$$

System (2) has three well known integrals of motion and a fourth integral discovered by Kowalevski

$$\begin{aligned} &2(p^2+q^2)+r^2 = 2c\gamma_1 + 6l_1 \\ &2(p\gamma_1 + q\gamma_2) + r\gamma_3 = 2l \\ &\gamma_1^2 + \gamma_2^2 + \gamma_3^2 = 1 \\ &\left((p+\imath q)^2 + \gamma_1 + \imath\gamma_2\right)\left((p-\imath q)^2 + \gamma_1 - \imath\gamma_2\right) = k^2. \end{aligned} \tag{3}$$

A change of variables

$$\begin{aligned} x_1 &= p + \imath q \\ x_2 &= p - \imath q \\ e_1 &= x_1^2 + c(\gamma_1 + \imath\gamma_2) \\ e_2 &= x_1^2 + c(\gamma_1 - \imath\gamma_2) \end{aligned} \tag{4}$$

transforms the four first integrals (3) into

$$\begin{aligned} r^2 &= E + e_1 + e_2 \\ rc\gamma_3 &= G - x_2e_1 - x_1e_2 \\ c^2\gamma_3^2 &= F + x_2^2e_1 + x_1^2e_2 \\ e_1e_2 &= k^2, \end{aligned} \tag{5}$$

with

$$\begin{aligned} E &= 6l_1 - (x_1+x_2)^2 \\ F &= 2cl + x_1x_2(x_1+x_2) \\ G &= c^2 - k^2 - x_1^2x_2^2. \end{aligned}$$

>From the first integrals, one gets

$$(E+e_1+e_2)(F+x_2^2e_1+x_1^2e_2) - (G - x_2e_1 - x_1e_2)^2 = 0$$

which can be rewritten in the form

$$e_1P(x_2) + e_2P(x_1) + R_1(x_1,x_2) + k^2(x_1-x_2)^2 = 0 \tag{6}$$

where polynomial P is

$$P(x_i) = x_i^2E + 2x_1F + G = -x_i^4 + 6l_1x_i^2 + 4lcx_i + c^2 - k^2,\ i = 1,2$$

and

$$R_1(x_1,x_2) = EG - F^2$$
$$= -6l_1x_1^2x_2^2 - (c^2-k^2)(x_1+x_2)^2 - 4lc(x_1+x_2)x_1x_2 + 6l_1(c^2-k^2) - 4l^2c^2.$$

Note that P from the formula above depends only on one variable, which is not obvious from its definition. Denote

$$R(x_1,x_2) = Ex_1x_2 + F(x_1+x_2) + G.$$

>From (6), Kowalevski gets

$$(\sqrt{P(x_1)e_2} \pm \sqrt{P(x_2)e_1})^2 = -(x_1-x_2)^2k^2 \pm 2k\sqrt{P(x_1)P(x_2)} - R_1(x_1,x_2). \tag{7}$$

After a few transformations, (7) can be written in the form

$$\left[\sqrt{e_1}\frac{\sqrt{P(x_2)}}{x_1-x_2} \pm \sqrt{e_2}\frac{\sqrt{P(x_1)}}{x_1-x_2}\right]^2 = (w_1 \pm k)(w_2 \mp k), \tag{8}$$

where w_1, w_2 are the solutions of an equation, quadratic in s:

$$Q(s,x_1,x_2) = (x_1-x_2)^2s^2 - 2R(x_1,x_2)s - R_1(x_1,x_2) = 0. \tag{9}$$

The quadratic equation (9) is known as **the Kowalevski fundamental equation**. Then, $Q(s,x_1,x_2)$ as a polynomial in three variables degree two in each of them satisfies

$$\mathscr{D}_s(Q)(x_1,x_2) = 4P(x_1)P(x_2)$$

$$\mathscr{D}_{x_1}(Q)(s,x_2) = -8J(s)P(x_2),\ \mathscr{D}_{x_2}(Q)(s,x_1) = -8J(s)P(x_1)$$

with

$$J(s) = s^3 + 3l_1s^2 + s(c^2-k^2) + 3l_1(c^2-k^2) - 2l^2c^2,$$

so it appeared to be an example of a member of the family of discriminantly separable polynomials, as it was shown in [4] (Theorem 3). Moreover, all main steps of the Kowalevski integration now follow as easy and transparent logical consequences of the theory of discriminantly separable polynomials. Let us mention here just one relation, see Corollary 1 from [4] (known in the context of the Kowalevski top as *the Kowalevski magic change of variables*):

$$\begin{aligned} \frac{dx_1}{\sqrt{P(x_1)}} + \frac{dx_2}{\sqrt{P(x_2)}} &= \frac{dw_1}{\sqrt{J(w_1)}} \\ \frac{dx_1}{\sqrt{P(x_1)}} - \frac{dx_2}{\sqrt{P(x_2)}} &= \frac{dw_2}{\sqrt{J(w_2)}}. \end{aligned} \tag{10}$$

Notice here that the equations of motion (2) can be rewritten in new variables $(x_1,x_2,e_1,e_2,r,\gamma_3)$ in the form:

$$\begin{aligned} 2\dot{x}_1 &= -if_1 \\ 2\dot{x}_2 &= if_2 \\ \dot{e}_1 &= -me_1 \\ \dot{e}_2 &= me_2 \end{aligned} \tag{11}$$

with two additional differential equations for $\dot{r}$ and $\dot{\gamma}_3$, where $m = \imath r$ and

$$f_1 = rx_1 + c\gamma_3,\ f_2 = rx_2 + c\gamma_3.$$

One can easily check that

$$\begin{aligned} f_1^2 &= P(x_1) + e_1(x_1 - x_2)^2 \\ f_2^2 &= P(x_2) + e_2(x_1 - x_2)^2. \end{aligned} \tag{12}$$

Further integration procedure is described in [10], and in the Subsection 2.3, we are going to develop analogue techniques for more general systems in details.

2 On new integrable systems of Kowalevski type

2.1 Systems of Kowalevski type. Defintion

Now, we are going to introduce a class of dynamical systems, which generalize the Kowalevski top. Instead of the Kowalevski fundamental equation (see formula (9)), we start here from an arbitrary discriminantly separable polynomial of degree two in each of three variables.

Given a discriminantly separable polynomial of the second degree in each of three variables

$$\mathscr{F}(x_1, x_2, s) := A(x_1, x_2)s^2 + B(x_1, x_2)s + C(x_1, x_2), \tag{13}$$

such that

$$\mathscr{D}_s(\mathscr{F})(x_1, x_2) = B^2 - 4AC = 4P(x_1)P(x_2),$$

and

$$\begin{aligned} \mathscr{D}_{x_1}(\mathscr{F})(s, x_2) &= 4P(x_2)J(s) \\ \mathscr{D}_{x_2}(\mathscr{F})(s, x_1) &= 4P(x_1)J(s). \end{aligned}$$

Suppose, that a given system in variables x_1, x_2, e_1, e_2, r, γ_3, after some transformations reduces to

$$\begin{aligned} 2\dot{x}_1 &= -if_1 \\ 2\dot{x}_2 &= if_2 \\ \dot{e}_1 &= -me_1 \\ \dot{e}_2 &= me_2 \end{aligned} \tag{14}$$

where

$$\begin{aligned} f_1^2 &= P(x_1) + e_1A(x_1, x_2) \\ f_2^2 &= P(x_2) + e_2A(x_1, x_2). \end{aligned} \tag{15}$$

Suppose additionally, that the first integrals of the initial system reduce to a relation

$$P(x_2)e_1 + P(x_1)e_2 = C(x_1, x_2) - e_1e_2A(x_1, x_2). \tag{16}$$

The equations for $\dot{r}$ and $\dot{\gamma}_3$ and m are not specified for the moment.

If a system satisfies the above assumptions we will call it *a system of Kowalevski type*. As it has been pointed out in the Introduction, see formulae (6, 9, 11,12), the Kowalevski top is an example of the systems of Kowalevski type.

The following theorem is quite general, and concerns all the systems of the Kowalevski type.

Theorem 1 *Given a system which reduces to (14, 15, 16). Then the system is linearized on the Jacobian of the curve*

$$y^2 = J(z)(z-k)(z+k),$$

where J is a polynomial factor of the discriminant of $\mathscr{F}$ as a polynomial in x_1 and k is a constant such that

$$e_1 e_2 = k^2.$$

Proof. Indeed, from the equations of motion on e_i we get

$$e_1 e_2 = k^2,$$

with some constant k. Now, we get

$$\left(\sqrt{e_1}\sqrt{P(x_2)} \pm \sqrt{e_2}\sqrt{P(x_1)}\right)^2 = C(x_1,x_2) - k^2 A(x_1,x_2) \pm 2\sqrt{P(x_1)P(x_2)}k.$$

From the last relations, we get

$$\left(\sqrt{e_1}\sqrt{\frac{P(x_2)}{A}} + \sqrt{e_2}\sqrt{\frac{P(x_1)}{A}}\right)^2 = (s_1-k)(s_2+k)$$

and

$$\left(\sqrt{e_1}\sqrt{\frac{P(x_2)}{A}} - \sqrt{e_2}\sqrt{\frac{P(x_1)}{A}}\right)^2 = (s_1+k)(s_2-k),$$

where s_1, s_2 are the solutions of the quadratic equation

$$\mathscr{F}(x_1,x_2,s) = 0$$

in s. From the last equations we get

$$\begin{aligned} 2\sqrt{e_1}\sqrt{\frac{P(x_2)}{A}} &= \sqrt{(s_1-k)(s_2+k)} + \sqrt{(s_1+k)(s_2-k)} \\ 2\sqrt{e_2}\sqrt{\frac{P(x_1)}{A}} &= \sqrt{(s_1-k)(s_2+k)} - \sqrt{(s_1+k)(s_2-k)}. \end{aligned}$$

Since s_i are solutions of the quadratic equation $F(x_1,x_2,s_i) = 0$, using Viète formulae and discriminant separability condition, we get

$$\begin{aligned} s_1 + s_2 &= -\frac{B}{A} \\ -(s_1 - s_2) &= \frac{\sqrt{4P(x_1)P(x_2)}}{A}. \end{aligned} \tag{17}$$

>From the last equation, we get

$$(s_1-s_2)^2 = 4\frac{P(x_1)P(x_2)}{A^2}.$$

Using the last equation, we have

$$\begin{aligned} f_1^2 &= \frac{P(x_1)}{(s_1-s_2)^2}\left[(s_1-s_2)^2 + 4e_1\frac{P(x_2)}{A^2}A\right] \\ &= \frac{P(x_1)}{(s_1-s_2)^2}\left[(s_1-s_2)^2 + \left(\sqrt{(s_1-k)(s_2+k)}+\sqrt{(s_1+k)(s_2-k)}\right)^2\right] \\ &= \frac{P(x_1)}{(s_1-s_2)^2}\left[\sqrt{(s_1-k)(s_1+k)}+\sqrt{(s_2+k)(s_2-k)}\right]^2. \end{aligned}$$

Similarly

$$f_2^2 = \frac{P(x_2)}{(s_1-s_2)^2}\left[\sqrt{(s_1-k)(s_1+k)}-\sqrt{(s_2+k)(s_2-k)}\right]^2.$$

>From the last two equations and from the equations of motion, we get

$$\begin{aligned} \frac{dx_1}{\sqrt{P(x_1)}}+\frac{dx_2}{\sqrt{P(x_2)}} &= -i\frac{\sqrt{(s_1-k)(s_1+k)}}{s_1-s_2}dt \\ \frac{dx_1}{\sqrt{P(x_1)}}-\frac{dx_2}{\sqrt{P(x_2)}} &= -i\frac{\sqrt{(s_2-k)(s_2+k)}}{s_1-s_2}dt. \end{aligned}$$

>From discriminant separability, one gets (see Corollary 1 from [4]):

$$\begin{aligned} \frac{dx_1}{\sqrt{P(x_1)}}+\frac{dx_2}{\sqrt{P(x_2)}} &= \frac{ds_1}{\sqrt{J(s_1)}} \\ -\frac{dx_1}{\sqrt{P(x_1)}}+\frac{dx_2}{\sqrt{P(x_2)}} &= \frac{ds_2}{\sqrt{J(s_2)}} \end{aligned} \tag{18}$$

and finally

$$\begin{aligned} \frac{ds_1}{\sqrt{\Phi(s_1)}}+\frac{ds_2}{\sqrt{\Phi(s_2)}} &= 0 \\ \frac{s_1\,ds_1}{\sqrt{\Phi(s_1)}}+\frac{s_2\,ds_2}{\sqrt{\Phi(s_2)}} &= \imath dt, \end{aligned} \tag{19}$$

where

$$\Phi(s) = J(s)(s-k)(s+k),$$

where Φ is a polynomial of degree up to six.

Thus, relations (19) define the Abel map on a genus 2 curve

$$y^2 = \Phi(s).$$

□

2.2 A new example of an integrable system of the Kowalevski type

Now, we are going to present a new example of system of the Kowalevski type.

Let us consider the next system of differential equations:

$$\begin{aligned} \dot{p} &= -rq & \dot{\gamma}_1 &= 2(q\gamma_3 - r\gamma_2) \\ \dot{q} &= -rp - \gamma_3 & \dot{\gamma}_2 &= 2(p\gamma_3 - r\gamma_1) \\ \dot{r} &= -2q(2p+1) - 2\gamma_2 & \dot{\gamma}_3 &= 2(p^2 - q^2)q - 2q\gamma_1 + 2p\gamma_2. \end{aligned} \tag{20}$$

After a change of variables

$$\begin{aligned} x_1 = p + q, \quad x_2 = p - q, \\ e_1 = x_1^2 + \gamma_1 + \gamma_2, \quad e_2 = x_2^2 + \gamma_1 - \gamma_2, \end{aligned}$$

system (20) becomes

$$\begin{aligned} \dot{x}_1 &= -rx_1 - \gamma_3 & \dot{e}_1 &= -2re_1 \\ \dot{x}_2 &= rx_2 + \gamma_3 & \dot{e}_2 &= 2re_2 \\ \dot{r} &= -x_1 + x_2 - e_1 + e_2 & \dot{\gamma}_3 &= x_2e_1 - x_1e_2. \end{aligned} \tag{21}$$

We can write down the first integrals of system (21) in the next form

$$\begin{aligned} r^2 - 2(x_1 + x_2) - e_1 - e_2 &= h \\ r\gamma_3 + x_1x_2 + x_2e_1 + x_1e_2 &= -\frac{g_2}{4} \\ \gamma_3^2 - x_2^2e_1 - x_1^2e_2 &= -\frac{g_3}{2} \\ e_1 \cdot e_2 &= k^2. \end{aligned} \tag{22}$$

In order to write down explicit formulae for solution of system directly in terms of Weierstrass $\wp$ function, we will suppose that constant of motion $h = 0$. Then, like in Kowalevski's case, from integrals (22) we get a relation in the form of (16)

$$\begin{aligned} &(x_1 - x_2)^2e_1e_2 + \left(2x_1^3 - \frac{g_2}{2}x_1 - \frac{g_3}{2}\right)e_2 + \left(2x_2^3 - \frac{g_2}{2}x_2 - \frac{g_3}{2}\right)e_1 \\ &- \left(x_1^2x_2^2 + x_1x_2\frac{g_2}{2} + g_3(x_1 + x_2) + \frac{g_2^2}{16}\right) = 0. \end{aligned} \tag{23}$$

Following the procedure described in Theorem 1 we get

$$\begin{aligned} \frac{dx_1}{\sqrt{P(x_1)}} + \frac{dx_2}{\sqrt{P(x_2)}} &= \frac{ds_1}{\sqrt{P(s_1)}} \\ \frac{dx_1}{\sqrt{P(x_1)}} - \frac{dx_2}{\sqrt{P(x_2)}} &= \frac{ds_2}{\sqrt{P(s_2)}} \end{aligned} \tag{24}$$

where $P(x)$ denotes the polynomial

$$P(x) = 2x^3 - \frac{g_2}{2}x - \frac{g_3}{2}, \tag{25}$$

and s_1, s_2 are the solutions of quadratic equation in s:

$$\begin{aligned}\mathscr{F}(x_1,x_2,s) &:= A(x_1,x_2)s^2 + B(x_1,x_2)s + C(x_1,x_2)\\ &= (x_1-x_2)^2 s^2 + \left(-2x_1x_2(x_1+x_2) + \frac{g_2}{2}(x_1+x_2) + g_3\right)s\\ &+ x_1^2x_2^2 + x_1x_2\frac{g_2}{2} + g_3(x_1+x_2) + \frac{g_2^2}{16} = 0.\end{aligned} \tag{26}$$

Finally, we get

Proposition 1 *The system of differential equations defined by (20) is integrated through the solutions of the system*

$$\begin{aligned}\frac{ds_1}{\sqrt{\Phi(s_1)}} + \frac{ds_2}{\sqrt{\Phi(s_2)}} &= 0\\ \frac{s_1\,ds_1}{\sqrt{\Phi(s_1)}} + \frac{s_2\,ds_2}{\sqrt{\Phi(s_2)}} &= 2\,dt,\end{aligned} \tag{27}$$

where

$$\Phi(s) = P(s)(s-k)(s+k).$$

2.3 Explicit integration in genus two theta functions

This Section is devoted to explicit integration of the system (20). Integration procedure will be done in two ways. The first one is based on Kowalevski [10] and uses properties of elliptic functions. The second one follows Kötter [9] and Golubev [7]. A generalization of Kötter transformation was derived in [4] for a polynomial $P(x)$ of degree four. Here we will reformulate such a transformation for $P(x)$ of degree three.

We are going to consider here, as in [10], the case where the zeros l_i, $i = 1, 2, 3$ of the polynomial P of degree three are real and $l_1 > l_2 > l_3$. Denote

$$l = (l_1 - l_2)(l_2 - l_3)(l_3 - l_1).$$

Following Kowalevski, we consider functions

$$P_i = \sqrt{(s_1 - l_i)(s_2 - l_i)}, \quad i = 1,2,3 \tag{28}$$

and

$$P_{ij} = P_iP_j\left(\frac{\dot{s}_1}{(s_1-l_i)(s_1-l_j)} + \frac{\dot{s}_2}{(s_2-l_i)(s_2-l_j)}\right). \tag{29}$$

Then by simple calculations one gets

$$\begin{aligned}\dot{P}_{ij} &= \frac{1}{2}P_iP_j\\ \dot{P}_1 &= \frac{P_3P_{13} - P_2P_{12}}{2(l_2-l_3)}, \dot{P}_2 = \frac{P_1P_{12} - P_3P_{23}}{2(l_3-l_1)}, \dot{P}_3 = \frac{P_2P_{23} - P_1P_{13}}{2(l_1-l_2)}.\end{aligned} \tag{30}$$

We will now derive expressions for p, q, r, γ_1, γ_2, γ_3 in terms of P_i, P_{ij} functions for i, $j = 1, 2, 3$.

Denote by

$$du_i = \frac{dx_i}{\sqrt{4x_i^3 - g_2 x_i - g_3}}, \quad i = 1,2.$$

Then

$$x_i = \wp(u_i),$$

and dividing both equations of system (24) with $\sqrt{2}$ we see that

$$s_1 = \wp(u_1 + u_2), \quad s_2 = \wp(u_1 - u_2).$$

We use the next properties of $\wp$-function, see [10]:

$$\begin{aligned}
\wp(u_1) + \wp(u_2) &= -2\frac{(l_2^2 - l_3^2)P_1 + (l_3^2 - l_1^2)P_2 + (l_1^2 - l_2^2)P_3}{(l_2 - l_3)P_1 + (l_3 - l_1)P_2 + (l_1 - l_2)P_3}, \\
\wp(u_1) - \wp(u_2) &= \frac{-2l}{(l_2 - l_3)P_1 + (l_3 - l_1)P_2 + (l_1 - l_2)P_3}, \\
\wp(u_1) \cdot \wp(u_2) &= -\big[\frac{(l_2 - l_3)(l_1^2 + l_2 l_3)P_1 + (l_3 - l_1)(l_2^2 + l_1 l_3)P_2}{(l_2 - l_3)P_1 + (l_3 - l_1)P_2 + (l_1 - l_2)P_3} \\
&\quad + \frac{(l_1 - l_2)(l_3^2 + l_1 l_2)P_3}{(l_2 - l_3)P_1 + (l_3 - l_1)P_2 + (l_1 - l_2)P_3}\big].
\end{aligned} \tag{31}$$

After some calculations, we get the next expressions for variables $p, q, r, \gamma_1, \gamma_2, \gamma_3$ in terms of P_i and P_{ij} functions for $i, j = 1,2,3$:

$$p = \frac{x_1 + x_2}{2} = \frac{\wp(u_1) + \wp(u_2)}{2} = -\frac{(l_2^2 - l_3^2)P_1 + (l_3^2 - l_1^2)P_2 + (l_1^2 - l_2^2)P_3}{(l_2 - l_3)P_1 + (l_3 - l_1)P_2 + (l_1 - l_2)P_3}, \tag{32}$$

$$q = \frac{x_1 - x_2}{2} = \frac{\wp(u_1) - \wp(u_2)}{2} = -\frac{l}{(l_2 - l_3)P_1 + (l_3 - l_1)P_2 + (l_1 - l_2)P_3}, \tag{33}$$

$$r = -\frac{\dot{p}}{q} = \frac{1}{2}\frac{(l_1 - l_2)P_{12} + (l_2 - l_3)P_{23} + (l_3 - l_1)P_{13}}{(l_2 - l_3)P_1 + (l_3 - l_1)P_2 + (l_1 - l_2)P_3}, \tag{34}$$

$$\begin{aligned}
\gamma_1 &= \frac{r^2}{2} - p^2 - q^2 - 2p \\
&= \frac{\left((l_1 - l_2)P_{12} + (l_2 - l_3)P_{23} + (l_3 - l_1)P_{13}\right)^2}{8\left((l_2 - l_3)P_1 + (l_3 - l_1)P_2 + (l_1 - l_2)P_3\right)^2} \\
&\quad - \frac{\left((l_2^2 - l_3^2)P_1 + (l_3^2 - l_1^2)P_2 + (l_1^2 - l_2^2)P_3\right)^2 + l^2}{\left((l_2 - l_3)P_1 + (l_3 - l_1)P_2 + (l_1 - l_2)P_3\right)^2} \\
&\quad + 2\frac{(l_2^2 - l_3^2)P_1 + (l_3^2 - l_1^2)P_2 + (l_1^2 - l_2^2)P_3}{(l_2 - l_3)P_1 + (l_3 - l_1)P_2 + (l_1 - l_2)P_3},
\end{aligned} \tag{35}$$

$$
\begin{aligned}
\gamma_2 &= -q(2p+1) - \frac{\dot{r}}{2} \\
&= \frac{l}{\left((l_2-l_3)P_1+(l_3-l_1)P_2+(l_1-l_2)P_3\right)^2} \\
&\cdot \left[(l_2-l_3-2l_2^2+2l_3^2)P_1+(l_3-l_1-2l_3^2+2l_1^2)P_2\right. \\
&\left.+(l_1-l_2-2l_1^2+2l_2^2)P_3\right] \\
&- \frac{((l_2-l_3)P_2P_3+(l_3-l_1)P_1P_3+(l_1-l_2)P_1P_2)}{8(l_2-l_3)P_1+(l_3-l_1)P_2+(l_1-l_2)P_3} \\
&- \frac{(l_2-l_3)P_{23}+(l_3-l_1)P_{13}+(l_1-l_2)P_{12}}{8\left((l_2-l_3)P_1+(l_3-l_1)P_2+(l_1-l_2)P_3\right)^2} \\
&\cdot (P_3P_{13}+P_1P_{12}+P_2P_{23}-P_2P_{12}-P_1P_{13}-P_3P_{23}),
\end{aligned} \tag{36}
$$

$$
\begin{aligned}
\gamma_3 &= -(\dot{q}+rp) \\
&= \frac{1}{2}\frac{(l_2^2-l_3^2)P_1+(l_3^2-l_1^2)P_2+(l_1^2-l_2^2)P_3}{\left((l_2-l_3)P_1+(l_3-l_1)P_2+(l_1-l_2)P_3\right)^2} \\
&\cdot ((l_1-l_2)P_{12}+(l_2-l_3)P_{23}+(l_3-l_1)P_{13}) \\
&- \frac{l}{2}\frac{P_3P_{13}+P_1P_{12}+P_2P_{23}-P_2P_{12}-P_1P_{13}-P_3P_{23}}{\left((l_2-l_3)P_1+(l_3-l_1)P_2+(l_1-l_2)P_3\right)^2}.
\end{aligned} \tag{37}
$$

Now, we will perform integration following Kötter [9] and Golubev [7]. First, we will formulate an extension of Kötter's transformation for a degree three polynomial $P(x) = 2x^3 - \frac{g_2}{2}x - \frac{g_3}{2}$.

Proposition 2 *For a polynomial $\mathscr{F}(x_1,x_2,s)$ given with formula (26), there exist polynomials $\alpha(x_1,x_2,s)$, $\beta(x_1,x_2,s)$, $P(s)$ such that the following identity*

$$
\mathscr{F}(x_1,x_2,s) = \alpha^2(x_1,x_2,s) + P(s)\beta(x_1,x_2,s), \tag{38}
$$

is satisfied. The polynomials are defined by the formulae:

$$
\begin{aligned}
\alpha(x_1,x_2,s) &= 2s^2 + s(x_1+x_2) - x_1x_2 - \frac{g_2}{4} \\
\beta(x_1,x_2,s) &= -2(x_1+x_2+s) \\
P(s) &= 2s^3 - \frac{g_2}{2}s - \frac{g_3}{2},
\end{aligned}
$$

where P coincides with the polynomial from formula (25).

Proof. The proof follows by a direct calculation. □

Define

$$
\hat{\mathscr{F}}(s) = \frac{\mathscr{F}(x_1,x_2,s)}{(x_1-x_2)^2},
$$

and consider the identity

$$\hat{\mathscr{F}}(s) = (s-u)^2 + (s-u)\hat{\mathscr{F}}'(u) + \hat{\mathscr{F}}(u).$$

Then, from (38) we get

$$(s-u)^2(x_1-x_2)^2 + 2(s-u)\left(u(x_1-x_2)^2 + \frac{B(x_1,x_2)}{2}\right)$$
$$+ \alpha^2(x_1,x_2,u) + P(u)\beta(x_1,x_2,u) = 0.$$

Corollary 1 *(a) The solutions s_1, s_2 of the last equation in s satisfy an identity in u:*

$$(s_1-u)(s_2-u) = \frac{\alpha^2(x_1,x_2,u)}{(x_1-x_2)^2} + P(u)\frac{\beta(x_1,x_2,u)}{(x_1-x_2)^2},$$

where $P(u)$ is a polynomial defined with (25).

(b) Functions P_i satisfy

$$P_i = \frac{\alpha(x_1,x_2,l_i)}{x_1-x_2} = \left(2l_i^2 - \frac{g_2}{4}\right)\frac{1}{x_1-x_2} + l_i\frac{x_1+x_2}{x_1-x_2} - \frac{x_1x_2}{x_1-x_2}. \tag{39}$$

Now we introduce a more convenient notation

$$X = \frac{x_1x_2}{x_1-x_2}, \quad Y = \frac{1}{x_1-x_2}, \quad Z = \frac{x_1+x_2}{x_1-x_2}.$$

Lemma 1 *The quantities X, Y, Z satisfy the system of linear equations*

$$\begin{aligned} -X + \left(2l_1^2 - \frac{g_2}{4}\right)Y + l_1Z &= P_1 \\ -X + \left(2l_2^2 - \frac{g_2}{4}\right)Y + l_2Z &= P_2 \\ -X + \left(2l_3^2 - \frac{g_2}{4}\right)Y + l_3Z &= P_3. \end{aligned} \tag{40}$$

The solutions of the system (40) are

$$\begin{aligned} Y &= \frac{(l_2-l_3)P_1 + (l_3-l_1)P_2 + (l_1-l_2)P_3}{-2l}, \\ Z &= \frac{(l_2^2-l_3^2)P_1 + (l_3^2-l_1^2)P_2 + (l_1^2-l_2^2)P_3}{l}, \\ X &= -\Big(\frac{(g_2+8l_2l_3)(l_2-l_3)P_1 + (g_2+8l_3l_1)(l_3-l_1)P_2}{8l} \\ &\quad + \frac{(g_2+8l_1l_2)(l_1-l_2)P_3}{8l}\Big). \end{aligned} \tag{41}$$

Using Viète formulae for polynomial $P(x)$ we can rewrite X in the form

$$X = \frac{(l_2-l_3)(l_1^2+l_2l_3)P_1+(l_3-l_1)(l_2^2+l_1l_3)P_2+(l_1-l_2)(l_3^2+l_1l_2)P_3}{2l}.$$

Now, from the expressions for X, Y, Z we get

$$q = \frac{x_1-x_2}{2} = \frac{1}{2Y},$$

$$p = \frac{x_1+x_2}{2} = \frac{Z}{2Y}.$$

Expressions for r and γ_i, $i = 1,2,3$ can be derived in terms of P_i, P_{ij} functions from equations of the system (20), see formulae (32)-(37).

3 Integrable subclass of systems of the Kowalevski type

Now we will present a whole new class of integrable systems of the same type as systems introduced in the previous section. We are looking for a system with possible first integrals of the form

$$\begin{aligned} r^2 &= E + p_2e_1 + p_1e_2 \\ r\gamma_3 &= F - q_2e_1 - q_1e_2 \\ \gamma_3^2 &= G + r_2e_1 + r_1e_2 \\ e_1 \cdot e_2 &= k^2, \end{aligned} \tag{42}$$

Here E, F, G, p_i, q_i, r_i are functions of x_1, x_2.

Theorem 2 *For a system which reduces to (14), (15), (16) with*

$$f_i = x_i^{m_i} \cdot r + x_i^{n_i} \cdot \gamma_3$$

for $m_i, n_i \in \mathbb{Z}$, $i = 1,2$ and at least on of conditions $m_1 \neq n_1$ or $m_2 \neq n_2$ is valid, relations (42) are satisfied for following coefficients:

$$p_1 = \frac{Ax_1^{2n_1}}{(x_1^{m_1}x_2^{n_2} - x_2^{m_2}x_1^{n_1})^2} \quad p_2 = \frac{Ax_2^{2n_2}}{(x_1^{m_1}x_2^{n_2} - x_2^{m_2}x_1^{n_1})^2}$$

$$q_1 = \frac{Ax_1^{n_1+m_1}}{(x_1^{m_1}x_2^{n_2} - x_2^{m_2}x_1^{n_1})^2} \quad q_2 = \frac{Ax_1^{n_2+m_2}}{(x_1^{m_1}x_2^{n_2} - x_2^{m_2}x_1^{n_1})^2}$$

$$r_1 = \frac{Ax_1^{2m_1}}{(x_1^{m_1}x_2^{n_2} - x_2^{m_2}x_1^{n_1})^2} \quad r_2 = \frac{Ax_2^{2m_2}}{(x_1^{m_1}x_2^{n_2} - x_2^{m_2}x_1^{n_1})^2}$$

$$E_i = \frac{x_2^{2n_2}P(x_1)+x_1^{2n_1}P(x_2)\pm B(x_1,x_2)x_1^{n_1}x_2^{n_2}}{(x_1^{m_1}x_2^{n_2}-x_2^{m_2}x_1^{n_1})^2},\ i=1,2$$
$$F_i = \frac{E_i(x_1^{2m_1}x_2^{2n_2}-x_1^{2n_1}x_2^{2m_2})+x_1^{2n_1}P(x_2)-x_2^{2n_2}P(x_1)}{2x_1^{n_1}x_2^{n_2}(x_1^{n_1}x_2^{m_2}-x_1^{m_1}x_2^{n_2})},\ i=1,2$$
$$G_i = \frac{E_i x_1^{m_1}x_2^{m_2}(x_1^{m_1}x_2^{n_2}-x_1^{n_1}x_2^{m_2})+x_1^{m_1+n_1}P(x_2)-x_2^{m_2+n_2}P(x_1)}{x_1^{n_1}x_2^{n_2}(x_1^{m_1}x_2^{n_2}-x_1^{n_1}x_2^{m_2})},\ i=1,2.$$

Here by $B(x_1,x_2)$ we denoted a function in two variables such that

$$B^2(x_1,x_2) = 4A(x_1,x_2)C(x_1,x_2)+4P(x_1)P(x_2).$$

Proof. Replacing (42) into condition (15) with $f_i = x_i^{m_i}\cdot r + x_i^{n_i}\cdot\gamma_3$, we get $r^2x_i^{2m_i}+2r\gamma_3 x_i^{m_i+n_i}+\gamma_3^2x_i^{2n_i} = P(x_i)+e_iA(x_1,x_2)$. Collecting coefficients with e_i we obtain system

$$\begin{aligned}
p_2x_1^{2m_1}-2q_2x_1^{m_1+n_1}+r_2x_1^{2n_1} &= A(x_1,x_2)\\
p_1x_1^{2m_1}-2q_1x_1^{m_1+n_1}+r_1x_1^{2n_1} &= 0\\
Ex_1^{2m_1}+2Fx_1^{m_1+n_1}+Gx_1^{2n_1} &= P(x_1)\\
p_1x_2^{2m_2}-2q_1x_2^{m_2+n_2}+r_1x_2^{2n_2} &= A(x_1,x_2)\\
p_2x_2^{2m_2}-2q_2x_2^{m_2+n_2}+r_2x_2^{2n_2} &= 0\\
Ex_2^{2m_2}+2Fx_2^{m_2+n_2}+Gx_2^{2n_2} &= P(x_2)
\end{aligned} \tag{43}$$

with solutions:

$$p_1 = \frac{A(x_1,x_2)x_1^{2n_1}}{(x_1^{m_1}x_2^{n_2}-x_2^{m_2}x_1^{n_1})^2},\qquad r_1 = \frac{A(x_1,x_2)x_1^{2m_1}}{(x_1^{m_1}x_2^{n_2}-x_2^{m_2}x_1^{n_1})^2},$$
$$p_2 = \frac{A(x_1,x_2)x_2^{2n_2}}{(x_1^{m_1}x_2^{n_2}-x_2^{m_2}x_1^{n_1})^2},\qquad r_2 = \frac{A(x_1,x_2)x_2^{2m_2}}{(x_1^{m_1}x_2^{n_2}-x_2^{m_2}x_1^{n_1})^2},$$
$$F = \frac{(x_2^{2n_2}x_1^{2m_1}-x_1^{2n_1}x_2^{2m_2})E+x_1^{2n_1}P(x_2)-x_2^{2n_2}P(x_1)}{2(x_1^{2n_1}x_2^{m_2+n_2}-x_2^{2n_2}x_1^{m_1+n_1})},$$
$$G = -\frac{(x_2^{m_2+n_2}x_1^{2m_1}-x_2^{2m_2}x_1^{m_1+n_1})E-x_2^{m_2+n_2}P(x_1)+x_1^{m_1+n_1}P(x_2)}{x_1^{2n_1}x_2^{m_2+n_2}-x_2^{2n_2}x_1^{m_1+n_1}}.$$

The second assumption is that the relation

$$(E+p_2e_1+p_1e_2)(G+r_2e_1+r_1e_2)-(F-q_2e_1-q_1e_2)^2 = 0 \tag{44}$$

is in the form (16). According to (16), the coefficients of e_i^2 should vanish, so we get:

$$q_1 = \frac{A(x_1,x_2)x_1^{n_1+m_1}}{(x_1^{m_1}x_2^{n_2}-x_2^{m_2}x_1^{n_1})^2},\qquad q_2 = \frac{A(x_1,x_2)x_2^{n_2+m_2}}{(x_1^{m_1}x_2^{n_2}-x_2^{m_2}x_1^{n_1})^2}.$$

Replacing these results into (44) it becomes

$$\frac{A}{(x_1^{m_1}x_2^{n_2}-x_1^{n_1}x_2^{m_2})^2}(Ae_1e_2+P(x_2)e_1+P(x_1)e_2+\varphi(E))=0$$

with $\varphi(E)$, a quadratic function of E

$$\varphi(E)=-E^2\frac{(x_1^{m_1-n_1}-x_2^{m_2-n_2})^2}{4}+E\frac{\frac{P(x_1)}{x_1^{2n_1}}+\frac{P(x_2)}{x_2^{2n_2}}}{2}-\frac{(P(x_1)x_2^{2n_2}-P(x_2)x_1^{2n_1})^2}{4x_1^{2n_1}x_2^{2n_2}(x_1^{n_1}x_2^{m_2}-x_1^{m_1}x_2^{n_2})^2}.$$

Finally, solving the quadratic equation

$$\frac{A}{(x_1^{m_1}x_2^{n_2}-x_1^{n_1}x_2^{m_2})^2}\varphi(E)=-C,$$

we get the solutions

$$E_i=\frac{x_2^{2n_2}P(x_1)+x_1^{2n_1}P(x_2)\pm B(x_1,x_2)x_1^{n_1}x_2^{n_2}}{(x_1^{m_1}x_2^{n_2}-x_2^{m_2}x_1^{n_1})^2},\ i=1,2. \tag{45}$$

□

Remark 1 *The discriminant of*

$$\mathscr{F}(x_1,x_2,s)=A(x_1,x_2)s^2+B(x_1,x_2)s+C(x_1,x_2)$$

as a polynomial in s is factorizable

$$\mathscr{D}_s\mathscr{F}(x_1,x_2)=B^2(x_1,x_2)-4(x_1-x_2)^2C(x_1,x_2)=4P(x_1)P(x_2).$$

If we choose $A(x_1,x_2), C(x_1,x_2)$ to be quadratic polynomials in each x_1, x_2 and $P(x)$ to be a polynomial of degree three or four, an integration of the systems which satisfy assumption of Theorem 1, will be performed in terms of theta-function of genus two.

Remark 2 *Relations (42) with values of p_i,q_i,r_i,E,F,G obtained in Theorem 2 will represent either the first integrals or will define submanifold on which corresponding system is integrable, as we will show on next example.*

Example 1 *Now we will apply Theorem 2 to the Kowalevski case, which has been briefly presented in the Introduction. Denote by*

$$A=(x_1-x_2)^2,$$

$$B=x_1^2x_2^2-6l_1x_1x_2-2cl(x_1+x_2)-(c^2-k^2),$$
$$C=6l_1x_1^2x_2^2+(c^2-k^2)(x_1+x_2)^2+4lcx_1x_2(x_1+x_2)-6l_1(c^2-k^2)+4l^2c^2,$$
$$P(x)=x^4-6l_1x^2-4clx_2-c^2+k^2$$

the polynomials that appear in the Kowalevski fundamental equation (9). Applying Theorem 2 we get

$$p_1=1,\ p_2=1,\ q_1=x_1,\ q_2=x_2,\ r_1=x_1^2,\ r_2=x_2^2.$$

The expressions for E,F,G we will denote by E_i,F_i,G_i, $i=1,2$ depending on choice of a sign in the expression for E:

$$\begin{aligned}E_1 &= 6l_1-(x_1+x_2)^2\\ F_1 &= x_1x_2(x_1+x_2)+2cl\\ G_1 &= -x_1^2x_2^2+c^2-k^2,\end{aligned}$$

and

$$\begin{aligned}E_2 &= -\frac{x_1^4-6x_1^2l_1-8clx_1+x_2^4-6l_1x_2^2-8clx_2-4c^2+4k^2+2x_2^2x_1^2-12l_1x_1x_2}{(x_1-x_2)^2}\\ F_2 &= \frac{1}{(x_1-x_2)^2}(x_1^4x_2+x_1^3x_2^2-12x_1^2l_1x_2-2x_1^2cl+2x_1(k^2-c^2)-12lcx_1x_2\\ &\quad +x_1x_2^4+x_1^2x_2^3-12x_1l_1x_2^2-2lcx_2^2+2x_2(k^2-c^2))\\ G_2 &= -\frac{x_1^2x_2^2(x_1^2+x_2^2)+2x_2^3x_1^3-24l_1x_1^2x_2^2+(k^2-c^2)(x_1+x_2)^2}{(x_1-x_2)^2}\\ &\quad +\frac{8lcx_1x_2(x_1+x_2)}{(x_1-x_2)^2}.\end{aligned}$$

The expressions E_1,F_1,G_1 correspond to the original Kowalevski case and for these values relations (42) are the first integrals of the Kowalevski's top.

The expressions E_2,F_2,G_2 correspond to a new system. By differentiating the first and the third relation (42) for E_2,F_2,G_2 instead of E,F,G, for a system which reduces to (14), (15), (16) with $f_i=rx_i+\gamma_3$ we get

$$\begin{aligned}\dot r &= \frac{\imath}{2r(x_1-x_2)^3}\big[(x_2^5+x_1^5)r-8(k^2-c^2)\gamma_3+24lcrx_1x_2+12l_1\gamma_3(x_1+x_2)^2\\ &\quad -2x_1^2x_2^2r(x_1+x_2)-3x_1x_2r(x_1^3+x_2^3)-4x_1x_2\gamma_3(x_1^2+x_2^2)\\ &\quad -4(k^2-c^2)r(x_1+x_2)+4lcr(x_1^2+x_2^2)+24l_1x_1x_2r(x_1+x_2)\\ &\quad +16cl\gamma_3(x_1+x_2)+m(x_1-x_2)^3(e_1+e_2)\imath\big],\end{aligned}$$

$$\begin{aligned}\dot\gamma_3 &= \frac{-\imath}{2\gamma_3(x_1-x_2)^3}\big[x_1x_2\gamma_3(x_1^4+x_2^4)+4x_1^3x_2^3r(x_1+x_2)+2(k^2-c^2)\gamma_3(x_1^2+x_2^2)\\ &\quad +2x_1^2x_2^2\gamma_3(x_1^2+x_2^2+x_1x_2)-16lc\gamma_3x_1x_2(x_1+x_2)+4(k^2-c^2)x_1x_2(x_1+x_2)\\ &\quad -32clx_1^2x_2^2r-24l_1x_1x_2\gamma_3(x_1^2+x_2^2)-24l_1x_1^2x_2^2r(x_1+x_2)+4k^2x_1x_2\gamma_3\\ &\quad +(mx_1\imath+\gamma_3+x_1r)x_1(x_1-x_2)^3e_2-(mx_2\imath+\gamma_3+x_2r)x_2(x_1-x_2)^3e_1\big].\end{aligned}$$

Finally, by differentiating of the second relation

$$r\gamma_3 = F_2-x_2e_1-x_1e_2$$

and by substituting obtained expressions for $\dot r$ and $\dot\gamma_3$, we get value for so far unknown func-

tion m:

$$m = \imath r + \frac{1}{(x_1-x_2)^3(rx_1+\gamma_3)^2 e_2 - (x_1-x_2)^3(rx_2+g)^2 e_1}$$
$$[4x_1x_2r^3(x_1^2x_2^2(x_1+x_2)+(k^2-c^2)(x_1+x_2)-6l_1x_1x_2(x_1+x_2)-8clx_1x_2)$$
$$+4\gamma_3r^2((k^2-c^2)(x_1^2+x_2^2+4x_1x_2)+2x_1^2x_2^2(x_1^2+x_2^2+x_1x_2)$$
$$-9l_1x_1x_2(x_1+x_2)^2-12lcx_1x_2(x_1+x_2))+4\gamma_3^2r(x_1x_2(x_1^3+x_2^3)$$
$$+2x_1^2x_2^2(x_1+x_2)-14clx_1x_2-15l_1x_1x_2(x_1+x_2)-3l_1(x_1^3+x_2^3)$$
$$+3(k^2-c^2)(x_1+x_2)-5lc(x_1^2+x_2^2))+4\gamma_3^3(x_1x_2(x_1^2+x2^2)-3l_1(x_1^2+x_2^2)$$
$$-4cl(x_1+x_2)-6l_1x_1x_2+2(k^2-c^2))].$$

Acknowledgements

The research was partially supported by the Serbian Ministry of Science and Technology, Project 174020 *Geometry and Topology of Manifolds, Classical Mechanics and Integrable Dynamical Systems* and by the Mathematical Physics Group of the University of Lisbon, Project *Probabilistic approach to finite and infinite dimensional dynamical systems, PTDC/MAT/104173/2008*.

References

[1] H. F Baker, *Abelian functions, Abel's theorem and the allied theory of theta functions*, Cambridge University Press, 1995.

[2] G. Darboux, *Principes de géométrie analytique*, Gauthier-Villars, Paris (1917) 519 p.

[3] V. Dragović, *Poncelet-Drboux curves, their complete decomposition and Marden theorem* Int. Math. Res. Notes (2010) doi:10.1093/imrn/rnq229, arXiv:0812.48290

[4] V. Dragović, *Generalization and geometrization of the Kowalevski top*, Communications in Math. Phys. 298 (2010), no. 1, 37-64

[5] V. Dragović, M. Radnović, *Poncelet porisms and beyond* Springer 2011

[6] B. Dubrovin, *Theta - functions and nonlinear equations* Uspekhi Math. Nauk, 36 (1981) 11-80

[7] V. V. Golubev, *Lectures on the integration of motion of a heavy rigid body around a fixed point*, Gostechizdat, Moscow, 1953 [in Russian], English translation: Israel program for scintific literature, 1960.

[8] V. Jurdjevic, *Integrable Hamiltonian systems on Lie Groups: Kowalevski type*, Annals of Mathematics, **150** (1999) 605-644

[9] F. Kotter, *Sur le cas traite par M-me Kowalevski de rotation d'un corps solide autour d'un point fixe*, Acta Math. **17** (1893)

[10] S. Kowalevski, *Sur la probleme de la rotation d'un corps solide autour d'un point fixe*, Acta Math. **12** (1889) 177-232

INTEGRABLE SYSTEMS ON STIEFEL VARIETIES

Yuri N. Fedorov[1], **Božidar Jovanović**[2]

[1] Department de Matemàtica I, Universitat Politecnica de Catalunya, Barcelona, E-08028 Spain
e-mail: Yuri.Fedorov@upc.es
[2] Mathematical Institute SANU, Serbian Academy of Sciences and Arts, Kneza Mihaila 36, 11000, Belgrad, Serbia
e-mail: bozaj@mi.sanu.ac.rs

Abstract. In this talk we present integrable variants of the Neumann systems on $V_{n,r}$. For more details and further generalizations, see our paper [6].

1. Introduction

1.1. A Stiefel variety $V_{n,r} \cong SO(n)/SO(n-r)$ is the variety of r ordered orthogonal unit vectors $(e_1,\dots,e_r)$ in the Euclidean space $\mathbb{R}^n$ or, equivalently, the set of $n\times r$ matrices

$$X = (e_1 \cdots e_r) \in M_{n,r}(\mathbb{R})$$

satisfying the condition $X^TX = \mathbf{I}_r$, where $\mathbf{I}_r$ is an $r\times r$ unit matrix. Thus $V_{n,r}$ is a smooth subvariety of dimension $N = rn - r(r+1)/2$ in the space of $n\times r$ real matrices $M_{n,r}(\mathbb{R}) = \mathbb{R}^{nr}$ and the components of X are redundant coordinates on it. In particular, $V_{n,1}$ is a sphere S^{n-1}, while both $V_{n,n}$ and $V_{n,n-1}$ are diffeomorphic to $SO(n)$.

The tangent bundle $TV_{n,r}$ is the set of pairs $(X,\dot X)$ subject to the constraints $X^TX = \mathbf{I}_r$, $X^T\dot X + \dot X^TX = 0$. On the other hand, the cotangent bundle $T^*V_{n,r}$ can be realized as the set of pairs of $n\times r$ matrices (X,P) that satisfy the constraints

$$X^TX = \mathbf{I}_r, \quad X^TP + P^TX = 0. \tag{1}$$

The canonical symplectic structure ω on $T^*V_{n,r}$ is the restriction of the canonical 2-form in the ambient space $T^*M_{n,r}(\mathbb{R})$, $\omega_0 = \sum_{i=1}^n \sum_{s=1}^r dp_s^i \wedge de_s^i$.

It is convenient to work with the redundant variables (X,P). The Hamiltonian equations with a Hamiltonian $H(X,P)$ read

$$\dot X = \frac{\partial H}{\partial P} - X\Pi, \tag{2}$$

$$\dot P = -\frac{\partial H}{\partial X} + X\Lambda + P\Pi, \tag{3}$$

where Λ and Π are $r\times r$ symmetric matrix Lagrange multipliers uniquely determined from the condition for the trajectory $(X(t),P(t))$ to satisfy constraints (1).

1.2. The famous Neumann system on the sphere S^{n-1} is defined as a natural mechanical system with the Hamiltonian (see [13, 11]):

$$H_{neum} = \frac{1}{2}(p,p) + \frac{1}{2}(Ae,e), \qquad A = \mathrm{diag}(a_1,\dots,a_n),$$

where the cotangent bundle T^*S^{n-1} is realized as a submanifold of $\mathbb{R}^{2n}\{e,p\}$ given by the constraints $(e,e) = 1$, $(e,p) = 0$. This system, together with the Jacobi problem on the geodesic flow on an ellipsoid, provides one of the basic and most beautiful examples of application of algebraic geometric tools to integrable systems (e.g, see [7, 12, 1]).

The Neumann systems on $V_{n,r}$ that we consider have the kinetic energy of $SO(n) \times SO(r)$-invariant metrics ds^2_κ (linear combinations of the *Euclidean* and *normal* metrics) and the potential function

$$V = \frac{1}{2}\,\mathrm{tr}(X^T A X) = \frac{1}{2}\sum_{i=1}^{r}(e_i, Ae_i). \tag{4}$$

The systems are completely integrable the noncommutative sense, that is, the motion occur on invariant isotropic tori of dimension less then the dimension of $V_{n,r}$ (Theorem 2, Section 2). In particular, for the motion without the Neumann potential, we get that the geodesic flows of the metric ds^2_κ is completely integrable in the non-commutative sense (Theorem 3).

Two matrix Lax representations are presented. The first, a "big" one, given by Theorem 1 is closely related to the symmetric Clebsch–Perelomov rigid body problem [14]. For $r = 1$, it was given by Moser in [11] and for $r > 1$ and the case of the Manakov type submersion metrics by Reyman and Semenov–Tian-Shanski [15] within the framework of the R-matrix method. Note that for $r > 1$ this Lax pair does not define a Neumann system on $V_{n,r}$ uniquely In contrast, the second (dual, or "small") Lax pairs, given by Theorem 4 are equivalent to the Neumann systems with the Euclidean and normal metrics up to an action of a finite discrete group. For the Neumann system with the Euclidean metric, the small Lax pair was first given in the unpublished manuscript [9].

In Section 3 we give a geometric interpretation of the integrals of the Neumann systems on $V_{n,r}$ obtained from the dual Lax representation. Our geometric model generalizes the celebrated Chasles theorem describing a geometric relation between the geodesic flow on an ellipsoid and common tangent lines of confocal quadrics ([4, 11, 10]). The Chasles theorem is adopted for the Neumann system on a sphere by Moser (see Theorem 4.10 in [12]).

2. The Neumann Systems and $SO(n) \times SO(r)$-invariant geodesic flows

2.1. While on the sphere S^{n-1} an $SO(n)$-invariant kinetic energy is unique (up to multiplication by a constant factor), on the variety $V_{n,r}$ with $r > 1$ there are many different $SO(n)$-invariant metrics. We consider the kinetic energy defined as follows.

The Lie groups $SO(n)$ and $SO(r)$ naturally act on $T^*V_{n,r}$ by left and right multiplications, respectively:

$$R \cdot (X,P) = (RX, RP), \quad R \in SO(n) \tag{5}$$

$$(X,P) \cdot Q = (XQ, PQ), \quad Q \in SO(r). \tag{6}$$

The actions (6) and (6) are Hamiltonian. The corresponding equivariant momentum mappings $\Phi : T^*V_{n,r} \to so(n)^* \cong so(n)$ and $\Psi : T^*V_{n,r} \to so(r)^* \cong so(r)$ are given by:

$$\Phi(X,P) = PX^T - XP^T, \qquad \Psi(X,P) = X^TP - P^TX.$$

The momentum mappings Φ and Ψ are invariant under the $SO(r)$ and $SO(n)$ actions, respectively. Therefore, the kinetic energy given by

$$H_\kappa(X,P) = \frac{1}{2}\langle\Phi,\Phi\rangle + \frac{\kappa}{2}\langle\Psi,\Psi\rangle = \frac{1}{2}\operatorname{tr}(P^TP) - \left(\frac{1}{2}+\kappa\right)\operatorname{tr}((X^TP)^2) \quad (7)$$

is $SO(n)\times SO(r)$-invariant. Within the class of the metrics ds^2_κ determined by the Hamiltonian functions (7) there is the normal metric ($\kappa = 0$) and the Euclidean metric ($\kappa = -1/2$). Moreover, for $r = 2$ there is a unique value of κ, while for $r > 2$ there are exactly two values, such that ds^2_κ is an Einstein metric (see [8]).

2.2. The Hamiltonian of the Neumann system has the form

$$H_{neum,\kappa}(X,P) = \frac{1}{2}\operatorname{tr}(P^TP) - \left(\frac{1}{2}+\kappa\right)\operatorname{tr}((X^TP)^2) + \frac{1}{2}\operatorname{tr}(X^TAX) \quad (8)$$

and the corresponding Hamiltonian equations (3) take the form

$$\begin{aligned}\dot X &= P - (1+2\kappa)XP^TX,\\ \dot P &= -AX - XP^TP + (1+2\kappa)PX^TP + XX^TAX.\end{aligned} \quad (9)$$

Note that Hamiltonians (8) are right $SO(r)$-invariant, so the momentum mapping Ψ is conserved by the flows (9) for any parameter κ. In particular, for $\kappa = 0$ we get the *Neumann system with the normal metric* given by

$$\begin{aligned}\dot X &= P - XP^TX,\\ \dot P &= -AX + PX^TP + X\Lambda = -AX + PX^TP - XP^TP + XX^TAX,\end{aligned} \quad (10)$$

while for $\kappa = -1/2$ we get the *Neumann system with the Euclidean metric* with the corresponding Hamilton equations

$$\begin{aligned}\dot X &= P,\\ \dot P &= -AX + X\Lambda = -AX - XP^TP + XX^TAX.\end{aligned} \quad (11)$$

2.3. Although for different κ the flows (9) do not coincide, the derivatives of the momentum Φ and of the symmetric matrix XX^T are the same:

$$\frac{d}{dt}\Phi = [XX^T, A], \qquad \frac{d}{dt}(XX^T) = [\Phi, XX^T]. \quad (12)$$

As a result, the following theorem holds.

Theorem 1 *Equations (9), in particular (10) and (11), imply the same $n\times n$ matrix Lax representation with a spectral parameter λ:*

$$\begin{aligned}&\frac{d}{dt}\mathscr{L}_{neum}(\lambda) = [\mathscr{A}_{neum}(\lambda), \mathscr{L}_{neum}(\lambda)]\\ &\mathscr{L}_{neum}(\lambda) = \lambda\Phi + XX^T - \lambda^2 A, \qquad \mathscr{A}_{neum}(\lambda) = \Phi - \lambda A.\end{aligned}$$

The coefficients of the spectral curve $\Gamma \subset \mathbb{C}^2\{\lambda,\nu\}$: $\det(\mathscr{L}_{neum}(\lambda) - \mu\mathbf{I}_n) = 0$ give us the commuting integrals of both systems, which can be expressed in the form

$$\mathfrak{F} = \{\operatorname{tr}(\lambda(PX^T - XP^T) + XX^T - \lambda^2A)^k \,|\, k = 1,\dots,n,\ \lambda\in\mathbb{R}\}. \quad (13)$$

By using Bolsinov's completeness condition for a set of Casimir functions of the pencil of compatible Poisson brackets on the reduced space $(T^*V_{n,r})/SO(r)$ (see [2]) and a construction of noncommutative integrable systems related to Hamiltonian actions of Lie groups (see [3]), we obtain:

Theorem 2 ([6]) *Let all the eigenvalues of A be distinct. Then the Neumann systems (9), in particular (10) and (11), are completely integrable in the non-commutative sense with the non-commutative set of integrals given by (13) and by the components of the $SO(r)$-momentum mapping Ψ. The generic trajectory $(X(t),P(t))$ corresponding to the maximal rank of the momentum Ψ is quasi-periodic over isotropic tori of dimension*

$$\frac{1}{2}\left(2r(n-r)+\frac{r(r-1)}{2}-\left[\frac{r}{2}\right]\right)+\left[\frac{r}{2}\right].$$

2.4. In particular, for the motion without the Neumann potential, we get

Theorem 3 ([6]) *The geodesic flows of metrics ds^2_κ with the Hamiltonian functions (7) are completely integrable in the non-commutative sense. The complete algebra of first integrals is*

$$\Phi^*(C^\infty(so(n))+\Psi^*(C^\infty(so(r))+C^\infty(T^*V_{n,r})^{SO(n)\times SO(r)},$$

where $C^\infty(T^*V_{n,r})^{SO(n)\times SO(r)}$ is the algebra of $SO(n)\times SO(r)$-invariant functions on $T^*V_{n,r}$.

3. The Chasles theorems for Neumann flows

3.1 The dual Lax pair for the generalized Neumann system (11) was first given in unpublished manuscript [9]. For $r=1$ it gives the known 2×2 Lax pair for the Neumann system (e.g.,see [11]). In general, we have:

Theorem 4 ([6]) *Up to the action of a discrete group $\mathbb{Z}_2^n$ generated by reflections with respect to the coordinate hyperplanes in $\mathbb{R}^n$,*

$$(X,P)\longmapsto(S_iX,S_iP),\qquad i=1,\dots,n,$$
$$S_i(x_1,\dots,x_n)=(y_1,\dots,y_n),\quad y_j=x_j,\quad j\neq i,\quad y_i=-x_i,$$

the Neumann flows (10) and (11) are equivalent to the following $2r\times 2r$ matrix Lax pair with a rational spectral parameter λ

$$\frac{d}{dt}\mathscr{L}^*_{neum}(\lambda)=[\mathscr{L}^*_{neum}(\lambda),\mathscr{A}^*_{neum}(\lambda)],$$
$$\mathscr{L}^*_{neum}(\lambda)=\begin{pmatrix}-X^T(\lambda\mathbf{I}_n-A)^{-1}P & -X^T(\lambda\mathbf{I}_n-A)^{-1}X\\ \mathbf{I}_r+P^T(\lambda\mathbf{I}_n-A)^{-1}P & P^T(\lambda\mathbf{I}_n-A)^{-1}X\end{pmatrix},$$

where for system (10), respectively (11), one should put

$$\mathscr{A}^*_{neum}(\lambda)=\begin{pmatrix}X^TP & \mathbf{I}_r\\ \Lambda-\lambda\mathbf{I}_r & -P^TX\end{pmatrix},\quad \mathscr{A}^*_{neum}(\lambda)=\begin{pmatrix}0 & \mathbf{I}_r\\ \Lambda-\lambda\mathbf{I}_r & 0\end{pmatrix},$$

where $\Lambda=X^TAX-P^TP$.

The statement is checked straightforwardly by using constraints (1) and the matrix identities

$$A(\lambda\mathbf{I}_n-A)^{-1}=(\lambda\mathbf{I}_n-A)^{-1}A=\lambda(\lambda\mathbf{I}_n-A)^{-1}-\mathbf{I}_n.$$

3.2. Let $a(\lambda)=(\lambda-a_1)\cdots(\lambda-a_n)$. The spectral curve of $\mathscr{L}^*_{neum}(\lambda)$ can be written in form

$$|a(\lambda)\mathscr{L}^*_{neum}(\lambda)-w\mathbf{I}_n|\equiv w^{2r}+w^{2r-2}a(\lambda)\mathscr{I}_2(\lambda)+\cdots+w^2a^{2r-3}(\lambda)\mathscr{I}_{2r-2}(\lambda)+a^{2r-1}\mathscr{I}_{2r}(\lambda)=0,$$

where $\mathscr{I}_{2l}(\lambda)$ are invariant polynomials in the components of the wedge products $e_{j_1}\wedge\cdots\wedge e_{j_j}$ and

$$\begin{aligned}
&e_1\ \wedge\cdots\wedge e_r,\\
&e_1\ \wedge\cdots\wedge e_r\wedge p_i,\quad i=1,\dots,r,\\
&\cdots\cdots\cdots\\
&e_1\ \wedge\cdots\wedge e_r\wedge p_1\wedge\cdots\wedge p_r.
\end{aligned}\tag{14}$$

Note that, due to the symplectic block structure of $\mathscr{L}^*_{neum}(\lambda)$, the coefficients at odd powers of w in the spectral curve are zero.

In the case $2r\le n$ the polynomials can be written in form

$$\begin{aligned}
\mathscr{I}_2(\lambda)\ &=\sum_{i=1}^{n}\frac{a(\lambda)}{\lambda-a_i}\left((e_1^i)^2+\cdots+(e_r^i)^2\right)+\sum_{1\le i<j\le n}\frac{a(\lambda)}{(\lambda-a_i)(\lambda-a_j)}\Phi_{ij}^2,\\
&\cdots\quad\cdots\\
\mathscr{I}_{2l}(\lambda)&=\sum_{I_l}\frac{a(\lambda)}{(\lambda-a_{i_1})\cdots(\lambda-a_{i_l})}\sum_{J_l=\{j_1,\dots,j_l\}}(e_{j_1}\wedge\cdots\wedge e_{j_l})^2_{I_l}\\
&\quad+\sum_{I_{l+1}}\frac{a(\lambda)}{(\lambda-a_{i_1})\cdots(\lambda-a_{i_{l+1}})}\sum_{J_l,1\le i\le r}(e_{j_1}\wedge\cdots\wedge e_{j_l}\wedge p_i)^2_{I_{r+1}}+\cdots,\\
&\cdots\quad\cdots\\
\mathscr{I}_{2r}(\lambda)&=\sum_{I_r}\frac{a(\lambda)}{(\lambda-a_{i_1})\cdots(\lambda-a_{i_r})}(e_1\wedge\cdots\wedge e_r)^2_{I_r}\\
&\quad+\sum_{I_{r+1}}\frac{a(\lambda)}{(\lambda-a_{i_1})\cdots(\lambda-a_{i_{r+1}})}\sum_{i=1}^{r}(e_1\wedge\cdots\wedge e_r\wedge p_i)^2_{I_{r+1}}\\
&\quad+\sum_{I_{r+2}}\frac{a(\lambda)}{(\lambda-a_{i_1})\cdots(\lambda-a_{i_{r+2}})}\sum_{1\le i<j\le r}(e_1\wedge\cdots\wedge e_r\wedge p_i\wedge p_j)^2_{I_{r+2}}+\cdots\\
&\quad+\sum_{I_{2r}}\frac{a(\lambda)}{(\lambda-a_{i_1})\cdots(\lambda-a_{i_{2r}})}|\Phi|^{I_{2r}}_{I_{2r}},
\end{aligned}\tag{15}$$

where $I_k=\{i_1,\dots i_k\}\subset\{1,\dots,n\}$ is the multi-index with distinct indices $1\le i_1<\cdots<i_k\le n$ and $|\Phi|^{I_k}_{I_k}$ is the $k\times k$ diagonal minor of the momentum matrix Φ corresponding to the multi-index I_k. Note that, in view of definition of Φ,

$$|\Phi|^{I_{2r}}_{I_{2r}}=(e_1\wedge\cdots\wedge e_r\wedge p_1\wedge\cdots\wedge p_r)^2_{I_{2r}}.$$

In the case $2r>n$ the polynomials $\mathscr{I}_{2l}(\lambda)$ have the same form with the only difference: the terms with the wedge products of e_i,p_j of order $>n$ are absent.

It follows that in both cases $\mathscr{I}_{2l}(\lambda)$ are polynomials in λ of degree $n-l$ and that the leading coefficients of $\mathscr{I}_2(\lambda),\dots,\mathscr{I}_{2r}(\lambda)$ produce trivial constants on $V(r,n)$. Note that, although the Lax matrix $\mathscr{L}^*_{neum}(\lambda)$ is not invariant under the right $SO(r)$-action, the spectral curve and therefore all the integrals $\mathscr{I}_{2l}(\lambda)$ are $SO(r)$-invariant. Like the "big" Lax matrix $\mathscr{L}_{neum}(\lambda)$ in (13), the dual Lax matrix $\mathscr{L}^*_{neum}(\lambda)$ does not produce explicitly the momenta integrals Ψ_{ij}.

3.3. The components of forms (14) that appear in the last invariant polynomial $\mathscr{I}_{2r}(\lambda)$ have a transparent geometric interpretation: they are Plücker coordinates of the $2r$-dimensional linear subspace ($2r$-plane)

$$\bar{\Sigma} = \bar{\Sigma}(X,P) \subset \mathbb{R}^{n+r}(x_1,\dots,x_n,y_1,\dots,y_r)$$

spanned by the columns of the $2r \times (n+r)$ matrix

$$\mathscr{V} = \mathscr{V}(X,P) = \begin{pmatrix} e_1 & \cdots & e_r & p_1 & \cdots & p_r \\ 0 & \cdots & 0 & & & \\ \vdots & & \vdots & & \mathbf{I}_r & \\ 0 & \cdots & 0 & & & \end{pmatrix}, \tag{16}$$

$\mathbf{I}_r$ being the identity $r \times r$ matrix. Indeed, for any $k, m\,(k < m)$, the Plücker coordinates of a k-plane π in $\mathbb{R}^m(x_1,\dots,x_m)$ spanned by independent vectors $v_1,\dots,v_k \in \mathbb{R}^m$ are the coefficients G_I of the polynomial

$$v_1 \wedge \cdots \wedge v_k = \sum_I G_I\, dx_{i_1} \wedge \cdots \wedge dx_{i_k},$$

where $I = \{i_1,\dots i_k\} \subset \{1,\dots,n\}$ is the multi-index with $1 \le i_1 < \cdots < i_k \le n$.

Then the Plücker coordinates of $\bar{\Sigma}$ are given by all $2r \times 2r$ minors of $\mathscr{V}$. In particular, the $2r \times 2r$ minors that completely contain $\mathbf{I}_r$ give the Plücker coordinates of the r-plane $\operatorname{span}(e_1,\dots,e_r) \subset \mathbb{R}^n$.

Now consider the following family of confocal cones in $\mathbb{R}^{n+r}(x_1,\dots,x_n,y_1\dots,y_r)$

$$\bar{Q}(\lambda) = \left\{ \frac{x_1^2}{\lambda - a_1} + \cdots + \frac{x_n^2}{\lambda - a_n} + y_1^2 + \cdots + y_r^2 = 0 \right\}, \quad \lambda \in \mathbb{R}. \tag{17}$$

Based on the method developed in [5], the following theorem is a first variant of a generalization of the remarkable Chasles theorem.

Theorem 5 ([6]) *Let the $2r$-plane $\bar{\Sigma}(t) \subset \mathbb{R}^{n+r}$ be associated to a generic solution $(X(t),P(t))$ of the Neumann systems (10) and (11) on $V_{n,r}$ as described above. Then $\bar{\Sigma}(t)$ is tangent simultaneously to $n-r$ fixed confocal cones $\bar{Q}(c_1),\dots,\bar{Q}(c_{n-r})$, where $c_1,\dots,c_{n-r}$ are the roots of the invariant polynomial $\mathscr{I}_{2r}(\lambda)$.*

One can show that for real solutions $(X(t),P(t))$ all these cones are real.

In the particular case $r = 1$, one can also consider the section of $\bar{\Sigma}$ and of the family $\bar{Q}(\lambda)$ by the subspace $\{y_1 = 1\} \cong \mathbb{R}^n$, which give respectively an affine line $l(t) = p(t) + \operatorname{span}\{e(t)\}$ and the family of confocal quadrics

$$Q(\lambda) = \left\{ \frac{x_1^2}{a_1 - \lambda} + \cdots + \frac{x_n^2}{a_n - \lambda} = 1 \right\}.$$

Then, due the above theorem, $l(t)$ is tangent to $n-1$ fixed quadrics $Q(c_1),\dots,Q(c_{n-r})$, and we recover Moser's variant of the Chasles theorem given for the Neumann system (see [12]).

3.4. By analogy with the case $r=1$, one can consider the restriction of family (17) to the linear subspace $\{y_1=\cdots=y_r=1\}$:

$$\begin{aligned} Q_r(\lambda) &= \mathfrak{i}^{-1}\left(\bar{Q}(\lambda)\cap\{y_1=1,\dots,y_r=1\}\right)\\ &= \left\{\frac{x_1^2}{a_1-\lambda}+\cdots+\frac{x_n^2}{a_n-\lambda}=r\right\}, \end{aligned} \tag{18}$$

where $\mathfrak{i}:\mathbb{R}^n\to\mathbb{R}^{n+r}$ is the natural inclusion $\mathfrak{i}(x_1,\dots,x_n)=(x_1,\dots,x_n,1,\dots,1)$. This gives a family of confocal quadrics in $\mathbb{R}^n$.

Further, the section of $\bar{\Sigma}$ by the subspace $\{y_1=\cdots=y_r=1\}$ defines an affine r-plane

$$\Sigma(t)=\mathfrak{i}^{-1}\left(\bar{\Sigma}\cap\{y_1=\cdots=y_r=1\}\right)\subset\mathbb{R}^n(x_1,\dots,x_n),$$

which is spanned by the orthogonal vectors $e_1,\cdots,e_r$ and passes through the point $p_1+\cdots+p_r$. As a result, to a generic solution $(X(t),P(t))$ of the Neumann system on $V_{n,r}$ one can uniquely associate the moving r-plane

$$\Sigma(t)=p_1(t)+\cdots+p_r(t)+\operatorname{span}\{e_1(t),\cdots,e_r(t)\}.$$

In contrast to the case $r=1$, due to dimensional reasons, for $r>1$ the r-plane $\Sigma(t)$ is not necessarily tangent to the quadrics $Q_r(c_1),\dots,Q_r(c_{n-r})$. More precisely, since

$$d\,\mathfrak{i}\left(T_{(x_1,\dots,x_n)}Q(\lambda)\right)=T_{\mathfrak{i}(x_1,\dots,x_n)}\bar{Q}(\lambda)\cap\{y_1=1,\dots,y_r=1\},$$

the tangency of $\bar{\Sigma}(t)$ and $\bar{Q}(c_i)$, for a fixed t, either implies the tangency of the corresponding affine r-plane $\Sigma(t)$ and the quadric $Q_r(c_i)$, or $\Sigma(t)$ does not intersect $Q_r(c_i)$. As a result, one cannot formulate a natural generalization of the Chasles theorem in $\mathbb{R}^n$ that involves this r-plane.

Another feature of the case $r>1$ is that, although the first integrals given by the polynomial $\mathscr{I}_{2r}(\lambda)$ are invariant with respect to the right $SO(r)$-action on (X,P), the $2r$-plane $\bar{\Sigma}$ and r-plane Σ do not have this property. Thus, a generic polynomial $\mathscr{I}_{2r}(\lambda)$ corresponds to a whole family of $2r$-planes (r-planes, respectively) that are tangent to the same set of confocal cones and is obtained as the orbit of $\bar{\Sigma}$ (Σ, respectively) under the right $SO(r)$-action.

Then, it natural to replace $\bar{\Sigma}$ by the moving cylinder $\bar{\Delta}(t)$, the union of $2r$-planes $\bar{\Sigma}(X(t)B,P(t)B)$ spanned by the columns of the $2r\times(n+r)$ matrices

$$\mathscr{V}(X(t)B,P(t)B),\qquad B\in SO(r),$$

where $\mathscr{V}(X,P)$ is given by (16). The cylinder $\bar{\Delta}(t)$ is $SO(r)$-invariant and, due to the construction, is tangent simultaneously to $n-r$ fixed confocal cones $\bar{Q}(c_1),\dots,\bar{Q}(c_{n-r})$.

Next, the section of $\bar{\Delta}(t)$ by the subspace $\{y_1=\cdots=y_r=1\}$ defines the moving $(2r-1)$-dimensional cylinder

$$\Delta(t)=\left\{\sum_{i,j}B_{i,j}p_i(t)\,|\,B\in SO(r)\right\}+\operatorname{span}\{e_1(t),\cdots,e_r(t)\},$$

which is now an appropriate object for the second generalization of the Chasles theorem:

Theorem 6 ([6]) *Let the $(2r-1)$-dimensional cylinder $\Delta(t)\subset\mathbb{R}^n$ be associated to a generic solution $(X(t),P(t))$ of the Neumann systems (10) or (11) on $V_{n,r}$ as described above. Then $\Delta(t)$ is tangent simultaneously to $n-r$ fixed confocal quadrics $Q_r(c_1),\dots,Q_r(c_{n-r})$ of the confocal family (18), where $c_1,\dots,c_{n-r}$ are the roots of the invariant polynomial $\mathscr{I}_{2r}(\lambda)$.*

Acknowledgments The research of B. J. was supported by the Serbian Ministry of Science, Project 174020, Geometry and Topology of Manifolds, Classical Mechanics and Integrable Dynamical Systems. The research of Yu. F. was supported by the MICINN-FEDER grant MTM2009-06973 and CUR-DIUE grant 2009SGR859.

References

[1] Adams M R, Harnad J, Previato E (1988) Isospectral Hamiltonian flows in finite and infinite dimensions. I. Generalized Moser systems and moment maps into loop algebras. *Comm. Math. Phys*. **117**, no. 3, 451–500.

[2] Bolsinov A V (1991) Compatible Poisson brackets on Lie algebras and the completeness of families of functions in involution, *Izv. Acad. Nauk SSSR, Ser. matem*. **55** No.1, 68–92.

[3] Bolsinov A V, Jovanović B (2003) Non-commutative integrability, moment map and geodesic flows. *Annals of Global Analysis and Geometry* **23** no. 4, 305–322, arXiv: math-ph/0109031.

[4] Chasles M (1846) Les lignes géodésiques et les lignes de courbure des surfaces du segond degré. *Journ. de Math.* **11**, 5–20.

[5] Fedorov Yu N (1995) Integrable systems, Lax representation and confocal quadrics, Amer. Math. Soc. Transl. (2) Vol. **168**, 173-199.

[6] Fedorov Yu N, Jovanović B (2011) Geodesic flows and Neumann systems on Stiefel varieties: geometry and integrability, *Mathematische Zeitschrift* DOI: 10.1007/s00209-010-0818-y, arXiv:1011.1835 [nlin.SI]

[7] Flaschka H (1984) Towards an algebro-geometric interpretation of the Neumann system. *Tohoku Math. J*. (2) **36** no. 3, 407–426.

[8] Jensen G (1973) Einstein metrics on principal fiber bundles, *J. Diff. Geom.* **8**, 599-614.

[9] Kapustin S (1992) The Neumann system on Stiefel varieties. Preprint (Russian).

[10] Knörrer H (1982) Geodesics on quadrics and a mechanical problem of C.Neumann. *J. Reine Angew. Math.* **334**, 69–78.

[11] Moser J (1980) Geometry of quadric and spectral theory. In: Chern Symposium 1979, Berlin–Heidelberg–New York, 147–188.

[12] Mumford D (1984) Tata lectures on theta, Birkhaüser, Boston.

[13] Neumann C (1859) De probleme quodam mechanico, quod ad primam integralium ultra-ellipticoram classem revocatum. *J. Reine Angew. Math.* **56**.

[14] Perelomov A M (1981) Some remarks on the integrability of the equations of motion of a rigid body in an ideal fluid, *Funct. Anal. Appl.* **15**, 144-146.

[15] Reyman A G, Semonov-Tian-Shanski M A (1994) Group theoretical methods in the theory of finite dimensional integrable systems. In. Dynamical systems VII, Encyclopaedia of Math.Sciences, Vol. **16**, Springer.

FURTHER RESULTS ON $PI^{\alpha}D^{\beta}$ TYPE CONTROL OF EXPANSION TURBINE IN THE AIR PRODUCTION CRYOGENIC LIQUID

M.P.Lazarević[1],Lj. Bučanović, [2]

[1] University of Belgrade, Faculty of Mechanical Engineering,
Department of Mechanics; Kraljice Mrije 16,
11020 Belgrade 35,Serbia
e-mail: mlazarevic@mas.bg.ac.rs
[2] Department of production of technical gases,
RTB,Bor,Serbia
e-mail: kisikana@nadlanu.com

Abstract. Here, it suggests and obtains a new algorithms of PID control based on fractional calculus (FC) in the producing of technical gases, i.e air production cryogenic liquid. Production liquid air low pressure was first introduced by P. L. Kapica and includes production liquor air pressure $p_2 = 6 \div 7\left[bar\right]$ and expansion in the gas turbine. For application in the synthesis of control input temperature and the flow of air expansion turbine, it is necessary to determine the appropriate differential equations linear's part of the building guidance as well as the procedural object. The paper presents a new robust control algorithms of $PI^{\alpha}D^{\beta}$ type which based on using fractional calculus. The objective of this work is to find out suitable settings for a fractional $PI^{\alpha}D^{\beta}$ controller in order to fulfill different design specifications for the closed-loop system, taking advantage of the fractional orders, α and β. Last, problem of discretization of proposed $PI^{\alpha}D^{\beta}$ will be treated as a key step in digital implementation.

1. Introduction

In classical control theory, state feedback and output feedback are two important techniques in system control. While it is not satisfied in most cases, the former technique requires that all variables are obtained directly. Although output feedback may avoid the restriction of state feedback, rather strong conditions such as the strict positive real condition, output feedback passivity and minimum phase, etc., are often on the system. Specially, the PID controller is by far the most dominating form of feedback in use today. Due to its functional simplicity and performance robustness, the proportional-integral-derivative controller has been widely used in the process industries. Design and tuning of PID controllers have been a large research area ever since Ziegler and Nichols presented their methods in 1942, [1]. Specifications, stability, design, applications and performance of the PID controller have been widely treated since then [2,3].On the other hand, fractional calculus is a mathematical topic with more than 300 years old history, but its application to physics and engineering

has been reported only in the recent years. Moreover, it is remarkable the increasing number of studies related with the application of fractional controllers in many areas of science and engineering, where specially fractional-order systems are of interest for both modeling and controller design purposes. It has been found that in interdisciplinary fields, many systems can be described by the fractional differential equations i.e. in the fields of continuous-time modeling, fractional derivatives have proved useful in linear viscoelasticity, acoustics, rheology, polymeric chemistry, biophysics,*etc.* [4-6]. However, in the recent years, emergence of effective methods to solve differentiation and integration of noninteger order equations makes fractional-order systems more and more attractive for the systems control community. The fractional PD^{α} controller [7], the fractional PI^{α} controller [8], the fractional controller $PI^{\beta}D^{\alpha}$ [6], the CRONE controllers [9,10], and the fractional lead-lag compensator [11] are some of the well-known fractional order controllers. In some of these works, it is verified that the fractional-order controllers can have better disturbance rejection ratios and less sensitivity to plant parameter variations compared to the traditional controllers. The fractional controllers have been used in many practical applications such as lateral and longitudinal control of autonomous vehicles [12], control of power electronic buck converters [13], control of robotic time delay systems [7], control of hexapod robots [14], and etc.

In this paper, we suggest and obtain a new algorithms of PID control based on fractional calculus (FC) in the producing of technical gases, i.e air production cryogenic liquid. The objective of this work is to find out suitable settings for a fractional $PI^{\alpha}D^{\beta}$ controller in order to fulfill different design specifications for the closed-loop system, taking advantage of the fractional orders, α and β.

2. Fundamentals of fractional calculus

Fractional calculus (FC) as an extension of ordinary calculus has a 300 years old history. FC was initiated by Leibniz and L`Hospital as a result of a correspondence which lasted several months in 1695. Both Leibniz and L`Hospital, aware of ordinary calculus, raised the question of a noninteger differentiation (order $n=1/2$) for simple functions. It had always attracted the interest of many famous ancient mathematicians, including L'Hospital, Leibniz,Liouville, Riemann, Grünward, and Letnikov [4-6]. Futher, the theory of fractional-order derivative was developed mainly in the 19th century. In his 700 pages long book on Calculus, 1819 Lacroix [15] developed the formula for the n-th derivative of $y=x^m$, $m-$ is a positive integer, $D^n x^m = \dfrac{m!}{(m-n)!}x^{m-n}$ where $n\ (\le m)$ is an integer. Replacing the factorial symbol by the Gamma function, he further obtained the formula for the fractional derivative

$$D^{\alpha}x^{\beta} = \frac{\Gamma(\beta+1)}{\Gamma(\beta-\alpha+1)}x^{\beta-\alpha} \tag{1}$$

where α and β are fractional numbers and Gamma function $\Gamma(z)$ is defined for $z>0$ as:

$$\Gamma(z)=\int_0^{\infty} e^{-x}x^{z-1}dx,\quad \Gamma(z+1)=z\Gamma(z)\,. \tag{2}$$

On the other hand, Liouville (1809-1882) formally extended the formula for the derivative of integral order *n*

$$D^n e^{ax} = a^n e^{ax} \Rightarrow D^\alpha e^{ax} = a^\alpha e^{ax},\ \alpha - arbitrary\, order \tag{3}$$

Using the series expansion of a function, he derived the formula known as *Liouville`s first formula for fractional derivative,* where α may be rational, irrational or complex.

$$D^\alpha f(x) = \sum_{n=0}^{\infty} c_n a_n^\alpha e^{a_n x} \tag{4}$$

where $f(x) = \sum_{n=0}^{\infty} c_n \exp(a_n x),\ \mathrm{Re}\, a_n > 0$. However, it can be only used for functions of the previous form. Also, it was J. B. J. Fourier,[16] who derived the functional representation of function

$$f(t) = \frac{1}{2\pi} \int_R \int_R f(\zeta) \cos\left(\xi(x-\zeta)\right) d\zeta\, d\xi \tag{5}$$

where he also formally introduced the fractional derivative version. Since from 19th century as a foundation of fractional geometry and fractional dynamics, the theory of FO, in particular, the theory of FC and FDEs and researches of application have been developed rapidly in the world. The modern epoch started in 1974 when a consistent formalism of the fractional calculus has been developed by Oldham and Spanier,[4], and later Podlubny,[6]. Applications of FC are very wide nowadays, in rheology, viscoelasticity, acoustics, optics, chemical physics, robotics, control theory of dynamical systems, electrical engineering, bioengineering and so on, [4-12]. In fact, real world processes generally or most likely are fractional order systems. The main reason for the success of applications FC is that these new fractional-order models are more accurate than integer-order models, i.e. there are more degrees of freedom in the fractional order model. Furthermore, fractional derivatives provide an excellent instrument for the description of memory and hereditary properties of various materials and processes due to the existence of a ”memory” term in a model. This memory term insure the history and its impact to the present and future. A typical example of a non-integer (fractional) order system is the voltage-current relation of a semi-infinite lossy transmission line [17] or diffusion of the heat through a semi-infinite solid, where heat flow is equal to the half-derivative of the temperature [6].

2.1 Definition of fractional differintegral

As an essential preliminary consider some definitions concerning fractional derivatives. Fractional derivatives are typically treated as a particular case of pseudo-differential operators. Since they are nonlocal and have weakly singular kernels, the study of fractional differential equations seems to be more difficult and less theories have been established than for classical differential equations. Now, it is well known that, one may generalize the differential and integral operators into one fundamental D_t^α operator t which is known as fractional calculus:

$$ {}_aD_t^{\alpha} = \begin{cases} \dfrac{d^{\alpha}}{dt^{\alpha}} & \Re(\alpha) > 0, \\ 1 & \Re(\alpha) = 0 \ , \\ \displaystyle\int_a^t (d\tau)^{-\alpha} & \Re(\alpha) < 0. \end{cases} \tag{6} $$

The definition of fractional integral is described by

$$ {}_aD_t^{-\alpha} x(t) = \frac{1}{\Gamma(\alpha)} \int_a^t (t-s)^{\alpha-1} x(s) ds, \quad \alpha > 0. \tag{7} $$

where $\Gamma(.)$ is the well known Euler's gamma function. There are three kinds of widely used fractional derivatives, namely the Grunwald-Letnikov (GL) derivative, the Riemann-Liouville (RL) derivative, and the Caputo (C) derivative. The GL derivative and RL derivative are equivalent if the functions they act on are sufficiently smooth. Besides, the RL derivative is meaningful under weaker smoothness requirements. The G-L definition is given by

$$ {}_a^{GL}D_t^{\alpha} f(t) = \lim_{h \to 0} \frac{1}{h^{\alpha}} \sum_{j=0}^{[(t-a)/h]} (-1)^j \binom{\alpha}{j} f(t - jh) \tag{8} $$

where *a*, *t* are the limits of operator and [x] means the integer part of **x**. As indicated above, the previous definition of GL is valid for α > 0 (fractional derivative) and for α < 0 (fractional integral) and, commonly, these two notions are grouped into one single operator called *differintegral*. The RL derivative is given as:

$$ {}_a^{RL}D_t^{\alpha} x(t) = D^n \, {}_aD_t^{\alpha-n} x(t), \quad \alpha \in [n-1, n), \tag{9} $$

and the Caputo derivative

$$ {}_a^{C}D_t^{\alpha} x(t) = {}_aD_t^{\alpha-n} D^n x(t), \quad \alpha \in n(n-1, n), \tag{10} $$

where $n \in Z^+, D^n$ is the classical n-order derivative. Moreover, previous expressions show that the fractional-order operators are *global* operators having a memory of all past events, making them adequate for modeling hereditary and memory effects in most materials and systems. Also, for the RL derivative, we have

$$ \lim_{\alpha \to (n-1)^+} {}_a^{RL}D_t^{\alpha} x(t) = \frac{d^{n-1} x(t)}{dt^{n-1}} \quad \text{and} \quad \lim_{\alpha \to n^-} {}_a^{RL}D_t^{\alpha} x(t) = \frac{d^n x(t)}{dt^n} \tag{11} $$

But for the Caputo derivative, we have

$$ \lim_{\alpha \to (n-1)^+} {}_a^{C}D_t^{\alpha} x(t) = \frac{d^{n-1} x(t)}{dt^{n-1}} - D^{(n-1)} x(a) \quad \text{and} \quad \lim_{\alpha \to n^-} {}_a^{C}D_t^{\alpha} x(t) = \frac{d^n x(t)}{dt^n} \tag{12} $$

Obviously, ${}_a^{RL}D$, $n \in (-\infty, +\infty)$ varies continuously with n, but the Caputo derivative cannot do this. On the other side, initial conditions of fractional differential equations with Caputo derivative have a clear physical meaning and Caputo derivative is extensively used in real applications. For numerical calculation of fractional–order differ-integral operator one can use relation derived from the GL definition. This relation has the following form:

$$ {}_{((t-L)}D_t^{\pm\alpha} f(t) \approx h^{\mp\alpha} \sum_{j=0}^{N(t)} b_j^{(\pm\alpha)} f(t-jh) \tag{13} $$

where L is the "memory length", h is the step size of the calculation,

$$ N(t) = \min\left\{ \left[\frac{t}{h} \right], \left[\frac{L}{h} \right] \right\}, \tag{14} $$

$[x]$ is the integer part of x and $b_j^{(\pm\alpha)}$ is the binomial coefficient given by

$$ b_0^{(\pm\alpha)} = 1, \quad b_j^{(\pm\alpha)} = \left(1 - \frac{1 \pm \alpha}{j} \right) b_{j-1}^{(\pm\alpha)} \tag{15} $$

For convenience, Laplace domain is usually used to describe the fractional integro-differential operation for solving engineering problems. The formula for the Laplace transform of the RL fractional derivative has the form:

$$ \int_0^{\infty} e^{-st} {}_0D_t^{\alpha} f(t) dt = s^{\alpha} F(s) - \sum_{k=0}^{n-1} s^k {}_0D_t^{\alpha-k-1} f(t)_{|t=0} \tag{16} $$

For $\alpha < 0$ (*i.e.*, for the case of a fractional integral) the sum in the right-hand side must be omitted). A geometric and physical interpretation of fractional integration and fractional differentiation can be found in Podlubny's work [18].

3. Basic ideas of $PI^{\alpha}D^{\beta}$ feedack type control

In recent years, fractional calculus has been applied in the modeling and control of various kinds of physical systems, as it is well known and documented in many control theories or in the literature data. In what concerns the area of automatic control, the fractional-order algorithms are extensively investigated. Thanks to the widespread industrial use of PID controllers, even a small improvement in PID features, achieved by using $PI^{\alpha}D^{\beta}$, could have a relevant impact. Recently, published results [8-12] indicate that the use of a fractional-order PID controller can improve both the stability and performance robustness of feedback control systems. In [6],Podluny proposed a generalization of the PID controller namely fractional PID ($PI^{\alpha}D^{\beta}$) where α and β are the order of integration and derivation respectively that can be real numbers. In fact, in principle, they provide more flexibility in the controller design, with respect to the standard PID controllers, because they have five parameters to select (instead of three). However, this also implies that the tuning of the controller can be much more complex. Therefore classical design method may not be applied directly to adjust all fractional controller parameters. In order to address this problem, different methods for the design of a fractional order PID (FOPID) controller have been proposed in the literature. Further research activities are running in order to develop new tuning rules for fractional controllers, studying previously the effects of the non integer order of the derivative and integral parts to design a more effective controller to be used in real-life models. Some of these technics are based on an extension of the classical PID

control theory. To this respect, in [19] the extension of derivation and integration order from integer to non integer numbers provides a more flexible tuning strategy and therefore an easier achieving of control requirements with respect to classical controllers. In [20] an optimal fractional order PID controller based on specified gain margin and phase margin with a minimum ISE criterion has been designed by using a differential evolution algorithm. In [21] a tuning method for fractional PID controller based on Ziegler-Nichols-type rules was proposed. Monje et al., [22] present a frequency domain approach based on the expected crossover frequency and phase margin. A state-space tuning method based on pole placement was also used (see [23]). Recent tuning method based on Quantitative Feedback Theory (QFT) are presented in [24]. In this paper, a fractional order PID controller ($PI^{\alpha}D^{\beta}$) is used to control the production process of technical gases as follows:

$$u(t) = K_p e(t) + K_{d\ 0} D_t^{\alpha} e(t) + K_{i\ 0} D_t^{-\beta} e(t) \tag{17}$$

The most common form of a fractional order PID controller is the $PI^{\alpha}D^{\beta}$ controller [6], involving an integrator of order α and a differentiator of order β where α, β can be any real numbers. The transfer function of such a controller has the form

$$G_c(s) = K_p + K_I s^{-\alpha} + K_D s^{\beta}, \quad (\alpha, \beta > 0) \tag{18}$$

The integrator term is s^{α} , that is to say, on a semi-logarithmic plane, there is a line having slope -20αdB. /dec. Clearly, selecting $\alpha = \beta = 1$, a classical PID controller can be recovered. The selections of $\alpha = 1, \beta = 0,$ $\alpha = 0, \beta = 1,$ respectively corresponds conventional PI & PD controllers. All these classical types of PID controllers are the special cases of the fractional $PI^{\alpha}D^{\beta}$ controller given by (17), see Fig. 1. It can be expected that the controller $PI^{\alpha}D^{\beta}$ may enhance the systems control performance. One of the most important advantages of the $PI^{\alpha}D^{\beta}$ controller is the better control of dynamical systems, which are described by fractional order mathematical models. Another advantage lies in the fact that the $PI^{\alpha}D^{\beta}$ controllers are less sensitive to changes of parameters of a controlled system [6-12]. This is due to the two extra degrees of freedom to better adjust the dynamical properties of a fractional order control system. However, in theory, $PI^{\alpha}D^{\beta}$ itself is an infinite dimensional linear filter due to the fractional order in differentiator or integrator.

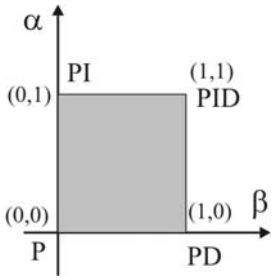

Figure 1. Generalization of the FOPID Controller: From point to plane

Fractional order controllers such as CRONE controller, TID controller, fractional PID controller and lead-lag compensator, [25] have so far been implemented to improve the performance and robustness in the closed loop control systems. As compared to

conventional PID compensators, the TID compensator allows for simpler tuning, better disturbance rejection, and smaller effects of plant parameter variations on the closed-loop response. Feedback control system compensator of the PID type is provided, wherein the proportional component of the compensator is replaced with a tilted component having a transfer function $s^{-1/n}$. The resulting transfer function of the entire compensator more closely approximates an optimal loop transfer function, thereby achieving improved feedback control performance. On the other hand, the CRONE control was proposed by Oustaloup in pursuing *fractal robustness* [9], [10] where "fractal robustness" is used to describe the following two characteristics: the iso-damping and the vertical sliding form of frequency template in the Nichols chart. Also, it is possible to extend the classical lead-lag compensator to the fractional-order case which was studied in [26]. The fractional lead-lag compensator is given by

$$C_r(s) = C_0\left(\frac{1+s/\omega_b}{1+s/\omega_h}\right)^r \tag{19}$$

where $0 < \omega_b < \omega_h, C_0 > 0$ and $r \in (0,1)$.Transfer functions such as (18) are not easy to implement for computational purposes. Simulations are usually carried out with software prepared to deal with integer powers of *s* only. Hardware implementations of controllers are nowadays usually achieved with electronic components allowing implementation of usual integer transfer functions easily, while how fractional transfer functions can be achieved with them is not clear at all. This makes the task of finding integer order approximations of fractional transfer functions a most important one where fractional transfer functions are usually replaced by integer transfer functions, with a behavior close enough to the one desired, but much easier to handle. Approximations are available both in the *s*-domain and in the *z*-domain. Moreover, one may find that many discretization schemes reported in literature which can be classified as either *direct* or *indirect*. The distinction is made based on whether an auxiliary continuous-time (*s* domain) approximation is constructed in the process. With direct methods, an intermediate continuous time approximation is not necessary, while with indirect methods such analogue approximation must be created. Most of the direct methods start with a suitable discrete approximation of the first order derivative or integral. Discretization scheme is then obtained by truncating some expansion of an appropriate non-integer power of the selected approximation. For example, a method based on power series expansion (PSE) of Euler operator,[27], or continued fraction expansion (CFE) is applied to Tustin operator,[28]. Further direct schemes are reported in [29-30]. Indirect methods are constructed in two steps where in the first step, a finite dimensional, continuous time approximation of the target fractional order system is found such as Oustaloup's rational approximation (ORA), [31] or sub-optimum H_2 rational approximation ,[32]. Once a satisfactory continuous-time approximation has been found, the second step of each indirect method is to find its discrete-time equivalent,as follows: approximations of Euler and Tustin, response invariant transformations (impulse-invariant and step invariant) and others, see[33].

4. Mathematical model of cryogenic process of mixing of two gaseous airs flows at different temperatures before entrance of expansion turbine

Cryogenics is the science and technology dealing with temperatures less than about 120 K, although this historical summary does not adhere to a strict 120K definition. The techniques used to produce cryogenic temperatures differ in several ways from those dealing with conventional refrigeration. Also, liquid air is air that has been cooled to very low temperatures(cryogenic temperatures) so that it has condensed to a pale blue mobile liquid. To protect it from room temperature, it must be kept in a vacuum flask. In practice, these two areas often overlap and the boundary between conventional and cryogenic refrigeration is often indistinct. Significant reductions in temperature often have very pronounced effects on the properties of materials and the behavior of systems. New way to technical production liquid air work is obtained by C. Linde at the end of the nineteenth century. On with the help of the reversing heat exchangers, slightly used cooling air, which appears in the damping of the higher of the lower pressure, the successful simple and economical production liquor large amounts of air. Production liquid air low pressure was first introduced in 1938. by the Russian academician P. L. Kapitsa, and includes production liquor air pressure $p_2 = 6 \div 7 \left[bar \right]$ and expansion in the gas turbine. So, expansion turbine in the air production liquid used for expansion air with thermodynamics state $P\left(p_p, T_p \right)$ to state $K\left(p_k, T_k \right)$ lowering when the air temperature with T_p at T_k and the pressure with p_p at p_k. Expansion of cold air after the start of equipment and waste heat arising due to exchange heat with the environment during the work. The amount of air that expansion in the gas turbine, according to [34], does not 25% exceed the amount of usable air. The air from the compressed state 1 turbocompressor, Fig. 2,(b) and cool to the state of the 2nd compressed air with pressure p_2 are in the reverse exchangers heat, where the cold to the state of 3rd Part of the air with the environment reverse heat state 3* and part of the state 3, which consists $m_e \left[kg / kg \right]$ of compressed air, are in expansion turbine where the expansion achieved by the state 8, where pressure p_1. Because of loss coefficient and other non-reverse expansion is not adiabatic line to state 8_{ad}, but to state 8, which is right. Place for removal of air state 4 elected to state 8, at the end of expansion, is in the area near the upper border curve (in the TS diagram $x = 1,0$ on $1 \div 3 \left[K \right]$ above the temperature saturated steam. Basic devices of the plant are (TK –turbocompressor, H - refrigerator air, RR – reverse exchangers heat, ET – expansion turbine, RK - exchangers heat i.e. air condenser, PV-damping valve)

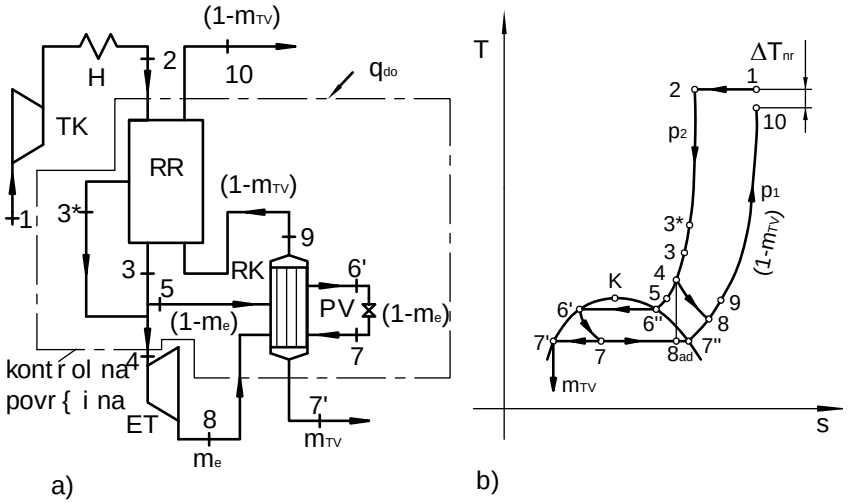

Figure 2. Scheme for plant liquid air flow pressure (a) and TS diagram of the process (b)

Liquid air quantity m_{TV} can be determined on the basis of heat balance,[34]:

$$h_2 = m_{TV} h_7^{'} + \left(1 - m_{TV}\right) i_{10} + m_e \left(h_4 - h_8\right) - q_{do}, \ [kJ/kg] \tag{20}$$

where are $q_{do}\left[kJ/kg\right]$- heat from the environment brought by kg air, $m_{TV}\left[kg/kg\right]$ - mass liquid air, $m_e\left[kg/kg\right]$ - mass air which expansion in expansion turbine. In the ideal case when the $q_{do} \approx 0$ and $\Delta T_{nr} = T_1 - T_{10} \approx 0$ liquid air mass is

$$m_{TV} = \frac{h_{10} - h_2}{h_{10} - h_7^{'}} + m_e \frac{h_4 - h_8}{h_{10} - h_7^{'}} \le \frac{h_1 - h_2}{h_{10} - h_7^{'}} + m_e \frac{h_4 - h_8}{h_{10} - h_7^{'}} \tag{21}$$

The main advantage of the procedure Kapic's according to the toe cap in relation to other procedures production liquid air [35] to be in the low pressure p_2 still does not have to spend inordinate work for production liquid $1\left[kg\right]$ air. Since the turbine is capable of much greater bandwidth than the reciprocating compressor is adapted to this process for large plants such as the face in practice. For qualitative assessment of gas turbine, with thermodynamics' point of view is used isentropic (internal) level of utility which is determined by the following terms:

$$\eta_T = \frac{\Delta h}{\Delta h'} = \frac{h_p - h_k}{h_p - h_{k'}} \approx \frac{T_p - T_k}{T_p - T_{k'}}, \ \ \eta_T = 0,80 \div 0,85 \tag{22}$$

For the development of the expansion works after refrigeration air, in the *" Factory of technical gas*" in Bor, built two expansion turbines, one gas turbine is always in operation, the other in the reserves, and the factory in preparation for the start after longer delays both turbine running in parallel. Energy received in expansion turbine in the work spent to drive fan that absorptive air from the atmosphere, regardless of air flow in the gas turbine. Ventilator compressed air and thus prevent an unlimited increase in the number of turbine rotor speed, a compressed air is emissive in the atmosphere which is not justified from the energy aspect. Technical adiabatic the work of expansion of air in gas turbine is:

$$l_{t,ad} = 10^{-3}\left(k/k-1\right)R\cdot T_p\left[1-\left(p_k/p_p\right)^{\frac{\kappa-1}{\kappa}}\right];\left[kJ/kg\right] \tag{23}$$

Power returned to the turbine - effective power, the expansion $\dot{m}\left[kg/s\right]$ of the pressure p_p to p_k have the value:

$$N_{eT} = N_i\cdot\eta_m = \dot{m}\cdot l_{t,ad}\cdot\eta_T\cdot\eta_m;\left[kW\right] \tag{24}$$

where are: $N_i\left[kW\right]$ - the internal (isentropic) gas turbine power, η_m - mechanical degree of utility gas turbines (due to friction in the bearings and stuffing box). $x_{i1}\left(t\right) = g_5\left(t\right)\left[m_N^3/h\right]$ - deviation values flow from the nominal value of gas's air flow at the entrance to the expansion turbine: $G_{56N} = 7600\left[m_N^3/h\right]$, $x_{i2}\left(t\right) = \theta_5\left(t\right)\left[K\right]$-value of temperature deviation from the nominal value of gas's air temperature at the entrance to the expansion turbine, $T_{5N} = 124\left[K\right]$, $z_1(t) = \theta_1\left(t\right)\left[K\right]$- value of temperature deviation from the nominal value of temperature gas's air environment with exchangers,heat $T_{1N} = 153\left[K\right]$, $z_2(t) = \theta_3\left(t\right)\left[K\right]$-value of temperature deviation from the nominal value of temperature air with the end of the cold heat exchangers $T_{3N} = 101\left[K\right]$, $y_A\left(t\right)\left[mm\right]$- deviation value position of the nominal value of the position control valves $TV946A$ $Y_{AN} = 14,7\left[mm\right]$, $y_B\left(t\right)\left[mm\right]$- deviation value position of the nominal value of the position control valves, $TV946B$ $Y_{BN} = 30,2\left[mm\right]$.On Fig. 3 it is presented diagram of process and symbolic-functional scheme with relevant variables.

4.1. *System description of mechatronic system in state space*

For application in the synthesis of proposed control input temperature and the flow of air expansion turbine, it is necessary to determine the appropriate differential equations linear's part of the cryogenic process of mixing of two gaseous airs flows at different temperatures before entrance of expansion turbine. Linear's differential equations that describe the work process are given as appropriate equation of state and output as follows

$$\begin{aligned}\dot{x}\left(t\right) &= \begin{bmatrix}-0,2 & 0\\ 0 & -0,2\end{bmatrix}x\left(t\right)+\begin{bmatrix}45,736 & 28,07\\ 0,174 & -0,085\end{bmatrix}u\left(t\right)+\begin{bmatrix}0 & 0\\ 0,088 & 0,112\end{bmatrix}z(t)\\ x_{\text{iz}}\left(t\right) &= \begin{bmatrix}1 & 0\\ 0 & 1\end{bmatrix}x\left(t\right)\end{aligned} \tag{25}$$

or, in condensed form is

$$\dot{x}\left(t\right) = Ax\left(t\right)+B_u u\left(t\right)+B_z z\left(t\right),\qquad x_i\left(t\right) = Cx\left(t\right) \tag{26}$$

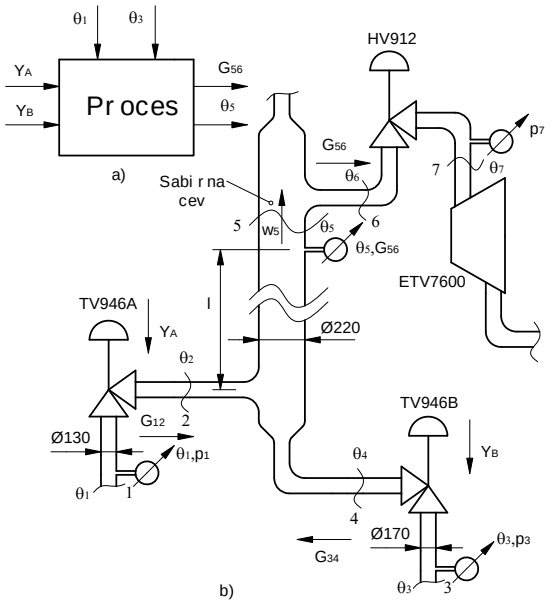

Figure 3. Diagram of the process (a) symbolic-functional scheme (b)

where corresponding vectors are, $u(t)=\left[y_A(t)\ y_B(t)\right]^T$, $z(t)=\left[z_1(t)\ z_2(t)\right]^T$, and A, B_u, B_Z, C are matrices with appropriate dimensions. From the above it is clear that model presents a MIMO system(multiple input, multiple output) where the number of inputs being to equal to that of outputs, system us square and it is possible to apply a control strategy uncoupling, whereby each of the inputs is made affect presented by one output only.In that way, one may obtain so called non-interactive system where is transfer function $W(s)$ of given system is decoupled, diagonal, and nonsingular matrix. To decouple the system, a new input $u(t)$ is introduced by means of feedback

$$u(t)=-K_c x(t)+F_c v(t) \tag{27}$$

where are $c_i - i$ -th row of matrix C and

$$N=\begin{bmatrix} c_1A^{p_1}B_u \\ c_2A^{p_2}B_u \\ \cdots\cdots \\ c_mA^{p_m}B_u \end{bmatrix}, \det N\neq 0 \quad p_i=\begin{cases} \min\left(j, c_iA^jB_u\neq 0\right) \\ n-1, c_iA^jB_u=0,\ \ \forall j \end{cases}, \forall j=0,1,2,...,n-1, \tag{28}$$

So, one can obtain

$$F_c=N^{-1},\ K_c=N^{-1}\left[c_1A^{p_1+1}\quad c_2A^{p_2+1}\quad \ldots\quad c_mA^{p_m+1}\right]^T \tag{29}$$

The transfer function $W(s)$ of the original system is

$$W(s) = C\left(sI - A\right)^{-1} B_u = \begin{bmatrix} \dfrac{45.736}{s+0.2} & \dfrac{28.07}{s+0.2} \\ \dfrac{0.174}{s+0.2} & \dfrac{-0.85}{s+0.2} \end{bmatrix} \tag{30}$$

and after applying new control is $W(s) = C\left(sI - A + B_u K_c\right)^{-1} B_u F_c$. Taking into account the proposed procedure for F_c, K_c it follows

$$\begin{aligned} &c_1 = [1 \;\; 0],\; c_2 = [0 \;\; 1],\; p_1 = 0,\; p_2 = 0, \\ &N = B_u,\; F_c = B_u^{-1},\; K_c = B_u^{-1} A \end{aligned} \tag{31}$$

and

$$W(s) = C\left(sI\right)^{-1} = \begin{bmatrix} 1/s & 0 \\ 0 & 1/s \end{bmatrix} \tag{32}$$

Now, decoupling system is

$$\begin{aligned} \dot{x}_1 &= v_1 \\ \dot{x}_2 &= v_2 + 0.088 z_1 + 0.112 z_2 \end{aligned} \tag{33}$$

5. The proposed fractional PIDs

Unlike conventional PID controller, there is no systematic and rigor design or tuning method existing for $PI^{\alpha}D^{\beta}$ controller. Here, design goals are choosing suitable α and β as well as load disturbance rejection.The controller parameters are the proportional gain K_p, the derivative gain K_d, the integral gain K_i, as well as noninteger order of derivative β and integrator α,Eq. 34. Load disturbances are typically low frequency signals and their attenuation is a very important characteristic of a controller. It is shown [1], that by maximizing the integral gain K_i, the effect of load disturbance at output will be minimum.

$$G_c(s) = \frac{K_p s^{\alpha} + K_I + K_D s^{\beta+\alpha}}{s^{\alpha}}, \quad (\alpha, \beta > 0) \tag{34}$$

Here, in order to obtain step response, simulation model has been developed using Simulink Library of MATLAB by using a special toolbox for non-integer control. For the simulation purpose, here we present the Crone approximation algorithm. It is based on the approximation of a function of the form:

$$C(s) = k s^{\nu},\; \nu \in R \tag{35}$$

which uses a recursive distribution of N poles and N zeros:

$$C(s) = k' \prod_{n=1}^{N} \frac{1 + \dfrac{s}{\omega_{z,n}}}{1 + \dfrac{s}{\omega_{p,n}}}, \tag{36}$$

Gain k' is adjusted so that if k is 1 then $\left|C(s)\right| = 0\,dB$ at $1\,rad/s$. Zeros and poles are found inside a frequency interval $\left[\omega_l, \omega_h\right]$ and are given, for a positive ν, by

$$\eta = \left(\omega_h / \omega_l\right)^{\frac{1-\nu}{N}}, \alpha = \left(\omega_h / \omega_l\right)^{\frac{\nu}{N}}, \quad \omega_{p,n} = \omega_{z,n-1}\alpha,\ n = 1,2,...,N$$
$$\omega_{z,n} = \omega_{p,n-1}\eta,\ n = 2,...,N, \quad \omega_{z,1} = \omega_l\sqrt{\eta} \tag{37}$$

For a negative ν the role of zeros and poles is interchanged. The controller is reckoned from $k, \nu, \omega_l, \omega_h$ and N. Here, they are presented simulation results for x_{i1}, Fig.4

$K_p = 1, K_d = 1, K_i = 0.1, \alpha = 0.99, \beta = 0.99$ $\quad$ $K_p = 50, K_d = 20, K_i = 10, \alpha = 0.9, \beta = 0.8$

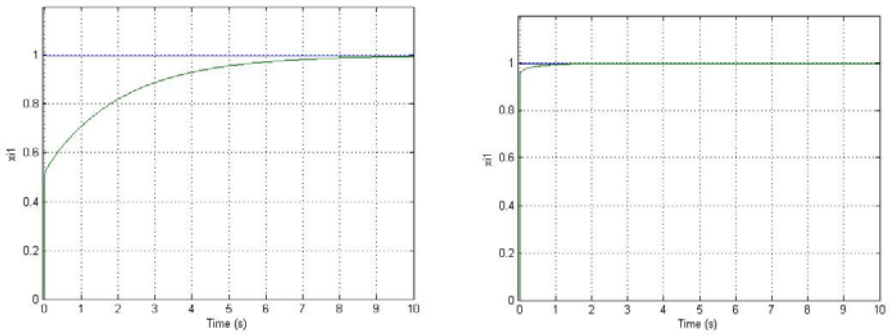

a) b)

Figure 4. **a)** step response of x_{i1}, for $K_p = 1, K_d = 1, K_i = 0.1, \alpha = 0.99, \beta = 0.99$

b)) step response of x_{i1}, for $K_p = 50, K_d = 20, K_i = 10, \alpha = 0.9, \beta = 0.8$

and for x_{i2} as follows, Fig.5:

$K_p = 1, K_d = 1, K_i = 0.1, \alpha = 0.99, \beta = 0.99$, $\quad K_p = 30, K_d = 10, K_i = 40, \alpha = 0.9, \beta = 0.5$

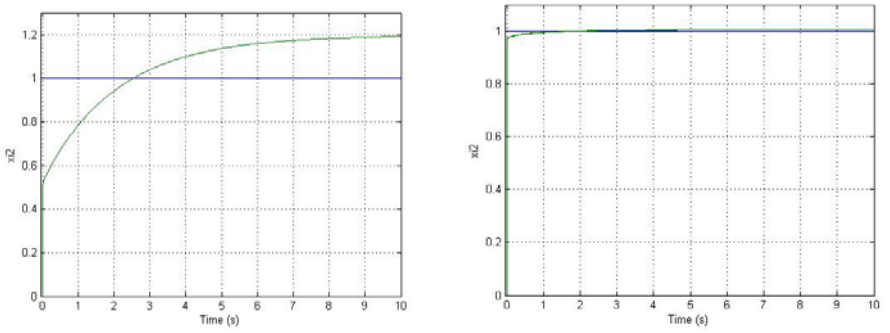

a) b)

Figure 5. **a)** step response of x_{i2}, for $K_p = 1, K_d = 1, K_i = 0.1, \alpha = 0.99, \beta = 0.99$

b)) step response of x_{i2}, for $K_p = 30, K_d = 10, K_i = 40, \alpha = 0.9, \beta = 0.5$

6. Discussion

Here, in this paper it is proposed new robust control algorithms of $PI^{\alpha}D^{\beta}$ type which based on using fractional calculus in the control of producing of technical gases, i.e air production cryogenic liquid. Design goals are suitable setting the controller parameters

K_i, K_d, K_p, noninteger order of derivative β and integrator α to fulfill different design specifications for the closed-loop system, for example, load disturbance rejection. Also, the problem of discretization of proposed $PI^{\alpha}D^{\beta}$ is considered as a one of important steps in digital implementation. In order to obtain step response, simulation model has been developed using Simulink Library of MATLAB by using a special toolbox for non-integer control.

Acknowledgement. This work is partially supported by the Ministry of Science and Environmental Protection of Republic of Serbia as Fundamental Research Project 41006 and 35006.

References

[1] K. Astrom and T. Hagglund. *PID controllers:Theory, design, and tuning*. Instrument Society of America, North Carolina, 1995.
[2] Y. Chen, C. Hu, and K. L. Moore, "Relay Feedback Tuning of Robust PID Controllers with Iso-Damping Property." *Accepted to present at the IEEE 2003 Conference on Decision and Control*, December 9-12, 2003, Maui, HI, USA.
[3] K. J. Astrom and T. Hagglund, "The Future of PID Control*," in IFAC Workshop on Digital Control. Past, Present and Future of PID Control,* (Terrassa, Spain), pp. 19–30, April 2000.
[4] K. B. Oldham and J. Spanier, The Fractional Calculus: Theory and Applications of Di.erentiation and *Integration to Arbitrary Order*, Academic Press, New York, NY, USA, 1974.
[5] R. Hilfer, Ed., *Applications of Fractional Calculus in Physics*,World Scientific, River Edge, NJ, USA, 2000.
[6] Podlubny, I*.: Fractional Differential Equations*. Academic Press, San Diego (1999)
[7] Lazarevic, M.P.: Finite time stability analysis of PD^{α} fractional control of robotic time-delay systems. *Mech. Res.Commun*. **33**, 269–279 (2006)
[8] Maione, G., Lino, P.: New tuning rules for fractional PI^{α} controllers. *Nonlinear Dyn*. **49**, 251–257 (2007)
[9] Oustaloup, A., Sabatier, J., Lanusse, P.: From fractal robustness to CRONE control. *Fractional Calc. Appl.* Anal. **2**(1), 1–30 (1999)
[10] Oustaloup, A.: La Commande CRONE. Hermes, Paris (1991)
[11] Monje, C.A., Feliu, V.: The fractional-order lead compensator. *In: IEEE International Conference on Computational Cybernetics*. Vienna, Austria, August 30–September 1(2004)
[12] Suárez, J.I., Vinagre, B.M., Calderón, A.J., Monje, C.A., Chen, Y.Q.: Using *fractional calculus for lateral and longitudinal control of autonomous vehicles. In*: Lecture Notes in Computer Science, vol. 2809. Springer, Berlin (2004)
[13] Calderon, A.J., Vinagre, B.M., Feliu, V.: Fractional-order control strategies for power electronic buck converters. *Signal Process*. **86,** 2803–2819 (2006)
[14] Silva, M.F., Machado, J.A.T., Lopes, A.M.: Fractional order control of a hexapod robot. *Nonlinear Dyn*. **38**, 417– 433 (2004)
[15] Lacroix, S. F. 1819, *Traite Du Calcul Differential et du Calcul Integral*,2nd edn.Vol .3 Paris Courcier,409-410,1819.
[16] Fourier J. Théorie analytique de la chaleur. Paris (1822)
[17] J. C. Wang: Realizations of generalized warburg impedance with RC ladder networks and transmission lines, J. of Electrochem. Soc., vol. 134, no. 8, August 1987, pp. 1915–1920.
[18] I. Podlubny. Geometric and Physical Interpretation of Fractional Integration and Fractional Differentiation. *Fractional Calculus and Applied Analysis*, vol. 5, no. 4, pp. 367-386, 2002.
[19] Caponetto, R., L. Fortuna and D. Porto,. Parameter Tuning of a Non Integer Order PID Controller. In: *Proceedings of the Fifteenth International Symposium on Mathematical Theory of Networks and Systems.* Notre Dame, Indiana,2002.
[20] Leu, J. F., S. Y. Tsay and C. Hwang , Design of Optimal Fractional-Order PID Controllers. *Journal of the Chinese Institute of Chemical Engineers* 33(2), 193.202,2002.
[21] D. Val´erio and J. S´a da Costa. Tuning of fractional pid controllers with ziegler-nichols-type rules. *Signal processing*, 86:2771–2784, 2006.

[22] C.A. Monje, A.J. Calder´on, B.M. Vinagre, Y.Q. Chen, and V. Felieu. On fractional PIalpha controllers: Some tuning rules for robustness to plant uncertainties. *Nonlinear Dynamics*, 8:369–381, 2004.
[23] L. Dorcak, I. Petras, I. Kostial, and J. Terpak. Statespace controller desing for the fractional-order regulated system. *International carpathian control conference*, 1: 2001, 2001.
[24] P.S.V. Natarj and S. Tharewal. On fractional-order qft controllers. *Journal of Dynamic Systems, Measurement, and Control*, 129:212–218, 2007.
[25] D. Xue and Y. Q. Chen: A Comparative Introduction of Four Fractional Order Controllers, *Proceedings of the 4th World Congress on Intelligent Control and Automation*, June 10 - 14, Shanghai, China, 2002
[26] C. A. Monje, B. M. Vinagre, A. J. Calder ´on, V. Feliu and Y. Q. Chen. *Self-tuning of Fractional Lead-Lag Compensators*, Prague, Czech, July 4-8 2005. IFAC World Congress.
[27] B. M. Vinagre, I. Podlubny, *et al.*, Some approximations of fractional order operators used in control theory and applications, *Fractional Calculus and Applied Analysis* 3:231-248, 2000
[28] B. M. Vinagre, Y. Q. Chen, I. Petráš, Two Direct Tustin Discretization Methods for Fractional-Order Differentiator/Integrator, *Journal of the Franklin Institute*, 340:349-362, 2003
[29] P. Ostalczyk, Fundamental Properties of the Fractional-Order Discrete-Time Integrator, *Signal Processing* 83:2367-2376, 2003
[30] G. Mainone, A Digital, Noninteger Order, Differentiator Using Laguerre Orthogonal Sequences. *International Journal of Intelligent Control and Systems*, vol. 11, no 2, 77-81, 2006
[31] I. Petras, I. Podlubny, et al., Analogue Realizations of Fractional Order Controllers. Fakulta Berg, TU Kosice, 2002
[32] J. Sabatier, O. P. Agrawal, J. A. Tenreiro Machado, *Advances in Fractional Calculus*, Springer, Netherlands, 2007
[33] K. J. Åström, B. Wittenmark, *Computer Controlled Systems: Theory and Design, 3. ed.*, Prentice-Hall, 1997
[34] Mitovski M. ,*Energetic efficiency of cryogen process*, Publisher “Bakar”, Bor,1994
[35] Bošnjaković F. Basic of heat transfer, Part I, Technical book,Zagreb,1970.

SOME NOTES ON STOCHASTICITY OF DYNAMIC RESPONSE OF 2D BRITTLE LATTICES

Sreten Mastilovic

Faculty of Construction Management, Union University
Cara Dusana 62-64, 11000, Belgrade, Serbia
e-mail: smastilovic@fgm.edu.rs

Abstract. A statistical approach to rupture of a disordered two-dimensional (2D) triangular lattice consisting of fragile nonlinear springs is used to elucidate some generic effects of the microstructural disorder and the strain rate on dynamic response of, and the damage evolution in, the low fracture energy materials. The emphasis is on the neighborhood of the critical point of the brittle response - the stress peak, the threshold of homogeneous-to-heterogeneous phase transition. The simulation results reveal increase of the mean and decrease of the standard deviation of the macroscopic tensile strength with increase of the structural and geometrical order till the "theoretical strength" saturation. At the same time, the increase in lattice disorder results in increase of the mean and standard deviation of the stress-peak damage energy rate, followed by the decrease of the same in the softening phase. Expressions are proposed to model the mean tensile strength dependence on the strain rate and the rate-driven change of damage energy during softening. The linearity of the rate dependence of the stress-peak macroscopic response parameters is observed and discussed.

1. Introduction

Brittle materials, such as ceramics, rocks, concrete, are frequently used in civilian and military applications for design of structures exposed to extreme dynamic loads. These applications require a thorough knowledge of the physics of high rate deformation of said materials, which is complex and subtle and influenced substantially by stochastic and random factors. The considered phenomena are, therefore, often too recondite to be modeled theoretically. Besides, although damage evolution by its very nature spans spatial scales, it has been recently suggested by Mastilovic et al. [12] that the governing spatial scale of damage and rupture phenomena in the low-fracture energy materials changes with the loading rate: the high-rate damage is governed by events at the submicroscopic scales while the medium-rate damage is governed substantially, if not predominantly, by cooperative phenomena at the mesoscopic scale ("the disorder of micro-texture controls the macroresponse"; [20]). Last but not least, the complexity of analytical and computational modeling is further burdened by a lack of detailed test data with respect to direct measurements under the high-rate tensile loading [13].

The present conference paper contains mainly the results recently published in the International Journal of Damage Mechanics [13, 14], which were focused on analysis of stochastic damage evolution of the dynamically loaded brittle systems. An objective of this research effort is to gain insights into some salient features of the deformation dynamics of

brittle solids, with emphasis on the ceramic materials with the inferior grain boundary strength and low fracture energy. With these materials in mind, the strain rate range of these "virtual" experiments, [10 s^{-1}, 1×10^{9} s^{-1}]—tentatively labeled medium-to-high—reaches the theoretical limit, $\dot{\varepsilon}_0 = \varepsilon_0/\tau_0 \approx 10^{9}\ s^{-1}$; defined by the limit failure strain, ε_0=0.001, and a temporal parameter of the order of Debye's atomic vibration period, $\tau_0 = 10^{-12}\ s$ [19].

Although a variety of experimental techniques are used to study the dynamic behavior of materials, the lower and upper ends of the range investigated herein are explored most commonly by the split Hopkinson pressure bar (up to the strain rates of $10^{4}\ s^{-1}$) and the plate impact tests ($10^{8}\ s^{-1}$), respectively [1]. It is important to point out that the direct comparison of results obtained by these two techniques is somewhat tentative [2] since the former is performed under one-dimensional (1D) stress conditions while the latter is performed under 1D strain conditions. On the other hand, the lattice simulation results presented herein are obtained at various strain rates are under practically identical stress conditions. Furthermore, the lattice simulations replicate rather well the underlining phenomenology of the sample response including the essential features of rate-dependent fracture and deterioration of the effective stiffness, and provide an elementary intuition on the phenomena [12]. Consequently, in spite of the recognized limitations and drawbacks [4, 5, 16, 18, 23], the lattice simulations prove a useful tool for qualitative analysis of universal trends of the dynamic behavior of brittle materials since they:

i. make possible the "virtual experiments" [10] into the regions that are still beyond capabilities of the presently available experimental techniques,
ii. offer detailed insights in the deformation process due to the practically unlimited control over the computer experiments,
iii. incorporate both aleatory variability and epistemic uncertainty in a straightforward manner [12].

The natural randomness of the mesoscale material texture is an example of the aleatory variability. The inherent disorder is, in the course of deformation, further enhanced by the extrinsic disorder due to the damage evolution that is governed by the local fluctuations of energy barriers quenched within the material and the local fluctuations of stress. The nonlocal and nonlinear character of these far-from-equilibrium processes is such that concepts of strain and damage based on spatial and temporal averaging are, at best, conditionally acceptable [8]. Nevertheless, the overall quantities exhibit universal trends [4] despite the random character of the local fluctuations of mechanical fields.

2. Simulation model

The present model is used extensively in the past to investigate stochastic damage evolution in low-fracture energy systems ([12, 13, 14] and references cited therein), thus, only a gist of the method is summarized herein. The idealized brittle mesoscale (tensile test) specimen is represented by a virtual 2D structure: a Delaunay simplicial graph dual to an irregular honeycomb system of Voronoi polyhedra representing, for example, grains of a ceramic material. In general, the identification of the microconstituent that dominates the macroresponse is a problem-specific task [17], which is at core of the definition of the representative volume element. In the present framework, the grain boundaries ("the most

common examples of weak interfaces in brittle materials" [9]) are considered to provide direct, first-order effects on the overall dynamic response; the average grain facet size defines the model resolution length, l_c; and the other microheterogeneities and defects (resulting in the local stress and strain fluctuations) on a smaller scale are accounted for by stiffness and strength distributions [7]. Consequently, the microstructural texture is represented by a network of grain boundaries while the cracking is necessarily intergranular. The size of grains and strength of grain boundaries in a polycrystalline ceramics are distinctively stochastic parameters.

The "continuum particles" [24] located in lattice nodes interact with their nearest neighbors through the nonlinear central-force links (defined by the Hook potential in tension and the Born-Meyer potential in compression). The coordination number z and link length λ define the randomness of the lattice morphology. The model is geometrically and structurally disordered since the equilibrium distances between particles and their mutual link stiffness are sampled from their respective distributions within the range $\alpha\ \bar{\lambda} \le \lambda \le (2-\alpha)\ \bar{\lambda}$ and $\beta\ \bar{k} \le k \le (2-\beta)\ \bar{k}$. The geometrical-order parameter, $(0 \le \alpha \le 1)$, and the structural-order parameter, ($0 \le \beta \le 1$), define bandwidths of the geometrical and stiffness disorder [12]. The link-rupture criterion is defined in terms of the critical link elongation $\varepsilon_{ij} = \Delta\lambda_{ij} / \lambda_{0ij} = \varepsilon_{cr} = const.$

The unnotched tensile specimen is a square of side length L = 1.9 mm. The problems of the loading at extremely high rates, including the uniform load distribution, are solved by imposing an instantaneous initial velocity field to the lattice in the loading direction, $\dot{x}_1(t=0) = \dot{\varepsilon}_1\, x_1$, and perpendicular to it, $\dot{x}_2(t=0) = -\upsilon_0^{(\varepsilon)}\, \dot{\varepsilon}_1\, x_2$, defined in the terms of the prescribed strain rate, $\dot{\varepsilon}_1 = \dot{L}/L$. (The preceding coordinates refer to the centroidal coordinate system and $\upsilon_0^{(\varepsilon)}$ is the apparent plane-strain Poisson's ratio [11].) Subsequently, at $t > 0$, only velocity of the particles located at the longitudinal boundaries ($x_1 = \pm L/2$) is controlled, $\dot{x}_1 = \pm \dot{\varepsilon}_1\, L/2$; while the motion of all other particles is governed by the Newton's equation of motion, discretized in time and integrated using one of many finite-difference algorithms to obtain the particle trajectories. Effects of this loading procedure are described in [12].

Finally, it is worthwhile to note that no attempt is made in this study to follow the procedures developed in [21] for constructing a mechanically equivalent lattice capable of matching the physical properties of polycrystalline ceramics, which would be futile keeping in mind the stated objectives. This, the reduced-units geometric and structural lattice parameters are: the coordination number $z = 6$, the average equilibrium distance between particle sites $\bar{\lambda} = l_c = 1$, the average link stiffness $\bar{k} = 50$, and the rupture strain of the links $\varepsilon_{cr} = 0.1\%$. The set of 30 simulations per each strain rate are performed on two lattices characterized by substantially different disorder levels labeled tentatively as:

- Large disorder (*LD*): (α, β) = (0.02, 0.5), and
- Small disorder (*SD*): (α, β) = (0.2, 0.9).

If no distinction is made between the large disorder and small disorder model, the simulation results refer to the later.

3. Results

The first set of results refers to simulations performed at four strain rates ($\dot{\varepsilon}$ = 10, 1×10^3, 1×10^5, and 1×10^7 s^{-1}) by using 30 different statistical realizations of the geometrical and structural disorder governed by the selection of the pseudorandom-number-generator seed. The basic tensile strength statistics is presented in Table 1 for the two sets of simulations performed on the models characterized by two different disorder levels (*LD* and *SD*) defined previously.

Table 1. Basic statistics of the dynamic tensile strength data for the large-disorder and small-disorder models (LD—SD)

$\log(\dot{\varepsilon})$ [1/s]	σ_m/E_0		
	MEAN [$\times10^{-3}$]	STANDARD DEVIATION [$\times10^{-3}$]	RATIO OF NON-OUTLIER MAX. & MIN.
1	0.0887—0.264	0.0155—0.0148	1.94—1.25
3	0.235—0.343	0.0115—0.0152	1.32—1.17
5	0.482—0.659	0.00209—0.0183	1.08—1.01
7	1.07—1.07	0.00185—0.000780	1.07—1.00

These results, recently published in [13], are in qualitative agreement with the experimental observations that the static tensile strength of brittle materials can be exceeded by an order of magnitude by the dynamic tensile strength introduced by shock waves [3]. The simulation results also confirm the relatively modest rate sensitivity of brittle materials at lower loading rates dominated by the subcritical crack growth. A single dominant macrocrack evolves from the most "favorably" positioned among weak links, which eventually results in a catastrophic failure along nearly-straight macro fracture at a small macro damage density level. The rapid strength ascent, depicted schematically in Figure 1 at two disorder levels, coincides with the transition of fracture pattern from a couple of dominant macrocracks to the web of uniformly distributed microcrack clusters [12, 13]. It should be emphasized that while stress and damage energy time histories for low and high strain rates generally reveal the brittle properties of the failure process[1], those in Figure 2, corresponding to this transition, reveal a number of quasi-ductile characteristics; most notably, the relatively significant damage accumulation in the hardening regime and the pronounced softening regime. These features are result of collective behavior of the microcracks comprising the web of microcrack clouds [12]. The reduction of tensile strength stochasticity in this strain rate range is attributed to the averaging effect within these clusters [25].

The scatter of strength data for the four loading rates and two material disorder levels, presented in Table 1, is depicted schematically by the shaded areas in Figure 1. The large scatter corresponding to $\dot{\varepsilon}$ = 10 s^{-1} is reduced to a single line at $\dot{\varepsilon}$ = 1×10^7 s^{-1}, which is

[1] The linear stress increases with time and the sudden drop upon failure with negligible damage accumulation prior to failure.

indicative of the substantial reduction of the tensile-strength scatter close to the "upper-plateau" loading rate range [13]. This suggests that the theoretical strength, defining the upper limit strength, is—similar to elastic properties—a deterministic property defined primarily by the chemical bonding (that is, at the atomic scale) and relatively insensitive to the subtle features of the material mesoscale texture [12]. The evident transition from the stochastic to the deterministic behavior—reflected by the reduction of the strength dispersion and change of damage evolution patterns discussed in [12]—is more pronounced in the case of the large microstructural disorder. It is observed that for the limit case of a slightly perturbed ideal lattice $(\alpha, \beta) = (0.99, 0.99)$ the strength scatter practically disappears, which suggests that the stochasticity of the materials response results from the structural disorder [13]; interestingly, the difference between the upper and lower strength thresholds remains and is reduced to $\sigma_m^{th} / \sigma_{m0} \approx 1.4$.

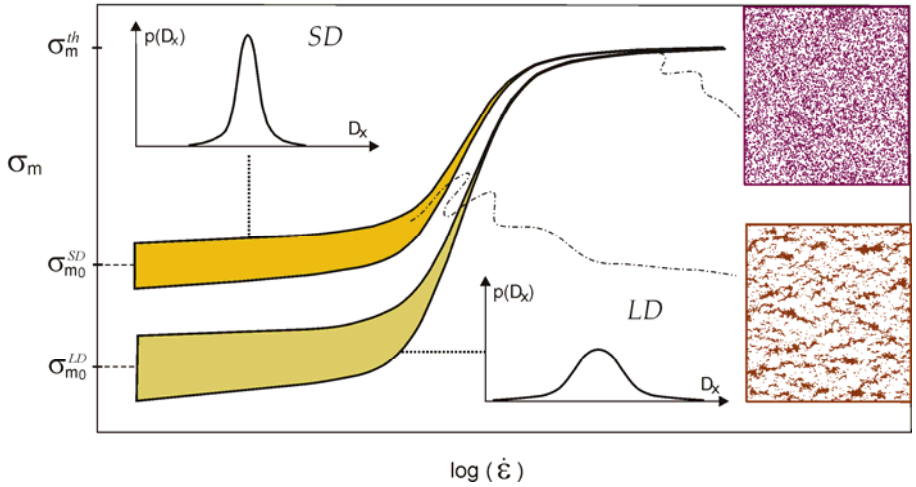

Figure 1. Schematic representation of the rate sensitivity of tensile strength outlining the ordering effect of kinetic energy and the effect of geometrical and structural disorder.

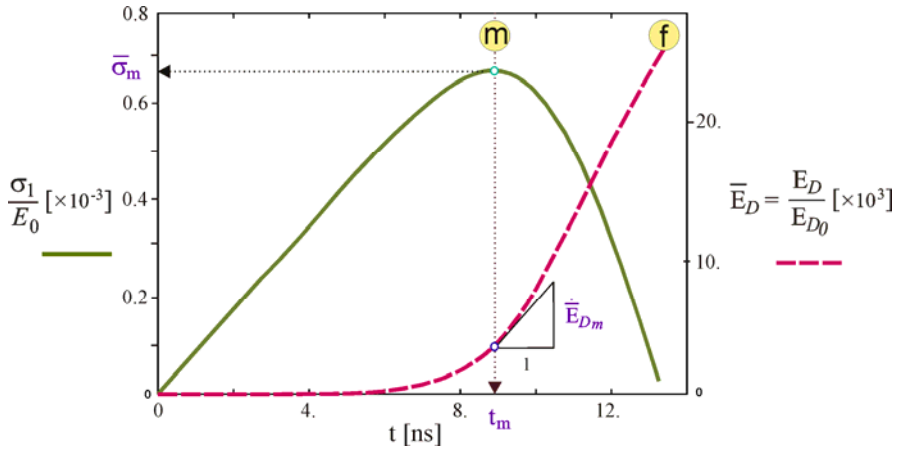

Figure 2. Typical time histories of the normal stress and damage energy at $\dot{\varepsilon}_1 = 1\times10^5\ s^{-1}$. The indices, m and f, refer to the stress peak and post peak (softening) quantities, respectively.

The importance of the microstructural events that take place at the critical point: the stress peak is worth to emphasize [23]. The present focus is on the stress-peak and post-peak damage energy rates (Tables 2, adopted from [13]). It should be noted that while the stress-peak damage energy rate is defined unambiguously, the post-peak damage energy rate reported herein refers to the maximum damage energy rate in the softening regime corresponding to the final deformation phase (as depicted in Figure 2) for the avalanche-type failures, but not necessarily in general.

Table 2. Statistics of the stress-peak ($\dot{\bar{E}}_{Dm}$) and the post-peak ($\dot{\bar{E}}_{Df}$) damage energy rates at the two levels of model disorder

$\log(\dot{\varepsilon})$ [1/s]	MEAN / STANDARD DEVIATION ($\times10^3$)			
1	0.0034 / 0.0030	1.2 / 0.36	0.0027 / 0.0028	1.5 / 0.56
3	0.27 / 0.25	2.1 / 0.84	0.22 / 0.10	2.6 / 1.7
5	22. / 1.1	37. / 1.0	25. / 1.3	55. / 2.1
7	6400. / 800.	11000. / 4200.	3600. / 680.	7600. / 400.
	$\dot{\bar{E}}_{Dm}$	$\dot{\bar{E}}_{Df}$	$\dot{\bar{E}}_{Dm}$	$\dot{\bar{E}}_{Df}$
	LARGE DISORDER		SMALL DISORDER	

First, it is interesting to note, from the simulation results, that for the displacement-controlled tension the mean value of the stress-peak damage energy rate scales reasonably well with the strain rate. More detailed investigation [14] revealed the linear dependence of the form

$$\dot{\bar{E}}_{Dm}\ \dot{\varepsilon}^{-1} = Const. \tag{1}$$

which is presented schematically in Figure 3 (the hollow squares).

Second, the increase of geometrical and structural disorder results in increase of both the mean value and the standard deviation of the $\dot{E}_{Dm}$ data. On the other hand, the basic statistics of the post-peak damage energy rate ($\dot{E}_{Df}$), presented in Table 2, reveals that the higher stress-peak damage energy rates—characteristic of the more disordered model—are followed by the lower post-peak (softening) damage energy rates, both in terms of the mean value and the data scatter [13].

Figure 3 also illustrates effect of the loading rate on the time, t_m, at which the stress peak is reached (the solid circles). This stress-peak time is tentatively affiliated with time-to-failure in [14] for two reasons: (i) the sample would fail at the stress-peak for the stress-controlled test, and (ii) the prevalent opinion, matured over the last two decades, is that the softening is not an intrinsic material property [7, 23]. All data points in Figure 3 represent mean values of 30 statistical realizations per strain rate for the SD model. The linearity

$$t_m \ \dot{\varepsilon} = Const. \tag{2}$$

is evident from Figure 3. As indicated in [14], Equation (2) is identical to the empirical relationship between creep rate and time to rupture for the constant-stress quasi-static loading [22], and the strain-controlled brittle creep fracture [6]. It also bears similarity with the time to failure derived in [15] by combining the main ideas of continuum damage mechanics and statistical and kinetic theories of strength.

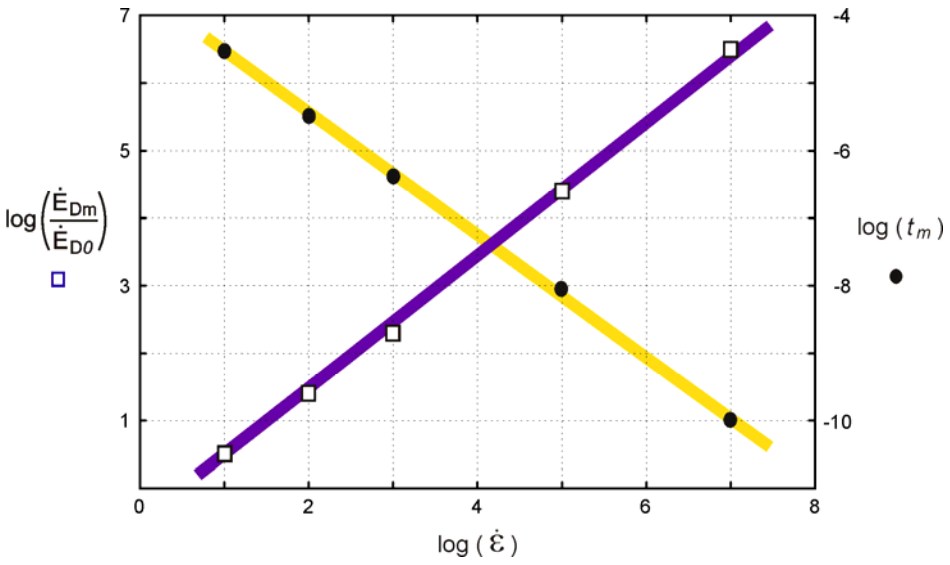

Figure 3. Change of the mean *stress-peak* parameters with the strain rate: the damage energy rate (hollow squares) and the time (solid circles).

The remarkable hardening of the brittle response with the rate increase, discussed previously [12, 13], is illustrated in Figure 4. The solid circle represents the mean strength obtained from 30 different statistical realizations at the five selected strain rates for the small-disorder model. The hollow circles depict one single realization at eight additional strain rates. The increase of the loading rate results in increase of the mean tensile strength, limited by the two horizontal asymptotes (σ_{m0} and σ_m^{th}) dependent on the system disorder [13]. The loading rate increase also results in reduction of the response stochasticity caused by the averaging effect of collective behavior of microcrack systems, which smoothens the randomness at the macroscopic scale. Another effect of that increasingly adiabatic deformation and damage is the diminishing flaw-sensitivity of brittle materials with the loading-rate increase [12].

Based on the simulation results, the following expression

$$\sigma_m = \sigma_{m0} + S_m \left\{ 1 - \exp\left[-\left(\frac{\log(\dot{\varepsilon}) + A}{2\log(\dot{\varepsilon}_\times)} \right)^C \right] \right\} \tag{3}$$

was proposed [14] to capture general features of the mean tensile strength dependence on the strain rate. The parameter $S_m = S_m(\alpha, \beta) = \sigma_m^{th} - \sigma_{m0}$ is a measure of hardening and A, C, and $\dot{\varepsilon}_\times$ are fitting parameters. As indicated on Figure 4, the crossover strain rate $\dot{\varepsilon}_\times$ corresponds to $\sigma_m = (\sigma_m^{th} + \sigma_{m0})/2$. It should be noted that the theoretical strength, associated by Grady [3] with the Hugeniot elastic limit obtained from shock compression experiments, is attained here by the virtual *tensile* experiments. The demonstrated disorder dependence of the hardening parameter S_m [13] suggests that the degree of structural heterogeneity of brittle solid governs substantially the process of activation and nucleation of micro-defects. (Roughly, the parameters A and $\dot{\varepsilon}_\times$ define the onset of the strength rapid increase, while C defines gradient of that increase.)

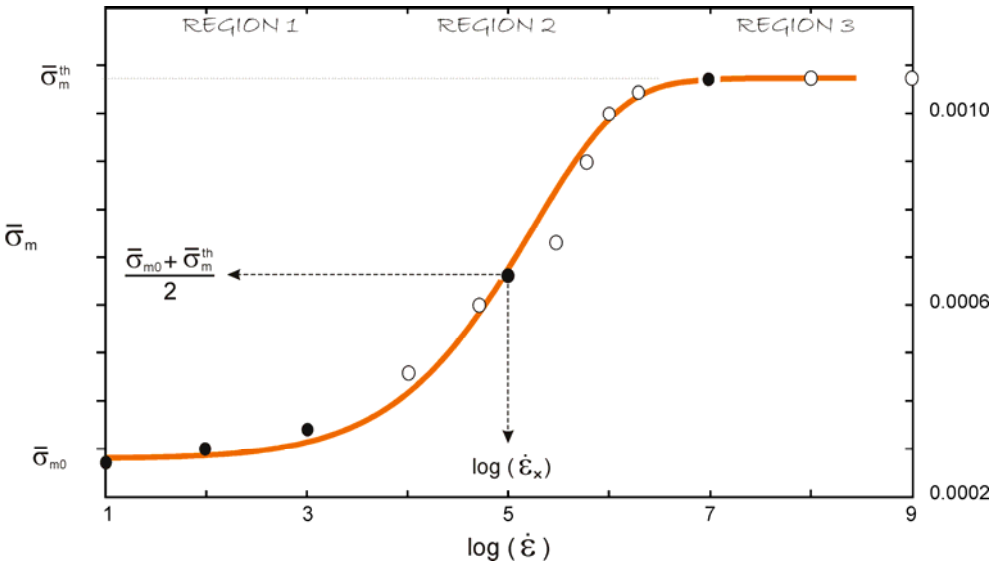

Figure 4. Rate dependence of the mean tensile strength. Solid line represents a fit obtained by using Equation (3) with parameters: A=4.7, C=12, and $\dot{\varepsilon}_x = 1\times10^5\ s^{-1}$.

The rate-driven change of the damage energy rate during softening is investigated in detail by Mastilovic [14] and summarized in the logarithmic plot in Figure 5. The hollow squares represent the mean of 30 statistical realizations for the small disorder lattice while the solid circles mark results of one single realization at the given rates. Note that, due to the observed reduction of the data scatter with the strain rate increase, any arbitrarily selected physical realizations at the high rates should represent reasonably well the mean value. The dashed line in Figure 5 represents the best fit of the simulation data:

$$\log\left(\frac{\dot{E}_{Df}}{\dot{E}_{Dm}}\right) = H_1\left\{\left(\log\dot{\varepsilon} - \log\dot{\varepsilon}_{eq}\right) - H_2\left[\exp\left(\frac{\log\dot{\varepsilon} - \log\dot{\varepsilon}_{eq}}{H_2}\right) - 1\right]\right\} \qquad (4)$$

where H_1 and H_2 are fitting parameters and $\dot{\varepsilon}_{eq}$ is the strain rate corresponding to the stress-peak damage energy rate equilibrium ($\dot{E}_{Df} = \dot{E}_{Dm}$) that marks the minimum of the curve in Figure 5 [14].

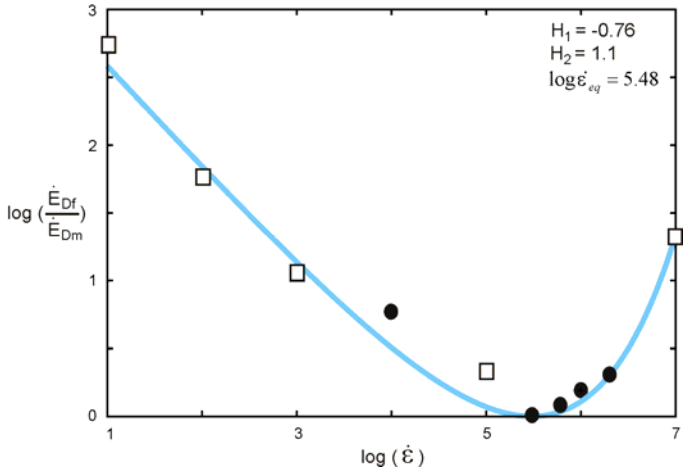

Figure 5. Change of the ratio of damage energy rates in the post-peak and peak regions of stress-strain curve with the strain rate. Dashed line represents the fit obtained by using Equation (4) with given fitting parameters.

It is obvious that the asymmetric data fit in Figure 5, defined by Equation (4), formally tends to infinity for both loading limits (the quasi-static and the "infinite"), but for different reason: $\lim_{\dot{\varepsilon}\to 0} \dot{E}_{Dm} = 0$ and $\lim_{\dot{\varepsilon}\to \infty} \dot{E}_{Df} = \infty$, respectively. In reality, the maximum possible strain rate in the material, $\dot{\varepsilon}_0$ (Introduction), provides the finite limit for $\dot{E}_{Df}$, while the stress peak is by definition associated by non-zero $\dot{E}_{Dm}$ (albeit very small and temporal-resolution dependent for the low rate "limits").

4. Summary

This study elucidates some universal trends that contribute to understanding of basic principles governing high-rate mesomechanics of disordered low-fracture-energy solids. An expression proposed to model the mean tensile strength dependence on the strain rate for the entire strain rate range is discussed. Although the fundamental arguments to support the form of this expression could not be provided at present, it appears simple and robust enough to capture reasonably well the entire rate-driven strength evolution with only a few experiments.

The damage dynamics is investigated based on change in the damage energy rate accompanying damage evolution in the critical point neighborhood. It is observed [14] that the medium of the transitional range rates (Region 2 in Figure 4), $\dot{\varepsilon}_{eq} = 3\times 10^5\, s^{-1}$, is characterized by the absence of change of the damage energy rate in the peak neighborhood ($\dot{E}_{Df} \approx \dot{E}_{Dm}$) and corresponds to an atypical stress-strain curve exhibiting many features of the quasi-ductile behavior.

The linearity of the rate dependence of the stress-peak macroscopic response parameters is observed and modeled. These models, based on simulation results, bridge the scales by offering connection between the macroscopic response parameters at the stress peak (t_m,

$\dot{E}_{Dm}$) and the microscopic failure criterion (ε_{cr}) for the dynamic loading within the wide range of the strain rates that encompasses variety of damage mechanisms.

References

[1] Field, J.E., Walley, S.M., Proud, W.G., Goldrein, H.T., Siviour, C.R. (2004). Review of experimental techniques for high rate deformation and shock Studies. *Int. J. Impact Eng.* **30**, 725-775.

[2] Grady, D.E. (1995). Dynamic Properties of Ceramic Materials. SAND 94-3266, Sandia National Laboratories, Albuquerque, USA.

[3] Grady, D.E. and Hollenbach, R.E. (1979). Dynamic fracture strength of rock. *Geophys. Res. Letters* **7**: 73-76.

[4] Hansen A., Roux S., Herrmann H.J. (1989). Rupture of central-force lattices. *J. Phys. France* **50**: 733-744.

[5] Jagota A., Bennison S.J. (1994). Spring-Network and Finite-Element Models for Elasticity and Fracture, in: Bardhan, K.K., Chakrabarti, B.K., Hansen, A. (Eds.), Proceedings of a workshop on breakdown and non-linearity in soft condensed matter, Springer-Verlag Lecture Notes in Physics, Berlin, Germany, pp. 186-201.

[6] Kachanov L.M. (1986). Introduction to Continuum Damage Mechanics. Martinus Nijhoff Publishers, Dordrecht, The Netherlands

[7] Krajcinovic D. (1996). Damage Mechanics. North-Holland, Amsterdam, The Netherlands

[8] Krajcinovic D., Mastilovic S. (1999) Statistical models of brittle deformation Part I: Introduction, *Int. J. Plasticity* **15**: 401-426

[9] Lawn, B. (1993). Fracture of Brittle Solids (2nd ed.), Cambridge University Press, Cambridge, UK.

[10] Mastilovic, S. (2008) Investigation of Dynamic Behavior of Brittle Solids by Discrete Systems, Faculty of Construction Management, Union University, Belgrade, Serbia.

[11] Mastilovic, S. (2008). A Note on Short-Time Response of Two-Dimensional Lattices During Dynamic Loading. *Int. J. Damage Mech*. **17**: 357-361.

[12] Mastilovic, S., Rinaldi, A., Krajcinovic, D. (2008). Ordering effect of kinetic energy on dynamic deformation of brittle solids. *Mech. Mater.* **40** (4-5): 407-417.

[13] Mastilovic, S. (2011). Some Observations Regarding Stochasticity of Dynamic Response of 2D Disordered Brittle Lattices. *Int. J. Damage Mech.* **20**: 267-277.

[14] Mastilovic, S. (2010). Further Remarks on Stochastic Damage Evolution of Brittle Solids Under Dynamic Tensile Loading. *Int. J Damage Mech.* doi: 10.1177/1056789510385294.

[15] Mishnaevsky, Jr., L. (1998). Damage and Fracture of Heterogeneous Materials. A.A. Balkema, Rotterdam, The Netherlands

[16] Monette, L., Anderson, M.P. (1994) Elastic and fracture properties of the two-dimensional triangular and square lattices, *Modelling Simul. Mater. Sci. Eng* **2**: 53-62

[17] Nemat-Nasser, S., Hori, M. (1999). Micromechanics: Overall Properties of Heterogeneous Materials (2nd ed.). North-Holland, Amsterdam, The Netherlands

[18] Ostoja-Starzewski, M. (2002). Lattice models in micromechanics. *Appl. Mech. Rev*. **55** (1): 35-60.

[19] Qi, C., Wang, M, Qian, Q. (2009). Strain rate effects on the strength and fragmentation size of rocks, *Int. J. Impact Eng.* **36**, 1355-1364.

[20] Rinaldi, A. (2009). Rational Damage Model of 2D Disordered Brittle Lattices Under Uniaxial Loadings. *Int. J. Damage Mech.* **18**, 233-257.

[21] Rinaldi, A., Krajcinovic, D., Peralta, P., Lai, Q. (2008). Lattice models of polycrystalline microstructures: A quantitative approach. *Mech. Mater.* **40**, 17-36.

[22] Tetelman, A.S., McEvily Jr., A.J., 1967. Fracture of Structural Materials. John Wiley & Sons, New York, USA.

[23] Van Mier, J.G.M and Man, H. (2009). Some Notes on Microcracking, Softening, Localization, and Size Effect. *Int. J. Damage Mech*., **18 (3)**: 283-309.

[24] Wiener, J.H., 1983. Statistical Mechanics of Elasticity. J. Willey and Sons, New York, USA.

[25] Zhou, F. and Molinari, J.F. (2004). Stochastic fracture of ceramics under dynamic tensile loading. *Int. J. Solids Struct*. **41**: 6573-6596.

ON VISCOPLASTICITY OF TRANSVERSELY ISOTROPIC QUASI-RATE INDEPENDENT MATERIALS

M. Mićunović[1], **Lj. Kudrjavceva**[2]

[1] Mašinski fakultet, The University of Kragujevac, ul. Sestre Janjića 6, 34000 Kragujevac, Serbia,
e-mail: mmicun@kg.ac.rs
[2] The State University of Novi Pazar, ul. Vuka Karadziá bb., 36000 Novi Pazar, Serbia
e-mail: ljuta1@gmail.com

Abstract. As found by experiments *quasi rate independent materials* (*QRI*) describe very well behavior of steels in very wide range of strains and strain rates ([3],[4]). This property has been combined with tensor representation modeling using a generalized associative flow rule based not on the yield function but on a more general loading function. Seemingly rate independent QRI producing incremental evolution equations show rate sensitivity by means of variability of yield stress with stress rate. On the other hand transverse isotropy appears in metal forming issues like in rolled car body sheets [18]. Here an extension of tensor generators and invariants is needed to include the preferred anisotropy direction. Such a procedure has been made here. In addition we believe that the results of this paper are applicable to dynamic deformation of orthogneiss rocks treated recently in [5].

Keywords: Viscoplasticity, QRI materials, reactor stainless steels, orthogneiss rock

1. Introduction and preliminaries

Theoretical consideration of viscoplasticity has become an important issue for finite element codes which pretend to perform calculations of complex structures with a high precision. In a majority of them (like ABAQUS, ADINA, MARC, etc.) evolution equation for plastic strain rate is of associate type, i.e., it is perpendicular to yield surface in stress space. As another essential simplification yield function is firmly connected to the second invariant of the deviatoric stress, so called J_2 invariant. This leads to coaxiality of plastic stretching and stress deviator tensors. Such a surface most commonly is based on the above–mentioned unique flow curve. It should be noted that usually yield function is detected from tension tests and then applied to calculation during arbitrary stress–strain histories appearing in real structures. This procedure could produce significant errors destroying geometrical accuracy which FEM codes offer.

The best check for a theory is to compare it to experiments. We have at the disposal experiments performed in Dynamic testing laboratory of JRC-Ispra, Italy with specimen made of austenitic stainless steel AISI 316 in the range of small, medium and high strain rates from $0.001\ s^{-1}$ to $1000\ s^{-1}$. The testing has been done mainly at room temperature. Calibration of the theory shortly sketched below is explained in detail in [4].

Let us devote few words about the notions used in this paper. For finite elasto-visco-plastic strains it is commonly accepted for a considered body that aside from undeformed

configuration (χ_0) and deformed current configuration (χ_t) there exists a local reference configuration of natural state elements (ν_t)[4]. Then, Kröner's decomposition rule [6, 7] holds in the following form:

$$\mathbf{F}_P := \mathbf{F}_E^{-1}\mathbf{F}, \tag{1}$$

where

$\mathbf{F}$ is the deformation gradient tensor,

$\mathbf{F}_E$ the elastic distortion tensor and

$\mathbf{F}_P$ the plastic distortion tensor,

determined by the mappings $(\chi_0) \to (\chi_t)$, $\chi_n \to (\chi_t)$ and $(\chi_0) \to (\nu_t)$, respectively.

In the next section for brief review of constitutive models we will need the plastic stretching tensor being equal to

$$\mathbf{D}_P = \mathrm{sym}(\mathbf{L}_P) \equiv \frac{1}{2}(\mathbf{L}_P + \mathbf{L}_P^T)$$

determined by the symmetric part of plastic "velocity gradient" tensor

$$\mathbf{L}_P = (D_t\mathbf{F}_P)\,\mathbf{F}_P^{-1}.$$

Here aside of the usual notation where the superimposed dot stands for material time derivative, we have applied $D_t\mathscr{A} \equiv \dot{\mathscr{A}}$ for arbitrary $\mathscr{A}$.

Concerning state variables we will use plastic strain and stress. As an invariant measure of plastic strain the Hill's logarithmic tensor

$$\boldsymbol{\varepsilon}_P = \ln \mathbf{V}_P = 0.5 \ln\left(\mathbf{F}_P\mathbf{F}_P^T\right) \tag{2}$$

is chosen here. Its principal advantage lies in the fact that it is a deviatoric tensor. In other words, its three principal invariants read

$$\pi_1 = \mathrm{tr}\boldsymbol{\varepsilon}_P = 0, \qquad \pi_2 = \mathrm{tr}\boldsymbol{\varepsilon}_P^2 \neq 0, \qquad \pi_3 = \mathrm{tr}\boldsymbol{\varepsilon}_P^3 \neq 0, \tag{3}$$

if plastic volume change is neglected. In the above definition, the polar decomposition theorem for the plastic distortion tensor has been applied by means of

$$\mathbf{F}_P = \mathbf{R}_P\mathbf{U}_P = \mathbf{V}_P\mathbf{R}_P,$$

where $\mathbf{R}_P^{-1} = \mathbf{R}_P^T$ holds for the plastic rotation tensor.

Let the second Piola-Kirchhoff stress, related to (ν_t)-configuration, be denoted by $\mathbf{S}$. It is connected with the Cauchy ("true") stress via the expression

$$\mathbf{S} = \det\mathbf{F}_E\mathbf{F}_E^{-T}\mathbf{T}\mathbf{F}_E^{-1}.$$

By means of its deviatoric part $\mathrm{dev}(\mathbf{S}) \equiv \mathbf{S}_d$ and Hill's logarithmic plastic strain the following set of invariants will be used throughout this paper. ‡:

$$\gamma := \{s_1, s_2, s_3, \pi_2, \pi_3, \mu_1, \mu_2, \mu_3, \mu_4\}, \tag{4}$$

where

$$s_1 = \mathrm{tr}\,\mathbf{S}, \quad s_2 = \mathrm{tr}\mathbf{S}_d^2, \quad s_3 = \mathrm{tr}\mathbf{S}_d^3, \quad \mu_1 = \mathrm{tr}\{\mathbf{S}_d\boldsymbol{\varepsilon}_P\},$$

‡ The choice of the deviatoric stress is motivated by the traditional approach in the existing plasticity papers. Of course, everything derived in this chapter holds if instead of $\mathrm{dev}\mathbf{S} \equiv \mathbf{S}_d$ we use the invariants formed by means of $\mathbf{S}$.

$$\mu_2 = \mathrm{tr}\{\mathbf{S}_d \boldsymbol{\varepsilon}_P^2\}, \quad \mu_3 = \mathrm{tr}\{\mathbf{S}_d^2 \boldsymbol{\varepsilon}_P\}, \quad \mu_4 = \mathrm{tr}\{\mathbf{S}_d^2 \boldsymbol{\varepsilon}_P^2\}.$$

Finally, let us mention that in papers oriented to experiments it is customary to use the following notations:

$$\sigma_{eq} \equiv \Big(\frac{3}{2} s_2\Big)^{1/2}, \quad D_t \varepsilon_{eq}^p \equiv \Big(\frac{2}{3} \mathrm{tr}\{\mathbf{D}_P^2\}\Big)^{1/2}, \tag{5}$$

and names *equivalent stress* and *equivalent plastic strain rate*, respectively. They are used throughout this paper.

2. QRI viscoplasticity

2.1. Quasi rate independence

It is known fact that initial yield stress under dynamic loading depends on strain rate or stress rate: at higher stress rates the initial stress yield is larger. On the other hand, the phenomenon of delayed yielding inherent to some metals and alloys is observed [4]: stress under dynamic loading exceeds its static value and plasticity starts after a certain time called delay time. Let plastic deformation commence at time t^*. Denote by Y the initial equivalent dynamic yield stress, i.e. $Y = Y\big(\dot{\sigma}_{eq}(t^*)\big)$. Its static counterpart, the initial equivalent static yield stress, is denoted here by $Y_0 \equiv Y$,

Then, the accumulated plastic strain is governed by corresponding constitutive equation having the following form [8]:

$$\varepsilon_{eq}^p(t) = \int_0^t J(t-\tau)\, \dot{\sigma}_{eq}(\tau)\, d\tau \quad \text{and} \quad D_t \varepsilon_{eq}^p(t) = J(0)\, D_t \sigma_{eq}(t), \tag{6}$$

where $J(t-\tau) = \{0 \text{ if } \tau < t^*, \text{ and } \exp(-\mathscr{M}) \text{ if } \tau \geqslant t^*\}$. Here $\mathscr{M}$ is an "universal" constant for tension and shear at strain rates introduced and determined in [8] for the extremely wide range from $10^{-3}[s^{-1}]$ to $10[s^{-1}]$. This holds for reactor steels with large percentage of Nickel and Chromium as well as for ferritic steels. A calibration of experiments dealt with orthogneiss rocks as reported in [5] is in progress. It is expected that a similar behavior will be met. The first type of evolution equations used here is referred as MAM model [8]. Below, we use a simplified version of the model. The evolution equation for the plastic stretching (plastic "strain rate") is shortly is described by the following tensor representation:

$$\mathbf{D}_{\mathrm{P}} = \Lambda \sum \Gamma_\alpha \mathbf{H}_\alpha, \tag{7}$$

For the time being, scalars $\Gamma_1, \Gamma_2, \ldots$ and tensors $\mathbf{H}_1, \mathbf{H}_2, \ldots$ are not specified but the experimental evidence acquired at the Dynamic testing laboratory of JRC, Ispra (cf. [8]) strongly suggests that the scalar coefficient Λ takes the form:

$$\Lambda = \eta\, (\sigma_{eq} - Y)\Big(\frac{\sigma_{eq}}{Y_0} - 1\Big)^{\lambda} D_t \sigma_{eq} \exp(-\mathscr{M}). \tag{8}$$

Inserting of (8) into (7) leads to an evolution equation seemingly characteristic for rate independent materials. However, the rate dependence appears in stress rate dependent value of the initial yield stress Y, which has a triggering role for inelasticity onset. A model based on (8) could be named as "quasi rate independent". It is worth noting that the obtained evolution equations are endochronic permitting scaling of plastic strain rate, replacing time as independent variable by the von Mises equivalent stress. This is useful for calibration in very wide strain rate range from low to almost impact strain rates.

Note about the universal constant: Regardless of the form of a constitutive model for the stainless steel AISI 316H, the exponent $\lambda = 0.554$ whereas the "universal" material constant was found to have the value: $\mathscr{M} = 7.26$

2.2. MAM model for isotropic materials

According to ([9]) the increment of plastic strain tensor is perpendicular to a loading surface $\Omega = \text{const}$ where Ω depends on stress, temperature and *Pattern of Internal Rearrangement* (PIR). Translating this statement into the language of the previous section an evolution equation for plastic stretching should hold in the following form ([9]):

$$\mathbf{D}_P = \partial_{\mathbf{S}}\Omega(\mathbf{S}, T, PIR). \tag{9}$$

Here PIR is described by anholonomic internal variables representing crystal slips over active slip systems. Due to its significance, the whole first paper of this monograph is devoted to the related geometric issues.

The plastic deformation "gradient" (i.e. distortion) tensor is incompatible, represents also slips and may reflect transformation of anholonomic coordinates. Thus, taking into account that plastic rotation tensor may be either fixed or taken to be unity, it was assumed in [8] that in the above equation PIR may be represented by the plastic strain tensor. Moreover, we extend the above evolution equation inserting in it a scalar function Λ which must account for the linear connection between rates of Mises equivalent stress and equivalent plastic strain rate. The structure of Λ is shown in (8). Therefore,

$$\mathbf{D}_P(D_t\mathbf{S}, \mathbf{S}, \boldsymbol{\varepsilon}_P, T) \;=\; \Lambda\, \partial_{\mathbf{S}}\Omega(\mathbf{S}, \boldsymbol{\varepsilon}_P, T), \tag{10}$$

where Rice's loading function depends on temperature and the above given invariants, i.e.,

$$\Omega \;=\; \Omega(\gamma, T) \;\equiv\; \Omega(s_1, s_2, s_3, \pi_2, \pi_3, \mu_1, \mu_2, \mu_3, \mu_4, T).$$

Suppose that damage is negligible until localization onset and that this function is approximated by a fourth order polynomial with respect to $\mathbf{S}$ and first order in $\boldsymbol{\varepsilon}_P$. With such an approximation we would have [4]:

$$2\,\Omega = a_1 s_2 + (a_2 + a_4\mu_1)(s_1 s_2 - s_3) + \frac{1}{2}a_3 s_2^2 + \frac{1}{3}a_5(3\mu_3 s_2 - 2\mu_1 s_3). \tag{11}$$

Therefore, applying tensor representation to the evolution equation for plastic stretching allows the next equation:

$$\mathbf{D}_P = \Lambda \sum_{\alpha=1}^{4} \Gamma_\alpha(\gamma)\,\mathbf{H}_\alpha \tag{12}$$

with the next tensor generators:

$$\begin{aligned}
Y_0\,\mathbf{H}_1 \;&= \mathbf{S} - \frac{1}{3}\mathbf{1}\,\mathrm{tr}\mathbf{S} \equiv \mathrm{dev}\mathbf{S} \equiv \mathbf{S}_d,\\
Y_0^2\,\mathbf{H}_2 \;&= \mathrm{dev}(\mathbf{S}_d^2),\\
\mathbf{H}_3 \;&= \boldsymbol{\varepsilon}_P,\\
Y_0\mathbf{H}_4 \;&= \mathrm{dev}(\mathbf{S}_d\boldsymbol{\varepsilon}_P + \boldsymbol{\varepsilon}_P\mathbf{S}_d)
\end{aligned} \tag{13}$$

and corresponding scalar coefficients depending on the listed invariants in the following manner:

$$\begin{aligned}
\Gamma_1 &= a_1 + a_2 s_1 + a_3 s_2 + a_4 \mu_1 + a_5 \mu_3, \\
\Gamma_2 &= -\frac{3}{2}(a_2 + a_4 \mu_1) - 2 a_5 \mu_1, \\
\Gamma_3 &= \frac{1}{2} a_4 (s_1 s_2 - s_3) - \frac{2}{3} a_5 s_3, \\
\Gamma_4 &= a_5 s_2.
\end{aligned} \tag{14}$$

The coefficient Λ has the form (8) given above.

Calibration of the MAM-model was done in [4] for a AISI 316H stainless steel. The material constants of this model were found to be: $\mathscr{A} = \{a_1, a_2, a_3, a_4, a_5\} = \{0.925,\ -0.065,\ -0.039,\ 0.017,\ -0.134\}$ with $\lambda = 0.554$ and correlation constant $\eta = 0.985$.

Two special cases of the loading function leading to reduced forms of the evolution equation (12) have remarkable simplicity.

- If $a_4 = 0$ and $a_5 = 0$, then the plastic stretching is of third–order power of stress. The loading function becomes

$$2\Omega = a_1 s_2 + a_2 (s_1 s_2 - s_3) + \frac{1}{2} a_3 s_2^2. \tag{15}$$

- For the second–order stress–dependent plastic stretching the loading function is specified with only two material constants

$$2\Omega = a_1 s_2 + a_2 (s_1 s_2 - s_3). \tag{16}$$

2.3. Transversely isotropic materials

When the material body possesses a single preferred anisotropy direction, say $\vec{N}$, then the arguments of the evolution equation (7) have to be extended to include the diadic $\mathbf{N} \equiv \vec{N} \otimes \vec{N}$. If $\vec{N}$ is unit vector then $\vec{N} \cdot \vec{N} = tr\mathbf{N} = 1$. Therefore,

$$\begin{aligned}
\mathbf{D}_{\mathrm{P}} &= \Lambda \, \partial_{\mathbf{S}} \Omega \left(\mathbf{S}, \boldsymbol{\varepsilon}_{\mathbf{p}}, \mathbf{N} \right), \\
\Omega &= \Omega \left(\mathbf{S}, \boldsymbol{\varepsilon}_{\mathbf{p}}, \mathbf{N} \right)
\end{aligned} \tag{17}$$

Accordingly the set of invariants to be used as the source of tensor generators reads:

$$\begin{aligned}
& s_1 = tr\mathbf{S}, \quad s_2 = tr\mathbf{S}_d^2, \quad s_3 = tr\mathbf{S}_d^3, \\
& \pi_1 = \mathrm{tr}\boldsymbol{\varepsilon}_{\mathbf{p}} = 0, \quad \pi_2 = \mathrm{tr}\boldsymbol{\varepsilon}_{\mathbf{p}}{}^2, \quad \pi_3 = \mathrm{tr}\boldsymbol{\varepsilon}_P^3, \quad \pi_4 = \mathrm{tr}\mathbf{N}\boldsymbol{\varepsilon}_{\mathbf{p}}, \quad \pi_5 = \mathrm{tr}\mathbf{N}\boldsymbol{\varepsilon}_{\mathbf{p}}{}^2, \\
& \mu_1 = tr\mathbf{S}_d\boldsymbol{\varepsilon}_{\mathbf{p}}, \quad \mu_2 = tr\mathbf{S}_d^2\boldsymbol{\varepsilon}_{\mathbf{p}}, \quad \mu_3 = tr\mathbf{S}_d\boldsymbol{\varepsilon}_{\mathbf{p}}{}^2, \quad \mu_4 = tr\mathbf{S}_d^2\boldsymbol{\varepsilon}_{\mathbf{p}}{}^2, \\
& \varkappa_1 = tr\mathbf{N}\mathbf{S}_d, \quad \varkappa_2 = tr\mathbf{N}\mathbf{S}_d^2, \\
& \lambda_1 = tr\mathbf{N}\mathbf{S}_d\boldsymbol{\varepsilon}_{\mathbf{p}}, \lambda_2 = tr\mathbf{N}\mathbf{S}_d^2\boldsymbol{\varepsilon}_{\mathbf{p}}, \lambda_3 = tr\mathbf{N}\mathbf{S}_d\boldsymbol{\varepsilon}_{\mathbf{p}}{}^2, \ \lambda_4 = tr\mathbf{N}\mathbf{S}_d^2\boldsymbol{\varepsilon}_{\mathbf{p}}{}^2
\end{aligned}$$

Suppose now that Ω is a polynominal of third order in $\mathbf{S}$ and linear in $\boldsymbol{\varepsilon}$. Then the loading function has the following form:

$$
\begin{aligned}
2\Omega = {} & a_0 s_1^2 + a_1 s_2 + a_2 s_3 + a_3 s_1 s_2 + a_4 s_1^3 + a_5 s_1 \mu_1 + \\
& a_6 s_1 \mu_2 + a_7 s_2 \mu_1 + a_8 \mu_2 + \\
& b_1 \varkappa_1^2 + b_2 \varkappa_2 + b_3 \varkappa_1^3 + b_4 \varkappa_1 \varkappa_2 + b_5 \varkappa_1 s_1 + \\
& b_6 \varkappa_1 s_2 + b_7 \varkappa_2 s_1 + b_8 \mu_1 \varkappa_1 + b_9 \varkappa_1 \mu_2 + \\
& b_{10} \varkappa_1 s_1 \mu_1 + b_{11} \varkappa_2 s_1 + b_{12} \varkappa_2 \mu_1 + \\
& c_1 \lambda_1 s_1 + c_2 \lambda_1 s_1^2 + c_3 \lambda_1 s_1 + c_4 \lambda_1 \varkappa_1 + c_5 \lambda_1 \varkappa_1^2 + \\
& c_6 \lambda_1 \varkappa_2 + c_7 \lambda_2 \varkappa_1 .
\end{aligned} \tag{18}
$$

For convenience, we introduce notations:

$$
\begin{array}{llll}
\bar{a}_1 \equiv a_1, & \bar{a}_2 \equiv a_2, & \bar{a}_3 \equiv a_5, & \bar{a}_4 \equiv a_7, \\
\bar{b}_1 \equiv b_1, & \bar{b}_2 \equiv b_2 & \bar{b}_3 \equiv b_6, & \\
\bar{b}_4 \equiv b_8, & \bar{b}_5 \equiv b_9, & \bar{b}_6 \equiv b_7, & \\
\bar{c}_1 \equiv c_1 & \bar{c}_2 \equiv c_2 & \bar{c}_3 \equiv c_5, &
\end{array}
$$

If damage is neglected, then $tr\mathbf{D}_{\mathrm{P}} = 0$ holds. On the other hand, the plastic stretching vanishes when stress is absent i.e. $\mathbf{D}_{\mathrm{P}/\mathbf{S}=0}$. With these two restrictions number of relevant material constants is much smaller so that is reduced into

$$
\begin{aligned}
2\Omega = {} & \bar{a}_1 s_2 + \bar{a}_2 (s_3 - s_1 s_2) + \bar{a}_3 \left(s_1 \mu_1 - \frac{3}{2} \mu_2 \right) + \bar{a}_4 \mu_1 s_2 + \\
& \bar{b}_1 \left(\frac{1}{9} s_1^2 + \varkappa_1^2 - \frac{2}{3} s_1 \varkappa_1 \right) + \bar{b}_2 \left(\frac{1}{9} s_1^2 + \varkappa_2 - \frac{2}{3} s_1 \varkappa_1 \right) + \\
& \bar{b}_3 \left(-\frac{1}{3} s_1 s_2 + \varkappa_1 s_2 \right) + \bar{b}_4 \left(\mu_1 \varkappa_1 - \frac{1}{2} \mu_2 \right) + \\
& \bar{b}_5 \left(-\frac{1}{3} s_1 \mu_2 + \varkappa_1 \mu_2 + \varkappa_1 s_1 \mu_1 - \mu_1 \varkappa_2 \right) + \\
& \bar{c}_1 (s_1 \lambda_1 - 3\lambda_1 \varkappa_1 + \pi_4 s_1 \varkappa_1) + \\
& \bar{c}_2 \left(\lambda_1 s_1^2 - 3 s_1 \lambda_2 - 9 \lambda_1 \varkappa_2 + 9 \varkappa_1 \lambda_2 - \frac{1}{9} \pi_4 s_1^3 - 6 \pi_4 \varkappa_1^3 + 6 \pi_4 \varkappa_1 \varkappa_2 \right) + \\
& \bar{c}_3 \left(\lambda_1 \varkappa_1^2 - \lambda_1 \varkappa_2 - \pi_4 \varkappa_1^3 + \pi_4 \varkappa_1 \varkappa_2 \right) .
\end{aligned} \tag{19}
$$

Special case of negligible plastic strain $\mu_1 \approx 0, \quad \mu_2 \approx 0, \lambda_1 \approx 0, \quad \lambda_2 \approx 0, \pi_4 \approx 0.$

$$
\begin{aligned}
2\Omega \approx {} & \bar{a}_1 s_2 + \bar{a}_2 (s_3 - s_1 s_2) + \bar{b}_1 \left(\frac{1}{9} s_1^2 + \varkappa_1^2 - \frac{2}{3} s_1 \varkappa_1 \right) + \\
& \bar{b}_2 \left(\frac{1}{9} s_1^2 + \varkappa_2 - \frac{2}{3} s_1 \varkappa_1 \right) + \bar{b}_3 \left(-\frac{1}{3} s_1 s_2 + \varkappa_1 s_2 \right)
\end{aligned} \tag{20}
$$

For further analysis only the simplest evolution equation following from the above reduced loading function is shown:

$$\mathbf{D}_{\mathrm{P}} = \bar{a}_1\mathbf{S}_d + \bar{a}_2\left(\frac{3}{2}\mathbf{S}_d^2 - s_1\mathbf{S}_d - s_2 1\right) +$$
$$\bar{b}_1\left(\frac{1}{9}s_1 1 + \varkappa_1\mathbf{N} - \frac{1}{3}s_1\mathbf{N} - \frac{1}{3}\varkappa_1\mathbf{1}\right) +$$
$$\bar{b}_2\left(\frac{1}{9}s_1 1 + \frac{1}{2}\mathbf{N}\mathbf{S}_d + \frac{1}{2}\mathbf{S}_d\mathbf{N} - \frac{1}{3}s_1\mathbf{N} - \frac{1}{3}\varkappa_1\mathbf{1}\right) + \tag{21}$$
$$\bar{b}_3\left(-\frac{1}{3}s_1\mathbf{S}_d - \frac{1}{6}s_2 1 + \frac{1}{2}s_2\mathbf{N} + \varkappa_1\mathbf{S}_d\right)$$

2.4. Classical theory of transversely isotropic materials

In classical theory of plasticity of transversely isotropic materials the evolution equation is based on the equivalent stress:

$$\sigma_{eq}^2 = \frac{3}{2}\left(s_2 + \frac{1}{2}\bar{R}\varkappa_1^2\right)$$

and the corresponding yield function

$$f = \frac{1}{3}\frac{\sigma_{eq}^2}{h(\varepsilon_{Peq})} = 1$$

Then

$$\mathbf{D}_P = \partial_{\mathbf{S}} f = \frac{1}{2h(\varepsilon_{peq})}\partial_{\mathbf{S}}\sigma_{eq}^2 = \frac{1}{2h(\varepsilon_{peq})}\left(\mathbf{S}_d + \bar{R}\varkappa_1\mathbf{N}\right). \tag{22}$$

Comparing these expressions with the simplest loading function in MAM theory we see that anisotropy coefficient $\bar{R}$ is proportional to $\bar{b}_1$. However this classical theory does not contain either coefficients $\bar{b}_2$ and $\bar{b}_3$ or new invariant expressions present in (21). Indeed analyzing data in [12] we conclude that evolution (22) is not able to cover deformation behavior of car body sheet.

2.5. Some loading histories

In order to illustrate significance of coefficients in (21), let us consider some special cases of loading calculating plastic stretching from the simplest evolution equation:

(a) longitudinal uniaxial tension:

$$\mathbf{S} = \sigma\begin{Bmatrix} 1 & 0 & 0 \\ 0 & 0 & 0 \\ 0 & 0 & 0 \end{Bmatrix} \Longrightarrow$$

$$\mathbf{D}_P = \left(\frac{a_1}{3}\sigma - \frac{a_2}{6}\sigma^2 + \frac{b_1+b_2}{9}\sigma + \frac{2b_3}{6}\sigma^2\right) = \begin{Bmatrix} 2 & 0 & 0 \\ & -1 & 0 \\ & & -1 \end{Bmatrix}.$$

$$\varkappa = \frac{D_{P22}}{D_{P11}} = -\frac{1}{2}$$

(b) transverse uniaxial tension

$$\mathbf{S}=\sigma\left\{\begin{array}{ccc}0&0&0\\0&1&0\\0&0&0\end{array}\right\}\Longrightarrow D_{P\alpha\beta}=0,\alpha\neq\beta,$$

$$D_{P11}=-\frac{a_1}{3}\sigma+\frac{a_2}{6}\sigma^2-\frac{4(b_1+b_2)}{9}\sigma+\frac{4b_3}{6}\sigma^2$$

$$D_{P22}=\frac{2a_1}{3}\sigma-\frac{a_2}{3}\sigma^2+\frac{2(b_1+b_2)}{9}\sigma-\frac{5b_3}{9}\sigma^2$$

$$D_{P33}=-\frac{a_1}{3}\sigma+\frac{a_2}{6}\sigma^2+\frac{2(b_1+b_2)}{9}\sigma+\frac{b_3}{9}\sigma^2$$

$$\varkappa=6\frac{2(b_1+b_2)-b_3\sigma}{6a_1-3a_2\sigma^2+8(b_1+b_2)-8b_3\sigma}$$

(c) longitudinal-transverse shear

$$\mathbf{S}=\tau\left\{\begin{array}{ccc}0&1&0\\1&0&0\\0&0&0\end{array}\right\}\Longrightarrow$$

$$\mathbf{D}_P=\left\{\begin{array}{ccc}a_2\tau^2/2+2b_3\tau^2/3 & a_1\tau+b_2\tau/2 & 0\\ & a_2\tau^2/2-2b_3\tau^2/3 & 0\\ Sym & & -a_2\tau^2-b_3\tau^2\end{array}\right\}$$

$$\varkappa=1-\frac{6b_3}{3a_2+4b_3}$$

(d) transverse shear

$$\mathbf{S}=\tau\left\{\begin{array}{ccc}0&0&0\\0&0&1\\0&1&0\end{array}\right\}\Longrightarrow\mathbf{D}_P=\left\{\begin{array}{ccc}-2\delta&0&0\\&\delta&0\\Sym&&a_1\tau/\delta\end{array}\right\}$$

where

$$\delta\equiv\frac{1}{2}a_2\tau^2-\frac{1}{3}b_3\tau^2$$

$$\varkappa=-\frac{1}{2}$$

3. Some concluding remarks

In the above loading cases to the direction of plastic strain a special attention is given. Meaning of coefficients b_2 and b_3 will be analyzed especially with relation to plastic strain induced anisotropy and transition form isotropy to transverse isotropy by previous loading. However, an immediate conclusion could be made now. Namely the coefficient b_3 is indispensable either for longitudinal-transverse shear or for the case of pure transverse shear.

Acknowledgement. This paper is made within the research project 174004 funded by the Serbian Ministry of Science.

References

[1] Hill R (1952) On Discontinuous Plastic States with Special Reference to Localized Necking in Thin Sheets, *Journal of Mechanics and Physics of Solids*, **1** , pp. 19-30.

[2] Hill R, Extremal Paths of Plastic Work and Deformation (1986) *Journal of Mechanics and Physics of Solids*, **34/5** , pp. 511-523.

[3] Mićunović M (2005) Self-consistent method applied to quasi-rate independent polycrystals, *Philosophical Magazine*, **85 (33-35)**, pp. 4031–4054

[4] Mićunović M (2009) *Thermomechanics of Viscoplasticity: Fundamentals and Applications* Springer, 2009.

[5] Cadoni E (2010) Dynamic characterization of orthogneiss rock subjected to intermediate and high strain rates in tension *Rock Mechanics and Rock Engineering*, **43-6**, pp. 667-67

[6] Kröner E (1960) Allgemeine Kontinuumstheorie der Versetzungen und Eigenspannungen *Arch. Rational Mech. Anal.*, **4**, pp. 273–334.

[7] Stojanović R (1962) On the reference-state problem in the non-linear elasticity theory of continua with dislocations *Physica Status Solidi,* **2**, pp. 566–575.

[8] Mićunović M, Albertini C, Montagnani M, High strain rate viscoplasticity of AISI 316 stainless steel from tension and shear experiments (1997) In: Miljanic, P. (ed) *Solid Mechanics*, *Serbian Acad. Sci. Meetings - LXXXVII*, *Dept. Techn. Sci.*, **3**, pp. 97–106.

[9] Rice J R (1971) Inelastic constitutive relations for solids: an internal variable theory and its application to metal plasticity, *J. Mech. Phys. Solids*, **19**, pp. 433–455.

[10] Vakulenko A A (1970) Superposition in continuum rheology (in Russian), *Izv. AN SSSR Mekhanika Tverdogo Tela*, **1**, 69–74

[11] Fomin V L (1975) *Continuum Mechanics for Engineers* (in Russian), St. Peterburg University Publ., St. Peterburg

[12] Aleksandrović S (1993): *F*ormability of thin sheets for non-monotonous plastic deformation processes, MSc-thesis, Fac.Mech.Engng., Kragujevac.

[13] Marciniak Z, Kuczynsky K (1967) Limit strains in the processes of stretch-forming sheet metal, *International Journal of Mechanical Sciences*, **9**, pp. 609–620

[14] Perzyna P (1971) Fundamental Problems in Viscoplasticity, *Advances in Applied Mechanics* **11**, pp. 313-387.

[15] Chaboche J L and Rousselier G (1983) On the plastic and viscoplastic constitutive equations, *Trans. ASME, PVT*, **105** pp. 153-164.

[16] Rabotnov Yu N (1980) *Elements of Hereditary Solids Mechanics*, Mir Publishers, Moscow

[17] Mićunović M (1992) Normality rule from plastic work extremals?, In: Anthony K.-H. & Wagner H.-J. (eds) *Continuum Models and Discrete Systems CMDS-7*, *Material Science Forum*, **123-125**, pp. 609–616, Trans Tech Publ, Aedermannsdorf

[18] Gambin W, Kowalczyk-Gajewska K, Kudrjavceva L, Mićunović M (2008) Two-scale approach to dynamic localization failure of AISI 316H stainless steel sheets *Theoretical and Applied Mechanics*, **35/1-3**, pp. 93-103

FUZZY OPTIMIZATION OF CANTILEVER BEAM

Z. Mitrović[1], S. Rusov[2], N. Nladenović[3], A. Obradović[4]

[1,3,4] Faculty of Mechanical Engineering,
The University of Belgrade, Kraljice Marije 16, 11120 Belgrade 35
e-mail:zmitrovic@mas.bg.ac.rs, nmladenovic@mas.bg.ac.rs, aobradovic@mas.bg.ac.rs
[2] Faculty of Transport and Traffic Engineering,
The University of Belgrade, Vojvode Stepe 305, 11000 Belgrade
e-mail: s.rusov@sf.bg.ac.rs

Abstract. It happens very often that we want to design a cantilever beam, while all project requirements are not fully known. Namely, we know roughly what the structure should realize. In classical optimization standard procedure should be applied in order to satisfy all the pre-requirements. What happens if the requirements can only be described, but not explicitly set? This paper starts from the premise that some requirements are expressed linguistically. We want that the length and the largest deflection of a cantilever beam are suitable to satisfy the predetermined conditions. Also, the goals are that the bending stress and the largest deflection have to be less than the allowable maximum value. The objective of this paper is: on known constraints and known fuzzy goal functions we must execute fuzzy projecting of a beam. Constraints are: the length of cantilever beam and its deflection, while the goal functions are maximum bending stress and maximum deflection. On this basis, with known cross-sectional dimensions, we can determine the maximum cantilever beam load.

1. Introduction

Optimization in any field of science, in any problem, provides a solution that satisfies the criteria prescribed in advance. Optimization problems are very often present in design of machines and their elements, optimal control, in finding the optimal trajectory of the system... In defining the optimal criteria there is a situation that some parameters of the system get advantage over the other parameters. A particular problem is the multi criteria optimization. In such cases we are never sure whether that we choose the right criteria, and in particular, whether the criteria are defined in an appropriate manner. What happens in cases where the criterion of optimality does not have clear boundaries? Today, there are available several procedures being able to successfully do mentioned job for us.
In case of the optimization problems with an analytical solution without special restrictions, existing methods provide an exact optimal solution. When the mentioned situation occurs in problems with analytical solution, usually expressed like derivatives of functions, the final solution may depend on the numerical skills. However, in those cases, the well-known classical methods of optimization are present.
Unconventional methods of optimization, in the cases without precisely defined constraints and optimality criteria, began its development about 20 years ago. More of these methods

are presented in [1]. A separate analysis of the process of optimization in engineering problems, using fuzzy logic is given in [2]. However, available methods have their disadvantages. The aim of this paper is to improve existing methods for optimization of fuzzy systems, so that the results are more realistic.

2. Theoretical postulation

Consider a function $y = f(x)$. It is necessary to determine the optimal solution x^*, for which the function $y = f(x)$ has a maximum value, whereas we need to be satisfied *n* constraints [2], for example

$$f_i(x) \le 0, \qquad i = 1,2,...,n \tag{1}$$

All constraints can be represented by a set A

$$A = A_1 \cap A_2 \cap ... \cap A_n = \{x \mid f_i(x) \le 0, \forall i = 1,2,...,n\}, \tag{2}$$

where is $A_i = \{x \mid f_i(x) \le 0\}$. That way we get to the optimal solution x^* defined as follows

$$f(x^*) = \max_{x \in A} \{f(x)\}. \tag{3}$$

In case of conflicting constraints and nonentity of analytical solutions, pre-defined problem can be expressed in a different way, using elements of fuzzy logic. Then, constraints presented with a set A, can be represented in an appropriate way, i.e. new set A, which is adopted in fuzzy set. This fuzzy set is the best way to set limits. It is now necessary to write the function $y = f(x)$ in the form of fuzzy. This can be done as follows [3], using the membership functions

$$\mu_B(x) = \frac{f(x) - m}{M - m}, \tag{4}$$

where are: $m = \inf_{x \in X} f(x)$ and $M = \sup_{x \in X} f(x)$. A set *X* denotes an area in which we look for the optimal solution, and a fuzzy set *B* is an appropriate goal function. Relation (4) is suitable for determining the maximum values, but in case you need to minimize a function, does not give proper results, and the membership functions of the goal function should be represented in the form of

$$\mu_B(x) = 1 - \frac{f(x) - m}{M - m}. \tag{5}$$

Obviously, the fuzzy solution obtained as $C = A \cap B$, i.e.

$$\mu_C(x) = \min\{\mu_A(x), \mu_B(x)\}, \tag{6}$$

and the optimal value x^* determined by the relation

$$\mu_C(x^*) \geq \mu_C(x), \qquad \forall x \in X\ . \tag{7}$$

If the goal functions and constraints are in conflict, fuzzy decision is taken in the form of [2]

$$\mu_C(x) = \alpha\mu_A(x) + (1-\alpha)\mu_B(x), \qquad \alpha \in [0,1]. \tag{8}$$

Applying the previous expression, in practice, does not yield to satisfactory solutions.

3. Problem of multicriteria optimization

Suppose the constraints given by fuzzy sets $A_i, i = 1,2,...,n$, and the goal functions with fuzzy sets $B_j, j = 1,2,...,m$. The corresponding membership functions are $\mu_{A_i}(x)$ and $\mu_{B_j}(x)$. Suppose that all constraints and all goal functions have not the same significance for the determination of the optimal solution.
Based on the above analysis it follows that the membership function of constraints

$$\mu_A(x) = \frac{1}{M_1}\sum_{i=1}^{n}\alpha_i\mu_{A_i}(x), \tag{9}$$

with $M_1 = \sup_{x\in X}\sum_{i=1}^{n}\alpha_i\mu_{A_i}(x)$, while α_i represent the weight coefficients for certain constraints. The same can be determined and the membership functions of goal, i.e.

$$\mu_B(x) = \frac{1}{M_2}\sum_{j=1}^{m}\beta_i\mu_{B_j}(x), \tag{10}$$

where is $M_2 = \sup_{x\in X}\sum_{j=1}^{m}\beta_i\mu_{B_j}(x)$, and β_j are the weight coefficients for certain goals.
In this case, fuzzy solution is obtained using (6), and the optimal solution is determined by relation (7).

4. Example

Suppose that the cantilever beam (Fig. 1.) of length l and square cross section with $a = 4cm$ is loaded with force $\vec{F}$ on its end. The cantilever beam is made of material whose elastic modulus is $E = 2{,}1 \cdot 10^4 \frac{kN}{cm^2}$, and allowed bending stress $200MPa$.

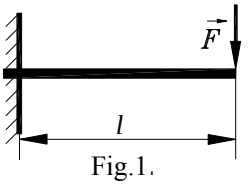

Fig.1.

It is well known, in this case, that the maximum value of bending stress and deflection can be determined by: $\sigma = \frac{Fl}{W_x}$ and $f = \frac{Fl^3}{3EI_x}$, where are $W_x = \frac{a^3}{6}$ and $I_x = \frac{a^4}{12}$.

Constraints are: $l \le 2m$ and $f \le 4mm$. Also, we ask that deflection at the end of cantilever beam of the length $1m$ is as close as possible to $0mm$. The goals are: to be sure the deflection does not exceed $4mm$, and that allowed bending stress does not exceed $200MPa$. All constraints and all goals are equally significant to us. On this basis, it is necessary to determine the intensity of force $\vec{F}$.

Using the given constraints, we can introduce them in the form of fuzzy sets

$$l = \begin{cases} d_1 & 0 \le d_1 \le 1 \\ 2 - d_1 & 1 \le d_1 \le 2 \end{cases}, \qquad f = \begin{cases} 4 - c_1 & 0 \le c_1 \le 4 \\ 0 & c_1 \ge 4 \end{cases}. \tag{11}$$

Previously shown functions express our demand that the length of a cantilever beam should be approximately $1m$, and the deflection is as small as possible and never exceeds $4mm$. Functions (11) remind us to the membership function expressions, which are interconnected [4-5]. Transformation of the previous function, for $x \in [0,1]$, we get

$$\mu_{A_1}(x = \frac{l}{2}) = \begin{cases} 2x & 0 \le x \le 0{,}5 \\ 2 - 2x & 0{,}5 \le x \le 1 \end{cases}, \qquad \mu_{A_2}(x = \frac{f}{4}) = \begin{cases} 1 - x & 0 \le x \le 1 \\ 0 & x \ge 4 \end{cases}. \tag{12}$$

Using (2) we obtain the membership function of constraints (Fig.2.)

$$\mu_A(x) = \begin{cases} 2x & 0 \le x \le \frac{1}{3} \\ 1 - x & \frac{1}{3} \le x \le 1 \end{cases}. \tag{13}$$

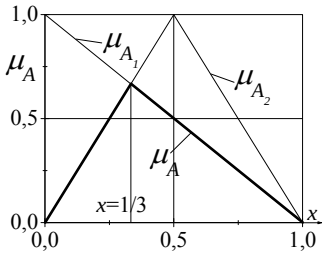

Fig.2.

As the goal functions of the linear functions of force $\vec{F}$, membership functions of goal functions can be expressed as

$$\mu_{B_1}(x=\frac{\sigma}{200})=x, \qquad \mu_{B_2}(x=\frac{f}{4})=x, \qquad x\in[0,1], \tag{14}$$

so $\mu_B(x)=x$. Then, based on (6) (Fig.3.)

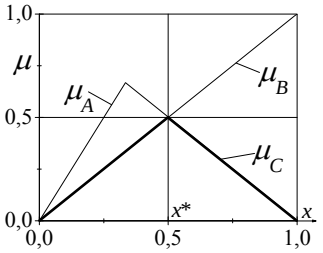

Fig.3.

$$\mu_C(x)=\begin{cases} x & 0\le x\le 0{,}5 \\ 1-x & 0{,}5\le x\le 1 \end{cases}, \tag{15}$$

whence, using (7), it follows that the optimal solution $x^*=0{,}5$. Therefore, obtained solutions are: $l=1m$, $f=2mm$, $\sigma=100MPa$, and the required intensity of the force is

$$F=\min\left\{\frac{W_x}{l}\sigma,\quad \frac{3EI_x}{l^3}f\right\}=\min\{1.07,\quad 0.27\}=0{,}27kN$$

Applying relation (9) and (10), we get

$$\mu_A^*(x)=\frac{1}{M_1}\mu_A(x)=\begin{cases} 3x & 0\le x\le \frac{1}{3} \\ \frac{3}{2}(1-x) & \frac{1}{3}\le x\le 1 \end{cases}, \quad \mu_B^*(x)=\frac{1}{M_2}\mu_B(x)=x, x\in[0,1], \tag{16}$$

as it is shown in Fig.4.

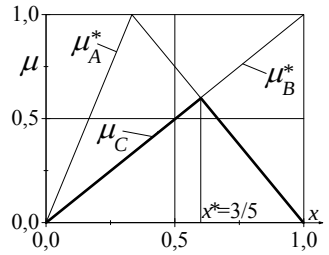

Fig.4.

Then $\frac{3}{2}\left(1-x^*\right)=x^*$, ie. $x^*=0{,}6$. Now the solutions are: $l=1{,}2m$, $f=2{,}4mm$, $\sigma=120MPa$, and the required intensity of the force is

$$F=\min\left\{\frac{W_x}{l}\sigma,\quad\frac{3EI_x}{l^3}f\right\}=\min\{1.28,\quad 0.32\}=0{,}32kN$$

5. Conclusion

This paper discusses the process of optimization using fuzzy sets. Theoretically, an optimization problem with the presence of more than one constraint and one goal function is considered. This procedure is generalized for the case of more constraints and more goal functions. It is especially considered the case when all the fuzzy constraints and fuzzy objective functions have the same practical significance. Improvement of existing methods, in order to obtain more realistic solutions, is done by a procedure of bringing the membership function to their maximum value. Theoretical studies of this optimization process are shown in the example of a cantilever beam.

Acknowledgement. This work was supported by the Republic of Serbia, Ministry of Science and Technological Development, through project No.TR35006

References

[1] Sakawa M (1993) Fuzzy sets and interactive multiobjective optimization, *Plenum Press*, New York.
[2] Ross T (2004) *Fuzzy logic with engineering applications*, Wiley&Sons.
[3] Zadeh L (1972) *On fuzzy algorithms*, Memo UCB/ERL M-325, University of California, Berkeley.
[4] Sridevi B and Nadarajan R (2009) Fuzzy similarity measure for generalized fuzzy numbers, *International Journal of Open Problems in Computer Science and Mathematics*, Vol. 2, No.2, pp. 240-253.
[5] Mitrović Z and Rusov S (2006) Z similarity measure among fuzzy sets, *FME transactions*, Vol. 34, No. 2, pp. 115-119.

STOCHASTIC MINIMAX DYNAMIC GAMES WITH INFORMATION CONSTRAINTS

Perišić M. Dragovan

Faculty of Transport and Traffic Engineering,
The University of Belgrade, Vojvode Stepe 305, Belgrade
e-mail: d.perisic@sf.bg.ac.rs

ABSTRACT. This paper analyzes zero-sum differential games for jump diffusion processes under incomplete state vector information. The problem is described by nonlinear stochastic equation with standard Wiener processes and compensated Poisson random measures. This problem is transformed by generalized Foker-Plank-Kolmogorov equation into deterministic dynamic game with distributed parameters. Necessary and sufficient conditions by which the solution of the game could be defined are presented. Finally, special cases of the problem with complete (full-feedback optimal control) and without information (open-loop optimal control), are observed in this paper.

Keywords: Zero-sum stochastic dynamic games, distributed parameters dynamic games, stochastic differential games with incomplete information, jump diffusion processes, functional Krotov's.

1. INTRODUCTION

The problem of stochastic differential games with zero-sum with two players under complete information vector state system considered in [1] in which conditions for existence and unity of viscose solution of respective Hamilton-Jacobi-Belman-Isaacs equations are given, a corresponding problem for stochastic dynamics games with jump diffusion processes considered in works [10], [11]. In the mentioned work summary of earlier works which mentioned this problem are given. One of the first works considering problems of stochastic differential games of N-persons with a complete vector of state information (without jump and control in diffusional member) is work [2]. In [5] authors consider simpler problem (similar to the problem previous work) for antagonistic games diffusion system with jump and incomplete state vector information.
The problem of stochastic differential games with control and with open loop is given in [7], Similar problem to be discussed here for differential stochastic games consider optimal control for system with random structure in [3], and for systems with fix structure in cited references in the above paper. The problem of antagonistic differential game with distributed parameters is considered in a similar way used here, is given in [4].
In the second part of this work presents stochastic differential equations which explain the dynamics of the differential games with price of the game in the form of general Bolcas problem. After responsive generalized equations Foker-Plank-Kolmogorov for density of distribution of probability vector of state system are given it is shown how the initial problem is transformed into antagonistic differential game with distributed parameters. In

the third part are defined requirements which have to be fulfilled in order to attain the solution for the differential games with partial information on the state of the system vector. The fourth part gives some conclusion remarks.

2. FORMULATION OF THE PROBLEM

Dynamic zero-sum two players stochastic differential games for jump diffusion processes is described by following nonlinear stochastic differential equations

$$\begin{aligned} &dx(s) = b(s,x(s),u(s),v(s))ds + \sigma(s,x(s),u(s),v(s))dB(s) + \\ &+ \int_{R^n} \gamma(x(s^-),u(s^-),v(s^-),z)\widetilde{N}(ds,dz) \\ &x(t_0) = x_0, \quad s \in T = [t_0,t_1], \end{aligned} \tag{1}$$

where the state vector x has n coordinates, and B is d – dimensional standard Brownian motion. Vectors γ and z have l-dimension and matrix σ is n×d –dimension, $\widetilde{N}(ds,dz) = ds\lambda(dz)$ - is compensated Poisson random measure Controls u and v take values from relevant compact metric spaces U and V. State vector x have four parts (x_1, x_2, x_3, x_4) dimension –minimum 0 and maximum n. Control u from first two parts and times, and v from x_2, x_3 and times, vector x_4 is unknown for two players. Cost functional where the first player intends to maximize and the second one to minimize is given in [4]

$$J = \int_{t_0}^{t_1} \int_{R^n} f_0(t, p(t,x), u(t,x_1,x_2), v(t,x_2,x_3))dxdt + \phi_0(p(t_1,x)), \tag{2}$$

where $p(t,x)$ – density probability of the state vector and satisfy the Fokker-Plank-Kolmogorov equations [12]

$$\partial_t p(t,x) = A_{uv}^S p(t,x) \tag{3}$$

where with A_{uv} marked operator defined of the equation (4), and with A_{uv}^S will be marked by the corresponding conjugate operator.

$$\begin{aligned} &A_{uv} = a^{ij}(t,x,u(t,x_1,x_2),v(t,x_2,x_3))\partial_i\partial_j p(t,x) + \\ &+ b^i(t,x,u(t,x_1,x_2),v(t,x_2,x_3))\partial_i p(t,x) + \\ &+ \int_R [p(x+\gamma^k(x,u,v,t,z),t) - p(x) - \nabla p(x,t)\cdot\gamma^k(x,u,v,t,z)]\lambda_k(dz_k) \end{aligned} \tag{4}$$

where $\partial_t, \partial_i, \partial_j$ - notational conventions for partial derivatives in time and relevant vector state components- respectively and by repeated indexes in equation (4) it is assumed to be addition. In the initial moment (t_0) normed density of probability $p_0(x)$, is known and for indefinite values of components of the state vector has in every moment of time $t \in (t_0,t_1)$ value for p equal 0. Matrix a *is* defined as a product of the relevant matrix in diffuse component and its transposed value.
Set of the admissible values for p and controls u and v we will mark with D ($d=(p,u,v)\in D$). The basic problem to be solved here is then

$$\sup_{u\in U}\inf_{v\in V} J(p_0(x),p(t,x),u(t,x_1,x_2),v(t,x_2,x_3)) = \sup_{u\in U}\inf_{v\in V} J(p_0(x),p(t,x),u(t,x_1,x_2),v(t,x_2,x_3))$$
$$= J(p_0(x),d^*) = J^*, \tag{5}$$

where with (*) are denoted those values which respond to the solution of the given game and other variables take values from admissible set of D.

3. EXTENSION PRINCIPLE AND STOCHASTIC DIFFERENTIAL GAMES WITH JUMP

Lets consider a set Z of continuously differentiable functionals $S(t,p(x))$: $T\times P\rightarrow \boldsymbol{R}$ which for each t from T have the continuous variation derivative continuous variation derivative $\delta S(t,p(x))/\delta p(x) = \delta_p S(t,p(x))$. Lets define set Z following functionals

$$R(t,p(x),u(t,x_1,x_2),v(t,x_2,x_3)) = \delta_t S(t,p(x)) + \\ + \int_{R^n} \delta_p S(t,p(x)) A_{uv} p(x) + f_0(t,p(x),u,v) \tag{6}$$

$$G(t_1,p(x)) = \phi_0(p(x)) - S(t_1,p(x)), \tag{7}$$

Now we can present functional R in the following shape

$$R(t,p(x),u(t,x_1,x_2),v(t,x_2,x_3)) = \delta_t S(t,p(x)) + \\ \int_{R^m}\{\int_{R^{n-m}}[p(x)A_{uv}^S \delta_p S(t,p(x)) + f_0(t,p(x),u,v)]dx_4\}dx_1dx_2dx_3, \tag{8}$$

or shorter

$$R(t,p(x),u(t,x_1,x_2),v(t,x_2,x_3)) = \delta_t S(t,p(x)) + H(t,p(x),u(t,x_1,x_2),v(t,x_2,x_3)), \tag{9}$$

where with H represents

$$H(t,p(x),u(t,x_1,x_2),v(t,x_2,x_3)) =$$
$$\int_{R^m}\{\int_{R^{n-m}}[p(x)A^S_{uv}\delta_p S(t,p(x)) + f_0(t,p(x),u,v)]dx_4\}dx_1dx_2dx_3.$$

(10)

In above expressions m denotes components of the state vector whose coordinates are known by the first or second player. For matrix component a with fixed value of t from set T we will assume that they have derivatives from second row by x for vector b,γ to have derivatives by x and matrix elements a and vector b,γ,λ and corresponding Jacobian transformation for conjugate operator in equation (3)are piecewise- continuous function in t for all x ($x\in\boldsymbol{R}^n$). These assumptions mean specified constrains and on a admissible controls u and v.

Now we can formulate theorem by which are determined necessary and sufficient conditions for existence of the solution for the given game and appropriate value function of the game.

Theorem 1. *If there exist an functional $S^*(t,p^*(x))\in Z$ and controls of both of players $u^*(t,x_1)$ and $v^*(t,x_1)$ such to fulfill the conditions*

1. $R(t,p^*,u^*,v^*) = 0,$

2. $\sup\limits_{u\in U}\inf\limits_{v\in V} H(t,p,u,v) = \inf\limits_{v\in V}\sup\limits_{u\in U} H(t,p,u,v),$

3. $G(t_1,p^*(x)) = 0,$

then there is a solution of antagonistic stochastic differential games with incomplete information of the state vector and respective cost of the game (5).

Proof. Lets consider the following functional (Krotov):

$$F(p_0(x),d) = \phi_0(p(t_1,x)) - S(t_1,p(t_1,x)) + S(t_0,p_0(x))$$
$$+\int_{t_0}^{t_1} R(t,p(t,x),u(t,x_1,x_2),v(t,x_2,x_3))dt,$$

(11)

using expression for functional R and expression for total time- derivative of functional S we get that

$$F(p_0(x),d) = \phi_0(p(t_1,x)) +$$
$$+\int_{t_0}^{t_1}\int_{R^n} f_0(t,p(t,x),u(t,x_1,x_2),v(t,x_2,x_3))dxdt = J(p_0(x),d)$$

(12)

Equation (12) can be applied for the solution of the game, so $S^*=J^*$ is the value of the criteria (3), which corresponds to the solution of the game. The functional S^* represents the value of criteria (2), for the solution of the game is the direct consequence of condition Isaacs′ 2. (which satisfied all values of admissible variables in expression for H) and 3. in theorem 1 [10]. It can be showed using Krotov method, that for fix values of controls u* or v* is not possible to get a smaller value or a bigger value of the criteria (2) from the value of functional S^*.
With proof of theorem 1. We will give the procedure how optimal values can be determined of control of both players u* and v*. Lets consider functional in expression for H:

$$q(t,u,v) = p^*(t,x)A^S_{uv}\delta_p S(t,p^*(t,x)) + f_0(t,p^*(t,x),u,v), \tag{13}$$

so optimal values now u* and v* have following shape:

$$u^*(t,x_1,x_2) = \arg\sup_{u\in U}\{\int_{R^{n-m1-m2}} q(t,x,u,v^*)dx_3dx_4\}, \tag{14}$$

and

$$v^*(t,x_2,x_3) = \arg\inf_{v\in V}\{\int_{R^{n-m2-m3}} q(t,x,u^*,v)dx_1dx_4\} \tag{15}$$

where *m1, m2, m3, m4* marked dimension four part vector *x*.

For the simpler problem without jump, when controls of both players participate only in vector *b* in equation (1), the solution is given in work [2] . This solution has a specific cases, solution for the problem with full information on the state and without information on the state. The problem here is not a deterministic problem with distributed parameters but an stochastic problem with concentrated parameters.
Similar solution is for the general problem (1), (2) with full information of the state of the system given in [10]. Here requirements that describe viscose solution of Hamilton-Jacobi-Bellman-Isaacs equations are given. The requirements which have to be fulfilled for existence of the solution of the stochastic differential game without information of the state vector given in [7] . Appropriate optimal values for u^* i v^* may be derived for formulas (14) and (15) where instead of integral on x_2 we have appropriate q when we have full information on the state and when we don't have information on the state- integration is done in whole space of the state (on x). In this case this controls can be determined over Krotovs functional and depends only on state vector.

4. CONCLUSION

Conditions defined in theorem 1 represent necessary and sufficient requirement for existence of solution of antagonistic stochastic differential game and its transformation in deterministic differential antagonistic game with distributed parameters. Required conditions may be defined in the form of maximum principle for antagonistic game with distributed parameters. The problem of stochastic differential games with insufficient

information on the state of the system is solved here in accordance with closed loop with known coordinates of the state. When we have full information of the state of the system we have full closed loop and we don't have the information on the state of the system then we have a problem with open loop.
More general problem with incomplete state information (without jumps) is considered in [6].

References

[1] Rainer Buckdahn and Juan Li, Stochastic differential Games and Viscosity Solutions of
Hamilton-Jacobi-Bellman-Isaacs Equations, *SIAM Journal on Control and Optimization*, Vol. 47, No 1. (2008), 444-475.
[2] A. Friedman, Stochastic Differential Equations and Applications Vol. 2*, Academic Press,*
New Jork (1976).
[3] K. A. Rybakov and I. L. Sotskova, An Optimal Control for Random-Structure Nonlinear
Systems under Incomplete State Vector Information*, Automation and Remote Control, Vol. 67, No. 7*, (2006), 62-75.
[4] D. Perišić, Stochastic differential game under incomplete state vector information*, Second*
International Congress of Serbian Society of Mechanics, Palić, Serbia, 1-5 june 2009.
[5] M. Friedman and Y. Yavin, Optimal control of partially observable jump diffusion processes, *International Journal of Systems Science,* Vol. 11, No. 3, 1980, 323-335.
[6] M. M. Khrustalev, Nash Equilibrium Conditions in Stochastic Differential Games where
the Pleyers Information about a State is Incomplete. I. Sufficient Equilibrium Conditions
and II. Lagrange Method, *Journal of Computer and Systems Sciences International*, I.
Vol. 34, No. 6,(1995), 821-830 and II. Vol. 35, No. 1, (1996), 67-73.
[7] T. T. K. An, B. Oksendal, Maximum Principle for Stochastic Differential Games with Partial Information, *Journal of Optimization Theory and Applications*,
Vol. 139, No. 3,
(2008), 463-483.
[8] A. Bensoussan and J.-L. Lions, Impulse control and quasivariational inequalities, Gauthier-Villars Montrouge, 1984.
[9] Imran H. Biswas, Espen R. Jakobsen and Kenneth H. Karlsen, Viscosity Solutions for a
System of Integro-PDES and Conections to Optimal Switching and Control of Jump-Diffusion Processes, University of Oslo, Pure Mathematics, No. 9, (2008), 1-27.
[10] R. Buckdahn, Y. Hu and J. Li, Integral-Partial Differential Equations of Isaacs` Type Related to Stochastic Differential Games with Jumps, arXiv:1004.2752v1[math.OC] 2010.
[11] I. H. Biswas, On Zero-sum Stochastics Differential Games with Jump-Diffusion Driven

State: A Viscosity Solution Framework, arXiv:1009.4949v1[math.OC] 2010.
[12] F. B. Hanson, Applied Stochastic Processes and Control for Jump-Diffusions: Modeling
Analysis and Computation, Chicago, Illinois, USA, 2007.

STOCHASTIC OPTIMAL CONTROL WITH JUMPS AND INFORMATION CONSTRAINTS

Perišić M. Dragovan

Faculty of Transport and Traffic Engineering,
The University of Belgrade, Vojvode Stepe 305, Belgrade
e-mail: d.perisic@sf.bg.ac.rs

ABSTRACT. This paper analyzes stochastic optimal control for jump diffusion processes under incomplete state vector information. The problem is described by nonlinear stochastic equation with standard Wiener processes and compensated Poisson random measures. This problem is transformed by generalized Foker-Plank-Kolmogorov equation into deterministic optimal control with distributed parameters. Necessary and sufficient conditions by which the solution of the optimal control are presented. Finally, special cases of the problem with complete (full-feedback optimal control) and without information (open-loop optimal control), are observed in this paper.

Keywords: Stochastic optimal control, distributed parameters optimal control, stochastic optimal control with incomplete information, jump diffusion processes, functional Krotov's.

1. INTRODUCTION

The problem of stochastic optimal control with jump diffusion processes under complete information vector state system considered in [1] in which conditions for existence and unity of viscose solution of respective Hamilton-Jacobi-Belman-Isaacs equations are given. Stochastic optimal control with jump diffusion processes also considered in [8]. In the mentioned work summary of earlier works which mentioned this problem are given. One of the first works considering problems of stochastic optimal control with incomplete vector of state information (without jump and control in diffusional member) is work [2]. In [5] authors consider simpler problem (similar to the problem previous work) for optimal control diffusion system with jump and incomplete state vector information.
The problem of stochastic optimal control with open loop is given in [7]. Similar problem to be discussed here is related to optimal control for system with random structure in [3], and for systems with fix structure in cited references in the above paper. The problem of antagonistic differential game with distributed parameters is considered in a similar way used here, is given in [4].
In the second part of this work presents stochastic differential equations which explain the dynamics of the control system with price in the form of general Bolcas problem. After responsive generalized equations Foker-Plank-Kolmogorov for density of distribution of probability vector of state system are given it is shown how the initial problem is transformed into optimal control with distributed parameters. In the third part are defined

sufficient conditions for optimal control with partial information on the state of the system vector. The fourth part gives some conclusion remarks.

2. FORMULATION OF THE PROBLEM

Dynamic for jump diffusion processes is described by following nonlinear stochastic differential equations

$$dx(s) = b(s, x(s), u(s))ds + \sigma(s, x(s), u(s))dB(s) + \\ + \int_{R^n} \gamma(x(s^-), u(s^-), z)\tilde{N}(ds, dz)$$

$$x(t_0) = x_0, \quad s \in T = [t_0, t_1], \tag{1}$$

where the state vector x has n coordinates, and B is d – dimensional standard Brownian motion. Vectors γ and z have l-dimension and matrix σ is n×d –dimension, $\tilde{N}(ds, dz) = ds\lambda(dz)$ - is compensated Poisson random measure Controls u take values from relevant compact metric spaces U. State vector x have two parts (x_1, x_2) dimension –minimum 0 and maximum n. Control u depend from first part state vector (x_1-known state) and times, and x_2 - is unknown coordinate. Cost functional where to maximize is given in [4]

$$J = \int_{t_0}^{t_1} \int_{R^n} f_0(t, p(t,x), u(t,x_1))dxdt + \phi_0(p(t_1, x)), \tag{2}$$

where $p(t,x)$ – density probability of the state vector and satisfy the Fokker-Plank-Kolmogorov equations [9]

$$\partial_t p(t,x) = A_u^S p(t,x) \tag{3}$$

where with A_u marked operator defined of the equation (4), and with A_u^S will be marked by the corresponding conjugate operator.

$$A_u = a^{ij}(t,x,u(t,x_1))\partial_i \partial_j p(t,x) + \\ + b^i(t,x,u(t,x_1))\partial_i p(t,x) + \\ + \int_R [p(x + \gamma^k(x,u,t,z),t) - p(x) - \nabla p(x,t)\cdot\gamma^k(x,u,t,z)]\lambda_k(dz_k) \tag{4}$$

where $\partial_t, \partial_i, \partial_j$ - notational conventions for partial derivatives in time and relevant vector state components- respectively and by repeated indexes in equation (4) it is assumed to be

addition. In the initial moment (t_0) normed density of probability $p_0(x)$, is known and for indefinite values of components of the state vector has in every moment of time $t \in (t_0,t_1)$ value for p equal 0. Matrix a *is* defined as a product of the relevant matrix in diffuse component and its transposed value.
Set of the admissible values for p and controls u and v we will mark with D ($d=(p,u,)\in D$).
The basic problem to be solved here is then

$$\sup_{d\in D} J(p_0(x), p(t,x), u(t,x_1)) == J(p_0(x), d^*) = J^*, \tag{5}$$

where with (*) are denoted those values cptimal control solution of the problem.

3. EXTENSION PRINCIPLE AND STOCHASTIC OPTIMAL CONTROL WITH JUMP

Lets consider a set Z of continuously differentiable functionals $S(t,p(x))$: $T\times P\rightarrow \mathbf{R}$ which for each t from T have the continuous variation derivative $\delta S(t,p(x))/\delta p(x) = \delta_p S(t,p(x))$. Lets define set Z following functionals

$$\begin{aligned} &R(t,p(x),u(t,x_1)) = \delta_t S(t,p(x)) + \\ &+ \int_{R^n} \delta_p S(t,p(x)) A_u p(x) + f_0(t,p(x),u) \end{aligned} \tag{6}$$

$$G(t_1,p(x)) = \phi_0(p(x)) - S(t_1,p(x)), \tag{7}$$

Now we can present functional R in the following shape

$$\begin{aligned} &R(t,p(x),u(t,x_1)) = \delta_t S(t,p(x)) + \\ &\int_{R^m} \{ \int_{R^{n-m}} [p(x) A_u^S \delta_p S(t,p(x)) + f_0(t,p(x),u)] dx_2 \} dx_1, \end{aligned} \tag{8}$$

or shorter

$$R(t,p(x),u(t,x_1)) = \delta_t S(t,p(x)) + H(t,p(x),u(t,x_1)), \tag{9}$$

where with H represents

$$\begin{aligned} &H(t,p(x),u(t,x_1)) = \\ &\int_{R^m} \{ \int_{R^{n-m}} [p(x) A_u^S \delta_p S(t,p(x)) + f_0(t,p(x),u)] dx_2 \} dx_1. \end{aligned} \tag{10}$$

In above expressions m denotes components of the state vector whose coordinates are known. For matrix component a with fixed value of t from set T we will assume that they have derivatives from second row by x for vector b,γ to have derivatives by x and matrix

elements a and vector b,γ,λ and corresponding Jacobian transformation for conjugate operator in equation (3)are piecewise- continuous function in t for all x ($x \in \boldsymbol{R}^n$). These assumptions mean specified constrains and on a admissible controls u .
Now we can formulate theorem by which are determined necessary and sufficient conditions for existence of the solution for optimal control.

Theorem 1. *If there exist an functional $S^*(t,p^*(x)) \in Z$ and controls $u^*(t,x_1)$ such to fulfill the conditions*

1. $R(t, p^*, u^*) = 0,$

2. $G(t_1, p^*(x)) = 0,$

then there is a solution of stochastic optimal control with incomplete information of the state vector condition (5) holds.

Proof. Lets consider the following functional (Krotov):

$$F(p_0(x), d) = \phi_0(p(t_1, x)) - S(t_1, p(t_1, x)) + S(t_0, p_0(x)) + \int_{t_0}^{t_1} R(t, p(t,x), u(t, x_1))dt, \tag{11}$$

using expression for functional R and expression for total time- derivative of functional S we get that

$$F(p_0(x), d) = \phi_0(p(t_1, x)) + + \int_{t_0}^{t_1}\int_{R^n} f_0(t, p(t,x), u(t, x_1))dxdt = J(p_0(x), d) \tag{12}$$

Equation (12) can be applied for the solution optimal control, so $S^*=J^*$ is the value of the criteria (2), which corresponds to the solution of the optimal control. It can be showed using Krotov method, that for fix values of controls u* is not possible to get a bigger value of the criteria (2) from the value of functional S^*.
With proof of theorem 1. We will give the procedure how optimal values can be determined of control u* . Lets consider functional in expression for H:

$$q(t,u) = p^*(t,x) A_u^S \delta_p S(t, p^*(t,x)) + f_0(t, p^*(t,x), u), \tag{13}$$

so optimal values now u* have following shape:

$$u^*(t, x_1) = \arg\sup_{d \in D} \{ \int_{R^{n-m}} q(t, x, u) dx_2 \}. \tag{14}$$

For the simpler problem with jump, when controls participate only in vector b in equation (1), the solution is given in work [5] . This solution has a specific cases, solution for the problem with full information on the state and without information on the state. The problem here is not a deterministic problem with distributed parameters but an stochastic problem with concentrated parameters.
Similar solution is for the general problem (1), (2) with full information of the state of the system given in [1] and [8]. Here requirements that describe viscose solution of Hamilton-Jacobi-Bellman-Isaacs equations are given. The requirements which have to be fulfilled for existence of the solution of the stochastic optimal control without information of the state vector given in [7] . Appropriate optimal value for u^* may be derived for formula (14) where instead of integral on x_2 we have appropriate q when we have full information on the state and when we don't have information on the state- integration is done in whole space of the state (on x). In this case this controls can be determined over Krotovs functional and depends only on state vector.

4. CONCLUSION

Conditions defined in theorem 1 represent necessary and sufficient requirement for existence of solution of stochastic optimal control and its transformation in deterministic optimal control with distributed parameters. Required conditions may be defined in the form of maximum principle for optimal control with distributed parameters. The problem of stochastic optimal control with insufficient information on the state of the system is solved here in accordance with closed loop with known coordinates of the state. When we have full information of the state of the system we have full closed loop and we don't have the information on the state of the system then we have a problem with open loop.
More general problem with incomplete state information (without jumps) is considered in [6].

References

[1] Juan Li, S. Peng, Stochastic Optimization Theory of BSDE with jumps and Viscosity Solutions of HJB Equations, *Nonlinear Analysis, Vol. 70, No 1, p(1176-1796).*
[2] W. H. Fleming, Optimal Control of Partially Observable Diffusions, *SIAM Journal on Control, Vol. 6, No2, 196.*
[3] K. A. Rybakov and I. L. Sotskova, An Optimal Control for Random-Structure Nonlinear
Systems under Incomplete State Vector Information*, Automation and Remote Control,*
Vol. 67, No. 7, (2006), 62-75.
[4] D. Perišić, Stochastic differential game under incomplete state vector information*, Second*
International Congress of Serbian Society of Mechanics, Palić, Serbia, 1-5 june 2009.
[5] M. Friedman and Y. Yavin, Optimal control of partially observable jump diffusion processes, *International Journal of Systems Science,* Vol. 11, No. 3, 1980, 323-335.
[6] M. M. Khrustalev, Nash Equilibrium Conditions in Stochastic Differential Games where

the Pleyers Information about a State is Incomplete. I. Sufficient Equilibrium Conditions
and II. Lagrange Method, *Journal of Computer and Systems Sciences International*, I. Vol. 34, No. 6,(1995), 821-830 and II. Vol. 35, No. 1, (1996), 67-73.

[7] B. Oksendal, A. Sulem, Applied Stochastic Control of Jump Diffusions, Springer 2007.

[8] A. Bensoussan and J.-L. Lions, Impulse control and quasivariational inequalities, Gauthier-Villars Montrouge, 1984.

[9] F. B. Hanson, Applied Stochastic Processes and Control for Jump-Diffusions: Modeling
Analysis and Computation, Chicago, Illinois, USA, 2007.

A NOTE ON KASNER METRIC

Dragi Radojević
Mathematical Institute SANU, Knez Mihailova 36, Belgrade, Serbia
e-mail: dragir@mi.sanu.ac.rs

Abstract. n a recent paper Stephen Hawking offered an interesting answer to the question of what happened before the beginning of the expansion of the Universe. We used the Kasner metric to illustrate that idea.

In a recent paper [2], Stephen Hawking offered an interesting answer to the question of what happened before the beginning of the expansion of the Universe:

" At this time, the Big Bang, all the matter in the Universe, would have been on top of itself. The density would have been infinite. It would have been what is called a singularity. At the singularity, all the laws of physics would have been broken down. This means that the state of the universe, after the Big Bang, will not depend on anything that may have happened before, because the deterministic laws that govern the universe , will break down in the Big Bang. The universe will evolve from the Big Bang, completely independently of what it was like before. Even the amount of matter in the universe, can be different to what it was before the Big Bang, as the Law of Conservation of Matter, will beak down at the Big Bang.

Since events before the Big Bang have no observational consequences, one may as well cut them out of the theory, and say that time began at the Big Bang. Events before the Big Bang are simply not defined, because there is no way one could measure what was happened at them."

We shall try to illustrate this idea using the Kasner cosmological model [1].

Kasner cosmological model is presented by the metric

$$ds^2 = t^{2p_1}\,dx^2 + t^{2p_2}\,dy^2 + t^{2p_3}\,dz^2 - dt^2$$

along with the "Kasner condition "

$$\begin{aligned} p_1 + p_2 + p_3 &= 1 \\ (p_1)^2 + (p_2)^2 + (p_3)^2 &= 1 \end{aligned}$$

These are two equations with three unknown constants. We could "solve" this system of equations by giving to one of the unknown constants the desired value.

If we are free to suppose $2p_3 = \frac{1}{4}$, we could get

$$p_1 = \frac{7 \pm \sqrt{77}}{16}\,, \qquad p_2 = \frac{7 \mp \sqrt{77}}{16}\,, \qquad p_3 = \frac{1}{8}$$

and in such a special case we obtaine

$$ds^2 = t^{2p_1}\,dx^2 + t^{2p_2}\,dy^2 + \sqrt{\sqrt{t}}\,dz^2 - dt^2 \qquad (\dagger)$$

The component g_{33} of the metric tensor is not defined for $t < 0$, and so we have the beginning of the universe (and time).

Another feasible choice could be $2p_3 = \frac{1}{2}$, and so

$$p_1 = \frac{3 \pm \sqrt{21}}{8}\ , \qquad p_2 = \frac{3 \mp \sqrt{21}}{8} \qquad p_3 = \frac{1}{4}$$

and this possibility provides —the metric

$$ds^2 = t^{2p_1}\,dx^2 + t^{2p_2}\,dy^2 + \sqrt{t}\,dz^2 - dt^2 \qquad (\ddagger)$$

In such a case $g_{33} = \sqrt{t}$, and it is not defined for $t < 0$, so we can choose the beginning !

References

[1] Kasner E (1921) Geometrical theorems on Einstein's cosmological equations: *Amer.J.Math* **43**, 217
[2] Hawking S, The beginning of time : Public lecture available on http.www.hawking. org.uk/lectures/bot.html
[3] Kramer D, Stephani L, Herlt E, Mac Callum M (1980) *E*xact Solutions of Einstein's field equations*Berlin*

MOND teorija
Modifikacija Njutnovske dinamike

Veljko Vujičić
Mathematical Institute SANU, Belgrade, Serbia
e-mail: vvujicic@mi.sanu.ac.rs

1. Uvod

Pod pojmom *Modifikacija* (lat. modificatio) ovde se podrazumeva: izmena, preinačenje, tačnije odredjenje. Prema tome značenje naslova MOND - Modifikacija njutnovske dinamike podrazumeva izmene ili utanačenje klasične i nebeske mehanike, u pojedinostima, kao i opštih osnova dinamike. U naslovu svog genijalnog dela [1] ističu se dve reči MATEMATIČKI PRINCIPI nauke o prirodi - *Philosophiae naturalis principia mathematica*‡ iza čega je nastala, po svemu velika knjiga, koja sadrži: *Osnovne definicije, aksiome ili zakone kretanja, leme, teoreme, zadatke, pretpostavke, pojave i pravila umnog rasudjivanja.* Autor ovog napisa smatra da svako otstupanje od tih principijelnih stavova jeste Modifikacija Njutnove dinamike, što ćemo kratko nazivati *MOND teorija - Modified Newtonian Dynamics*. To je znatno opštije od tog naziva koji smo preuzeli iz WIKIPEDIA, the free encyclopedia, koja se vezuje za ime Mordehai Milgrom (1983), fizičhara Weizmann Instituta u Izraelu.[2] §

‡ Pri obeležavanju jedne godišnjice izdavanja ove Njutnove knjige, u Kagujevcu 22. i 23. oktobra 1987. godine, profesor beogradskog univerziteta B.A. Aničin napisao sledeće:“Pisac ovih redova (Aničin) je smišljao školski zadatak u kojem se materijalna tačka kreće po poligonu pod dejstvom impulsivne centralne sile, u nameri da zadatak objavi; pretražio je literaturu inašao ga rešenom kod Njutna. Dodir sa ovom starom knjigom donio mu je svest o tome koliko je danas slabo poznat sadržaj Principia ali i svest o dan današnjoj predavačkoj vrednosti ovog dela, posebno kada je reč o pedagogiji centralnog kretanja.

I baš tu gde izgleda da u svetu nedostaju knjige sa kratkim , jasnim i operativnim komentarom mi imamo delo iz pera jednog..., nećete verovati, ni mehanočara, ni matematičara, ni fizičara, veţilozofa Branislava Petronijevića. Knjiga ima svega 64 strane, ali obuhvata skoro sve značajne teoreme, date korak po korak, skoro sasvim sa orginalnim Njutnovim oznakama, što znatno olakšava poredjenje.’

§ From Wikipedia, the free enciclopedia. In Phfysics Modified Newtonian dynamics - MOND is a hypothesis that proposed a modification of Newton’s law of gravity to explain the galaxy rotation problem. When the uniform velocity of rotation galaxies was first observed, it was unexpected because Newtonian theory of gravity predicts that objects that are farther out will have lower velocities. For example, planets in the Solar System orbit with velocities decrease as their distance from the Sun increases.

MOND was proposed by Mordehai Molgrom in 1983 as a way to model this observed uniform velocity data. Milgrom noted that Newton’s law for gravitation force has been verified only where gravitational acceleration is large, and suggested that for extremely low accelerations the theory may not hold MOND theory posits that acceleration is not linearly proportional to force at low values.

MOND was stands in contracts to the more widely accepted theory of dark matter. Dark matter theory suggests that each galaxy contains ahead of as yet undeniable type od matte that provides an overall mass description different from the observed description of normal matter. This dark matter modifies gravity so as to cause the uniform rotation velocity data.

Prva i opšta modifikacija Njutnove teorije javlja se upravo od matematičara uporedom sa razvojem matematičke analize. Njutn je svoje delo ispisao logički po principima i simbolima euklidske geometrije duži i njihovih odnosa. Post njutnovska dinamika napisana je rečnikom i relacijama osavremenje matematiǩe analaize. Nastoijalo se pri tom da matemativ cke transformacije ne menjaju prirodu dinamičkih objekata, ali je bilo i ne malih zastranjavanja. Sledeći Hamiltonov način svodjenja diferencijalnih jednaǐna drugog reda, na diferencijalne jednačine dva puta više diferencijalnih jednačina prvog reda, uveden je sasvim nenjutnovski pojam “Dinamički sistemi" u kojim su ispuštena osnovna svojstva njutnovske dinamike. Dinamika je nauka o silama, a u tako zvanim “dinamičkim sistemima” ne figurišu sile, niti svojstva mehanike. Istorijski gledano, modifikacija Njutnove teorije počela je i nastavljala se daleko pre ove nodifikacije, ali se drukčije nazivala i naziva, kao: Ojler-Lagranžova analitička mehanika ili Hamiltova mehanika. Njutn je zasnovao svoju teoriju na aksiomama poput geometrije, a Ojler i Lagranž na osnovu svojih principa. U svom predgovoru Njutn kazuje da racionalna mehanika ima dva zadatka; jedan, ako su poznati atributi kretanja, da se odredi sila i drugi, ako je poznata sila, da se tačno odredi kretanje. Medjutim, Hamilton u svojoj teoriji postavlja samo jedan zadatak - da se prointegrali $2n$ diferencijalnih jednačina, bez pomena reči i pojma sile, koji leži u osnovi Njutnove dinamike. Na toj osnovi razvijena je velika teorija dinamičkih sistema i neinvarijantno integralenje ldinearnih diferencijalnih jednačina prvog reda i proučavanje stabilnosti integrabilnih i neintegrabilnih sistema.

U cilju veće tačnosti razdvojmo poimanje reči *Njutnova* i *njutnovska*. Pod pojmom *Njutnova* podrazumevaćemo onako kako je Njutn pisao, a pod *njutnovska* klsičnu mehaniku, kako su to drugi autori pisali.

Najprostiji primer zastranjivanja je drugi Njutnov aksiom ili zakon kretanja. Ne mali broj autora klasične mehanike nazivaju taj aksiom *Osnovna jednačina kretanja* i zapisuju je u obliku

$$\frac{d}{dt}(m\mathbf{v}) = \mathbf{F}, \tag{1.0}$$

a drugi, tačnije, taj zakon pišu u obliku

$$m\frac{d\mathbf{v}}{dt} = \mathbf{F}. \tag{1.1}$$

To je velika razlika, što će se videti u daljem izlaganju. Pokazaće se da jednačina (1.0) ne nastaje po drugoj Njuytnovoj aksiomi ili zakonu kretanja. Kao takva nije u opštem tačna, pogotovo ne kao njutnovski opšti zakon kretanja tela.

MOND

Njutn je svoje matematičke principe o kretanju počeo sa osam definicija, osnovnih definicija kojim se utvrdjuju pojmovi:

1. masa,
2. količina kretanja,
3. sila inercije,
4. sila,
5. centripetalna sila,
6. apsolutna veličina centripetalne sile,
7. ubrzavajuća veličina centripetalne sile,
8. pokretačka veličina centripetalne sile.

MOND1.

Umesto tuh osnovnih Njutnovih definicija i njihovih tumačenja, dovoljno je za razvijanje teorijske mehanike 5 opštih definicija, stim što se pre definisanja uvode tri *preprincipa*:[3]

1. Postojanja,
2. Invarijantnosti, i
3. Kauzalne odredjenosti.

Svako odstupanje u razvijanju teorije mehanike, koje ne zadovoljava ova tri preprincipa, ne može se smatrati mehanikom.

Posle toga slede osnovne definicije:

1. brzine,
2. impulsa ili količine kretanja
3. ubrzanja,
4. sile inercije,
5. dejstva sile.

Naš pristup ne bi trebalo shvatiti kao negiranje Njutnovih matematičkih principa teorije o kretanju tela, nego kao preinačenje i popboljšanje opisa kretanja tela. Sam Njutn je ukazivao na modifikaciju pravilima rasudjivanja.

Pravilo IV

" *U eksperimentalnoj fizici tvrdjenja, izvedena iz savršenih pojava pomoću navoda, ne uzimasjući u obzir suprotna tvrdjenja, treba se opredeliti za vernije ili tačnije, ili približno tačne, dok se ne otkriju takve pojave, po kojim 'ce se oni isključiti. Tako treba postupiti da novi navodi ne bi poništili tvrdjenja.*"

U cilju veće jasnosti ovde se se polazi od predprincipa: postojanja, kauzalne odredjenosti i invariijantnosti.

Preprincip postojanja.

Na osnovu nasledjenih, postojećih i stečenih znanja mehanika polazi od toga da postoje: *tela, rastojanja, vreme*.([3], str. 13-15).

Dakle, prihvatamo da postoje tela, rastojanja i vreme. Za neprebrojivo mnoštvo raznoraznih tela ustanovljeno je jedno svojstvo M koje se naziva *masam*.

Za raznorazna moguća rastojanja ustanovljerno je jedno svojstvo ili atribut L, koju ima *dužina* l.

Za sva trenutna, mala, velika i prekidnog i neprekidnog trajanja kretanja i relativnog mirovanja uvedeno je jedno svojstvo T, zvano *vreme*.

Preprincip kauzalne odredjenosti.

Tačnost odredjivanja atributa kretanja zavisi od stepena tačnosti merenja parametara objekta.

Rastojanja, njihove promene i drugi činioci kretanja tela jednoznačno su odredjeni u toku celog vremena, kako u budućnosti, tako i u prošlosti, i to onolikom tačnošću, koliko su poznate odrednice kretanja u bilo kojem odredjenom trenutku vremena.

Princip invarijantnosti.

Kretanje i svojstva kretanja tela ne zavise od forme iskaza: utvrdjena istina o kretanju i zapisana jednom u odredjenom obliku nekog jezika jednako je sadržana u zapisu drugog oblika ili drugog pisma.

Do sada smo navedena svojstva ili atribute nazivali *dimenzije* ili *fiziv cke dimenzije* zapisivali

$$\dim m = M, \quad \dim l = L, \quad \dim t = T.$$

Medjutim, kako u matematici reč "dimenzija" najčešće se koristi kao broj elemenata, tj. mera nekog elementa mnoštva, a u fizici kao jedinice mera svojstava, ovde ćemo prirodna svojstva kretanja tela nazivati *atriburima*‖ i pisati:

$$\text{atr}\, m = M, \quad \text{atr}\, l = L, \quad \text{atr}\, t = T. \tag{1.2}$$

Definicije

I. Brzina kretanja **v**, te i kretanje, je promena rastojanja u toku vremena, tj

$$\mathbf{v} = \frac{d\mathbf{r}}{dt}. \tag{1.3}$$

Njeno svojstvo je

$$\text{atr}\mathbf{v} = LT^{-1}. \tag{1.4}$$

II. Proizvod mase i brzine je impuls kretanja ili količina kretana,

$$\mathbf{p} = m\mathbf{v}, \quad \text{atr}\, \mathbf{p} = MLT^{-1}.. \tag{1.5}$$

III. Ubrzanje **w** je promena brzine po bremenu **v** po vremenu t, tj.

$$\mathbf{w} = \frac{d\mathbf{v}}{dt}.\text{atr}\, \mathbf{w} = LT^{-2}. \tag{1.6}$$

IV Rroizvod mase objekta i ubrzanja je inerciona sila, tj

$$I = m\mathbf{w}, \quad \text{atr}\, I = MLT^{-2}. \tag{1.7}$$

Ova značajna definicija ustanovljava svojstvo svake sile **F** proizvodom MLT^{-2}, tj.

$$\text{atr}\, \mathbf{F} = MLT^{-2}. \tag{1.8}$$

Kao takva sila menja brzinu u toku vremena, te je proporcionalna ubrzanju, čiji je faktor proporcionalnosti masa objekta ili tela. Masa je reprezent svakog tela kao celine, a vezuje se za jednu tačku kao centar inercije tela. Tu tačku nazivamo materijalna ili masena tačka. Razlikuje se od pojma geometrijske i topološke tačke, po tome što, pored položaja pretstavlja i masu tela.

V. Dejstvo je prirodna skalarna invarijanta, koje se javlja kao integral impulsa kretanja i pomeranja, tj.

$$\mathscr{A} = \int \mathbf{p} \cdot \mathbf{dr}. \quad \text{atr}\, \mathscr{A} = MLT^{-1}. \tag{1.9}$$

Isto svojstvo ima i *dejstvo sile*,¶

$$\mathscr{A}(\mathbf{F}) = \int \Big(\int \mathbf{F} \cdot d\mathbf{r} \Big) dt. \tag{1.10}$$

Četvrta Njutnova definicija izjednačuje pojam sile i pojam dejstva, jer piše:

‖ l. Atribut - svojstvo, karakteristika, priroda ,...

¶ O prirodi dejstva videti više u radu [4].

Napadna sila je dejstvo, proizvedeno nad telom, da bi se izmenilo njegovo stanje mirovanja ili ravnomernog pravolinijskog kretanja.

U pojašnjenju svoje definicije se dodaje:"Sila se pojavljuje jedinstveno samo u dejstvu i podle prekida dejstva ne ostaje u telu." ([1], str 26)

Svoj treći aksiom ili zakon Njutn je ispisivao pomoću reči "dejstvo". Neki autori Racionalne mehanike prevode taj zakon na srpski: "Akciji odgovara uvek jednaka reakcija suprotnog smera ili dejstva dvaju tela jednog na drugo uvek su jednaka i suprotno usmerena." Pri tom zadržavaju reči *Action* i *Reaction*. Pri ograničenom kretanju vezama, pojmom "reakcija" tumači se kao sila, kojom se veza protivi akciji-sili.

Tu nejasnoću otklanja naša definicija V, kojom se karakteriše fizičko svojstvo dejstva $\mathscr{A}$,

$$\operatorname{atr}\mathscr{A} = MLT^{-1}, \tag{1.11}$$

Nazivi i formile raznih dejstava iskazuju se odgovarajućim rečima, kao: *Dejstvo impulsa kretanja, Dejstvo sile, Dejstvo energije, Dejstvo momenta sile, ...*, ali svojstvo dejstva (1.11) ostaje jedno te isto pri svim matematičkim transformacijama.

Dakle, naša prva modifikacija (MOND1) ne menja prirodu stvari, nego preinačuje definicije potrebnih pojmova o kretanju tela.

2. MOND 2

Princip dejstva sile i protivdejstva

Umesto tri aksiome ili zakona kretanja ovde se polazi od jednog opšteg principa, kojeg smo nazvali *Princip dejstva sile i protivdejstva*.

Autor ove modifikacije polazi od jednog principa, koji je nazvao *Princip dejstva sila*. Pod pojmom "princip" u mehanici podrazumevamo jedan opšti razumni analitički stav analitičke dinamike, na osnovu kojeg i uvedenih definicija može razviti cela teorija o kretanju realnih objekata.

Imenovanje 1. Dejstvo $\mathscr{A}(\mathbf{F})$ neke sile $\mathbf{F}$ je integralna skalarna invarijanta

$$\mathscr{A}(\mathbf{F}) = \int_{t_0}^{t} \Big(\int_{0}^{r} \mathbf{F} \cdot d\mathbf{r} \Big) dt, \tag{2.1}$$

kojim se iskazuje promena položaja bjekta pod dejstvom sile $\mathbf{F}$ u toku vremena $t - t_0$.

Imenovanje 2. Negativno dejstvo (2.1) sile inercije (IV) nazivać *Protivdejstvo*

$$\mathscr{A}(\mathbf{I}) = \int_{t_0}^{t} \Big(\int_{0}^{s} \mathbf{I} \cdot d\mathbf{r} \Big) dt, \tag{2.2}$$

Na osnovu tako imenovanih pojmova u osnovu mehanike uvodimo Princip dejstva sile i protivdejstva rečima:

Dejstvo sile jednako je protivdejstvu, što se iskazuje matematičkom simbolikom:

$$\mathscr{A}(\mathbf{I}) = \mathscr{A}(\mathbf{F}),$$

odsnosno

$$\mathscr{A}(\mathbf{I}) = \int_{t_0}^{t} \Big(\int_{s_o}^{s} \mathbf{I} \cdot d\mathbf{r} \Big) dt = \int_{t_0}^{t} \Big(\int_{0}^{r} \mathbf{F} \cdot d\mathbf{r} \Big) dt. \tag{2.3}$$

Ovaj princip obuhvata sve tri Njutnove aksiome ili zakona kretanja. Zaista,

Prvi zakon. Ako je dejstvo sile $\mathscr{A}(\mathbf{F}) = 0$, sledi da je

$$\int_{t_0}^{t} \Big(\int_{r_o}^{r} \mathbf{I} \cdot d\mathbf{r} \Big) dt = 0 \longrightarrow \int_{r_o}^{r} \mathbf{I} \cdot d\mathbf{r} = 0. \tag{2.4}$$

Odavde dalje sledi da je potrebno i dovoljno, saglasno definiciji IV, da bude

$$I = m\frac{d\mathbf{v}}{dt} = 0 \longrightarrow \mathbf{v} = \mathbf{c}. \tag{2.5}$$

Ova relacija simbolizuje prvi Njutnov aksiom ili zakon dinamike.

Drugi Njutynov zakon. Istim postupkom na osnovu (2.4) sledi da je

$$\int_{r_o}^{r} \mathbf{I} \cdot d\mathbf{r} = \int_{r_o}^{s} \mathbf{F} \cdot d\mathbf{r},$$

i dalje

$$\int_{r_o}^{r} (\mathbf{F} - \mathbf{I}) \cdot d\mathbf{r} = 0.$$

Pri bilo kojem pomeranju $d\mathbf{r}$ dobija se potreban i dovoljan uslov da je

$$\mathbf{I} = \mathbf{F}, \tag{2.6}$$

što predstavlja u suštini drugi Njutnov zakon ili *Osnovnu jednačinu kretanja* u Dalamberovom obliku.

Sa logičkog stanovišta pojam zakona se razlikuje od pojmova *jednačina, lema* ili *teorema* bez obzira na prisutne zapise u nekim udžbenicima fizike ili mehanike. Njutn je veoma jasno razdvoio te pojmove. Samo je tri svoje aksiome nazvao zakonima, pozivajući se na eksperimentalne dokaze prethodnika Hajgensa, Keplera i Galileja. Na osnovu tih znanja - zakona, pojava i razumskih zaključivanja opisuje atribute kretanja pomoću pedloga i teorema. Zkoni se ne izvode pomoću prethodno znanih matematičih relacija, kao što se to čini sa teoremama. U jednom autoritativnom univerzitetskom udžbeniku piše da drugi Njutnov zakon glasi:

Promena kretanja proporcionalna je sili i zbiva se u pravcu sile.

Zatim se nepravilno objašnjava: "U vektorskom obliku drugi Njutnov zakon glasi

$$\frac{d}{dt}(m\mathbf{v}) = \mathbf{F},$$

gde je $\mathbf{F}$ vektor sile i predstavlja rezultantu savih sila koje deluju na telo. Kad se pretpostavi da se masa menja za vreme kretanja,$m = const.$, i sem toga da je $m > 0$, kao što je Njutn prećutno pretpostavio, drugi Njutnov zakon svodi se na oblik

$$m\frac{d\mathbf{v}}{dt} = \mathbf{F}, \tag{2.7}$$

koji predstavlja osnovnu vektorsku jednačinu dinamike.."

S obzirom na veliki značaj ovog zakona neophodno je da se primeti slede:

1. Jednačina (1.0) ne predstavlja Njutnov aksiom ili zakon. Tekst zakona, kao što se vidi, ne pominje pojam *količine kretanja* $m\mathbf{v}$, koji figuriše u toj jednačini. Ovako ili onako ne može da se menja aksiom ili zakon, jer iz zakona ne mogu da slede mnoga tvrdjenja (teoreme) dinamike, kao što to slede iz zakona (2.7).

2. Pretpostavka da li je masa ovakva ili onakva ne može da menja zakon. Naprotiv iz zakona će slediti, kakvo može biti kretanje i sila.

3. Šta više, jednačina (1.0) nije tačna u fizičkom smislu, jer ne opisuje verno odgovarajuće kretanje raketa ili tela sa reaktivnim silama.

Ta greška je verovatno nastala zbog nepotpunog čitanja Njutnovog dela. Njutn je definisao "količinu kretanja", ali ne i pojam "kretanje"kojim se kazuje drugi aksiom ili zakon kretanja. Medjutim u pojašnjenju svoje osnovne definicije VIII piše: "Ubrzavajuća sila (čitaj: ubrzanje, prim V.V) odnosi se prema pokretačkoj (čitaj: sili), kao brzina prema količini kretanja. Zaista, količina kretanja je proporcionalna brzini i masi, a pokretačka sila je proporcionalna ubrzanju i masi" Pojam *kretanje* nije definisao, ali u opširnoj Njutnpvpj POUKI kazuje da su *vreme, prostor, mesto i kretanje* opšte poznati pojmovi. Ipak tačka IV ukazuje na "kretanje koje je premeštanje tela iz jednog mesta u drugo".

Promena količine kretanja. Jednačina (1.0) izvodi se na osnovu zakona (2.7), a ne obratno. Formalno ako levoj i desnoj strani jednačine (2.7) dodamo $\frac{dm}{dt}\mathbf{v}$, tj.

$$m\frac{d\mathbf{v}}{dt}+\frac{dm}{dt}\mathbf{v}=\mathbf{F}+\frac{dm}{dt}\mathbf{v},$$

dobiće se

$$\frac{d}{dt}(m\mathbf{v})=\mathbf{F}^{*}, \tag{2.8}$$

gde je sada $\mathbf{F}^{*}=\mathbf{F}+\frac{dm}{dt}\mathbf{v}$. Ta konstatacija pokazuje da sile nisu formalni brojevi, nego raznorazni uzročnici kretanja, čije je svojstvo MLT^{2}.

Raznovrsnost sila lepo pokazuje Njutnova teorema IV prve knjige ([1], str. 78-80). Dokažimo tu teoremu ovde analitički.

Data je jednačina trajektorije u obliku kružne linije

$$R=\sqrt{x^{2}+y^{2}}. \tag{2.9}$$

i diferencijalne jednačine kretanja materijalne tačke mase m po kružnoj liniji, saglasno zakonu (2.7), su

$$m\frac{d\dot{x}}{dt}=F_{x}, \qquad m\frac{d\dot{y}}{dt}=F_{y}.$$

Treba odrediti veličinu sile $F=\sqrt{F_{x}^{2}+F_{y}^{2}}$.

Dva uzastopna izvoda jednačine (2.9) po vremanu daje

$$\dot{x}^{2}+\dot{y}^{2}+x\ddot{x}+y\ddot{y}=0,$$

ili, s obzirom na prethodne diferencijalne jednačine kretanja,

$$v_{or}^{2}+x\frac{F_{x}}{m}+y\frac{F_{y}}{m}=0.$$

S obzirom da je $x=R\cos\theta$, $\quad y=R\sin\theta$; $\quad F_{x}=Fcos\theta$, $\quad F_{y}=Fsin\theta$, nalazimo da je

$$F=-m\frac{v^{2}}{R}. \tag{2.10}$$

Teorema je dokazana. Sila je direktno proporcionalna kvadratu brzine i obrnuto proporcionalna poluprečniku kružnice ako je brzina konstantna. Ali ako je i veličina brzine

konstantna, onda je sila proporcionalna masi materijalne tačke. Pri jednom obrtu po kružnici, obima $2R\pi$ za vreme T, biće

$$F = -m\frac{4\pi^2 R^2}{RT^2} = -m\frac{4\pi^2}{T^2}R = k_1 R, \tag{2.11}$$

gde je k_1 jedan konstantni faktor proporcionalnosti. Može se kazati: da je sila koja dejstvuje na materijalnu tačku po kružnici direktno proporcionalna poluprečniku kružnice ili masi materijalne tačke.

Suština stvari neće se promeniti ako se razlomak (2.11) pomnoži brojem

$$1 = \frac{R^{n-1}}{R^{n-1}};$$

formula će znatno izmeniti oblik, ali ne i značenje,

$$F = -m\frac{4\pi^2}{T^2}\frac{R^{n+1}}{R^n}.$$

Njutn posebno ističe šestu posledicu u kojoj uzima vrednost Keplerovske konstante,

$$\frac{a^3}{T^2} = \frac{R^3}{T^2},$$

, tj. slučaj ada je $n = 2$. Tada se dobija da je

$$F = -m\frac{4\pi^2}{T^2}\frac{R^3}{R^2} = -m\frac{\mu}{R^2},$$

gde je

$$\mu = \frac{4\pi^2 R^3}{T^2}.$$

za keplerovska kretanja konstanta.

Treći Njutnov aksiom.

Treći Njutnov zakon je iskazan pojmom *Action* - dejstvo, s tim što je Njutn svojom definicijom IV identifikovao pojam sile sa pojmom dejstva, tj. da dva tela dejstvuju jednon na drogo akcijom $\mathbf{F}$. Znatan broj autora knjiga o mehanici ne tumače dosledno Njutnovu teriju, te na taj način modifikuju Njutnovu dinamiku. Najbitnije odstupanje od Njutnovih matematičkih principa o kretanju tela jeste Hamilonova mehanika. Po Njutnu u mehanici je sila $\mathbf{F}$ i jednaka reakciji $-\mathbf{R}$, te sledi

$$\mathbf{F} = -\mathbf{R},$$

ili

$$\mathbf{F}_1 = -\mathbf{F}_2. \tag{2.12}$$

Medjutim naš princip dejstva sile i protivdejstva za kretanje dva tela - dve materijalne tačke tvrdi da je:

$$\int_{t_0}^{t}\int_{r_{01}}^{r_1} \mathbf{F}_1 \cdot d\mathbf{r}_1 dt = \int_{t_0}^{t}\int_{r_{01}}^{r_1} \mathbf{I}_1 \cdot d\mathbf{r}_1 dt, \tag{2.13}$$

$$\int_{t_0}^{t}\int_{r_{02}}^{r_2} \mathbf{F}_2 \cdot d\mathbf{r}_2 dt = \int_{t_0}^{t}\int_{r_{02}}^{r_2} \mathbf{I}_2 \cdot d\mathbf{r}_2 dt, \tag{2.14}$$

To su velike i suštinske razlike.

Prva i najvažnija razlika je se odnosi na svojstva - fizičke dimenzije. Sila ima svojstvo 1.7, a dejstvo sile (1.10). Drukčuje rečeno, to su različiti atributi kretanja.

Druga zamerka se ispoljava u nesigurnost o saglasnosti prve i treće Njutnove aksiome. Prva aksioma kazuje da telo ostaje u mirovanju ili ravnomernom pravolinijskom kretanju. To bi po jednačini (2.12) moglo da znači da je zbir sila dva medjusobna dejstva tela jednak nuli, i dalje da su dva tela u medjusobnom ravnomernom pravolinijskom kretanju, što je protivno pojavnom stanju u prirodi stvari. Dva tela mogu se kretati nezavisno jedan od drugog, mogu se približavati, ostajati na istom mestu, rastojanju ili se udaljavati jedno od drugog. Najprostiji ubedljiv i svakom dostupan opit je: ako ispustite jedan predmet iz ruke, ubrzano će krenuti prema Zemlji. Ali ako taj predmet vežete nekom vezicom, čiji godrnju kraj držite u raci, telo ce mirovati ako miruje ruka, ili ce se pokrenuti za pokretom ruke.

Ovaj prost primer, kao što se može odmah zaključiti, ne predstavlja samo dva tela, nego ima dodatni materijalni objekt-vezu, odredjene dužine. Dakle nije reč o dva nezavisna tela, nego o sistemu dva tela, koja povezuje neka realna veza, koja se može pretstaviti jednačinom

$$\mathbf{r}_2 - \mathbf{r}_1 = \boldsymbol{\rho}(t), \tag{2.15}$$

U mehanici je poznato da takve idealne veže skrivaju silu, koja se približno tačno odredjuje silom [+],

$$\mathbf{R} = -\lambda \, grad \, f. \tag{2.16}$$

Primenom principa dejstva sile i protivdejstva na kretanje dva tela, masa m_1 i m_2 na rastojanju

$$\rho(t) = |\mathbf{r}_2 - \mathbf{r}_1|,$$

pri uslovu (2,15) imamo dve jednačine kretanja, odnosno

$$m_1 \frac{d^2\mathbf{r}_1}{dt^2} = \mathbf{F}_1, \tag{2.17}$$

$$m_2 \frac{d^2\mathbf{r}_2}{dt^2} = \mathbf{F}_2, \tag{2.18}$$

gde jednačinu (2.15) možemo napisati u obliku

$$f = \rho^2 = (x_2 - x_1)^2 + (y_2 - y_1)^2 + (z_2 - z_1)^2 - \rho^2 = 0$$

Diferencijalne jednačine kretanja (2.17) konkretizuju se pomoću (2.16):

$$\begin{aligned}
m_1\ddot{x}_1 &= \lambda(x_2 - x_1) = X_1, \\
m_1\ddot{y}_1 &= \lambda(y_2 - y_1) = Y_1, \\
m_1\ddot{x}_1 &= \lambda(z_2 - z_1) = Z_1; \\
m_2\ddot{x}_2 &= -\lambda(x_2 - x_1) = X_2, \\
m_2\ddot{y}_2 &= -\lambda(y_2 - y_1) = Y_2, \\
m_2\ddot{z}_2 &= -\lambda(z_2 - z_1) = Z_2.
\end{aligned}$$

Očigledno je da postoji 6 diferencijalnih i jedna konačna jednačina, momoću kojih se megu odrediti 6 koordinata vektora sila i jedan množilac veze λ. Uporedjenjem desnih strana jednačina, zbog jedinstvenog značenja parametra λ, dobija se da je:

$$X_2 = -X_1, \quad Y_2 = -Y_1 =, \quad Z_2 = -Z_1,$$

[+] Vidi detaljnije “Sile veza”[3]

tj.

$$\mathbf{F}_1 = -\mathbf{F}_2,$$

što znači, da su sile uzajamnog dejstva po veličini i pravcu jednake, a po smeru suprotne. To je saglasno s trtećom Njutnovom aksiomom.

Prema navedenom dokazano je da iz našeg principa dejstva sila i protivdejstva, proizilaze sve tri Njutnove aksiome ili zakona, sa dodatkom ili pojašenjenjem razdvajanja pojmova sile i dejstva sile.

Drugi izvod po vremenu jednačine rastojanja (2.15) svodi se na:

$$\frac{d^2\boldsymbol{\rho}}{dt^2} = \frac{d^2\mathbf{r}_2}{dt^2} - \frac{d^2\mathbf{r}_1}{dt^2}.$$

Sobzirom na (2.17) i (2.18) dobija se

$$\frac{F_2}{m_2} - \frac{\mathbf{F}_1}{m_1} = \frac{d^2\boldsymbol{\rho}}{dt^2},$$

ili

$$\mathbf{F}_2 = -\mathbf{F}_1 = \frac{m_1 m_2}{m_1 + m_2}\frac{d^2\boldsymbol{\rho}}{dt^2}.$$

Primer dva tela. Posmatrajmo dva tela masa m_1 i m_2, čije položaje i rastojanje odredjuje relacija (2.15). Prvi i drugi izvodi veze (2.15) po vremenu su:

$$\dot{\mathbf{r}}_2 - \dot{\mathbf{r}}_1 = \mathbf{v}_2 - \mathbf{v}_1 = \dot{\boldsymbol{\rho}},$$

$$\ddot{\mathbf{r}}_2 - \ddot{\mathbf{r}}_1 = \dot{\mathbf{v}}_2 - \dot{\mathbf{v}}_1 = \ddot{\boldsymbol{\rho}}.$$

Zamenom ubrzanja iz jednačina (2.17) i (2.18) u prethodnu relaciju dobija se

$$\dot{\mathbf{v}}_2 = \frac{\mathbf{F}_2}{m_2}, \quad \dot{\mathbf{v}}_1 = \frac{\mathbf{F}_1}{m_1},$$

a odatle proizilazi sila uzajamnog privlačenja dva tela u obliku

$$\mathbf{F} = \frac{m_1 m_2}{m_1 + m_2}\ddot{\boldsymbol{\rho}}.$$

Pretpostavimo li da je materijalna tačka mase m_1 masa Sunca $M_\odot$, a druga materojalna tačka mase m_2 oznaäva masu bilo koje planeta m_p dobiće se formula veličine sile uzajamnog privlačenja Sunca i planeta

$$F = \frac{M_\odot m_p}{M_\odot + m_p}\ddot{\boldsymbol{\rho}}.. \tag{2.19}$$

Pomnožimo li skalarno ovu jednačinu jediničnim vektorom $\rho_0 = \frac{\rho}{\rho}$ dobija se, dobija se veličina sila uzajamnog privlačenja dva tela,

$$F = \frac{M_\odot m_p}{M_\odot + m_p}\frac{\dot{\rho}^2 + \rho\ddot{\rho} - v_{or}^2}{\rho}. \tag{2.20}$$

Primetno je da se ova formula znatno razlikuje od njutnovske formule uzjamnog privlačenja bilo koja dva tela Sunčevog planetarnog sistema.

$$F = k\frac{m_\odot m_p}{\rho^2}, \tag{2.21}$$

gde je je k takozvana "univerzalna konstanta gravitacije" čija je tabulisana brojna vrednost

$$k = 6,672 \times 10^{11} kg\, m^3\, s^{-2}.. \tag{2.22}$$

Sobzirom da formule (2.21) i (2.22) čine osnovu teorije klasične nebeske mehanike, neophdodno je u teoriji MOND dokazati preimućstvo formule (2.20), nad njutnovkom formulom (2.21).

Osnovna i bitna razlika izmedju formula (2.20) i (2.21) je u tome što formula (2.21) pokazuje da je sila funkcija rastojanja, a formula (2.20) pokazuje da je sila zavisna od masa, rastojanja i od kvadrata brzine.

Po njutnovskom trećem zakonu može se tumačiti da na pojedino telo dejstvuje istovremeno i sila jednog i sila drugog, koje se kao takve poništavaju, pa bi proizilazilo, da prema prvom Njutnovom zakonu kreću ravnomerno i pravolinijski, što faktički nije baš tako. Formula (2.20) kazuje da se radijalna sila poništava samo pri uslovu ako je

$$\dot{\rho}^2 + \rho\ddot{\rho} = v_{or}^2. \tag{2.23}$$

tj. kad je veličina centripetalne sile

$$F_{cp} = \frac{m_1 m_2}{m_1 + m_2} \frac{v^2}{\rho}$$

jednaka veličini centifugalne sile

$$F_{cf} = \frac{m_1 m_2}{m_1 + m_2} \frac{\dot{\rho}^2 + \rho\ddot{\rho}}{\rho},$$

ili, kako je S. Simić* primetio da se ova jednačina (20) može svesti na oblik

$$F_\rho = \frac{m_1 m_2}{m_1 + m_2} \frac{(\rho\dot{\rho})^{\cdot}}{\rho}.$$

gde

$$\frac{(\rho\dot{\rho})^{\cdot}}{\rho}$$

ukazuje na prome nu impulsa kretanja duž rastojana tela.

Napomenimo još da formula (21), koju nazivaju "opsti zakon gravitacije", odražava Njutnovu teoremu VII (III knjige, naslovljene O SISTEMU SVETA). Ta primedba znači da formula (21) nije zakon prirode, kako se uči u školama, nego matematičko tvrdjenje izvedeno na osnovu prethodnih teorema, koja ne opisuje verno kretanje Meseca. " Mesec pod jednovremenim dejstvom privlačenja Zemlje i Sunca kreće se po orbiti oko Zemlje, daleko od Keplerovske." "Lunarna teorija - jedna od najtežih problema nebeske mehanike - razvijala se sasvim različito od drugh planetarnih teorija."([5], str.9, [6])

Ovde se polazi polazi od osnovnih stavova klasične mehanike i matematičke analize. Kako i tu postoji nesaglasje izmedju stručnjaka visokih znanja i akademskih zvanja, citirajmo nekoliko Nutnovih stavova, važnih za rešavanje naslovljenog problema.

Isak Njutn ([1], str.2) *Racionalna mehanika je učenje o kretanjima, proizvedenim bilo kakvim silama, i o silama, poptrebnih za proizvodjenje bilo kakvog kretanja, tačno izloženo i dokazano.*

Od 8 Njutnovih definicija 4 se odnose na centripetalne sile:

* Dr Slavko Simić, Matematički instirut SANU.

Def. V: *Centripetalna sila je ona koja tela privlači ili gura prema nekoj tački kao središtu, ili što izaziva da mu na neki način teže da dodju do njega.*

Def. VI: *Apsolutna veličina centripetalne sile jeste njena veća ili manja mera prema dejstvu uzorka, koji je kružno rasprostire do središta okoline.*

Def. VII: *Ubrzavajuća veličina centripetalne sile proporcionalna je brzini koju proizvodi u datom vremenu.*

Def. VIII: *Pokretačka veliv cina centripetalne sile proporcionalna je kretanju, koje proizvodi u datom vremenu.*

POJAVA VI: *Mesec opisuje radijusom, povučenim ka centru Zemlje, površine proporcionalne vremenu.* ([2], str. 509).

TEOREMA III (Treća knjiga): *Sila kojom se Mesec održava na svojoj orbiti, usmerena je ka Zemlji i obrnuto je proporcionalna kvadratima rastojanja položaja od centra Zemlje.*

POUKA: *Do sada smo nazivali tu silu, sa kojom se nebeska tela zadržavaju na svojim orbitama, centripetalnim, ali kako se pokazalo da je to privlačenje, tako ćemo je ubuduće nazivati privlačenjem.*

Da bi izbegli prisutne nejasnoće i nedoslednosti citirajmo i treći Keplerov zakon ([7], str. 55):

"Proporcija izmedju vremena perioda bilo koje dve planete tav cno je jednaka polutronoj prpoporciji njihovih **srednjih** *rastojanja."*

Sobzirom da je reč o kretanju o ravni, pogodno jr upotrbiti ravanski polarni koordinatni sistem. Tada se naformula (2.20) dobija prostiji oblik:

$$F = \frac{m_1 m_2}{m_1 + m_2}(\ddot{\rho} - \rho\dot{\theta}^2). \tag{2.24}$$

Primetimo da je $F = 0$ ako je $\ddot{\rho} = \rho\dot{\theta}^2$, kao i to da je

$$F = -\frac{m_1 m_2}{m_1 + m_2}\frac{v_{or}^2}{\rho},, \tag{2.25}$$

ako je $\rho = const.$ ' Saglasno sa navedenim nespornim relacijama, autor ovog rada predložio je rešenje problema paradoksa Mesečevog kretanja na Prvom srpskom (26 YU) kongresu teorijske i primenjene mehanike, 10-13 aprila 2007. godine, Kopaonik, Srbija, i razdelio tekst rada DINAMIČKI PARADOKS TEORIJE MESEČEVOG KRETANJA (Jedno rešene vekovnog problema). Ali kako rad nije tada našao mesta u plikacijama Kongresa, ovde navodimo izvode iz tog rada; U celosti je objavljena ta verezija na engleskom jezziku [16].

Osnovni prilog tih radova pokaazali su da sila Sunčevog privlačenja Meseca nije veća, kako se smatra u literaturi, od sile Zenljinog privlačenja Meseca, nego je sila Zermljinog privlačenja veća više od 3 puta od odgovarajuće sile Sunca.

Primer. Za tabulisane vrednosti:
masa Zemlje $M_\oplus = 5,97 \times 10)^{24}\, kg$, masa Meseca $0.739 \times 10^{24}\, kg$,
rastojanje Meseca od Zemlje $\rho = 384\,400\, km$,
srednja brzina Meseca $v_{or} = 1,02\, kms^{-1}$
dobija se

$$F_\oplus = 0.987839876 \cdot 1,02^2 = 0,002673 \cdot 10^{-3}.$$

Za Sunce:

$$m_\odot = 1,9891 \cdot 10^{30} kg, \quad \rho_\odot = 149,6 \cdot 10^6 km, \quad v_\odot = 19,5 kms^{-1}, \qquad v_\oplus = 29,8 kms^{-1},$$
$$v_{or} = 29,8 + 1,02 - 19,5 = 11,32 kms^{-1},$$

dobija se

$$F_\odot = 0,999999 \frac{11,32^2}{149,6 \cdot 10^6} = 0,856559 \cdot 10^{-3}.$$

Sledi da je $F_\oplus = 3,1262566 F_\odot$, što dokazuje naše tvrdjenje da je sila plivlačenja Zemlje veća od privlačne sile Sunca, koje se odnose na Mesec.

3. MOND3

3.1. Deferencijalne jednačine kretanja planeta

"Ovo je vektorska diferencijalna jednačina kretanja oko Sunca [8]

$$m\frac{d^2\mathbf{r}}{dt} = -f\frac{m(M+m)}{r^3}\mathbf{r}, \tag{3.1}$$

gde je M masa Sunca, a m masa planete, a f predstavlja jednu konstantnu koja važi za ceo Sunčev sistem i koja izražava jednu opštu osobinu materije u tom delu vasione". ([8], str.18) U nastavku iste knjige (strana 30) nalazi se jednačina

$$\frac{a^3}{T^2} = \frac{f}{4\pi^2}(M+m) \tag{3.2}$$

sa pogovorom: *"Ova jednačna izražava značajnu jednu vezu izmedju velike poluose a planatske putanje i vremena T obilaženja planete oko Sunca koju je Njutn pronašao, a koja nije istovetna sa trećim Keplerpvim zakonom. Po tom Keplerovom zakonu, prednji izraz morao bi imati istu numeričku vrednost za sve planete, no znog prisustva planetske mase m menja se ta vrednost od planete do planete. No kada se uzme u obzir da je masa svake planete veoma mala prema masi Sunca, pa da se m može pored M zanemariti, onda se uvidja zašto treći Keplerov zakon važi dosta tačno. No mi ćemo ga od sada zameniti prednjim tačnijim zakonom kojeg je Njutn pronašao."*

Ovaj pogovor traži podrobniju analizu. Poslednja rečenica *...tačnijim zakonom od onog kako ga je Njutn pronašao*, može da znači, da se f odredjuje jednačinom (3.2). Kao što se vidi, jednačina (3.2) sadrži 4 merljive veličine: M, m, a, T i, za sada, još jedan neodredjeni, tj nepoznati faktor proporcionalnosti f. Ta jednačina po prirodi stvari ne predstavlja relaciju za odredjivanje Keplerove konstante,

$$K = \frac{a^3}{T^2}$$

koja je, kao takva uvedena trećim Keplerovim zakonom. Pri toj nespornoj činjenici i jednačini (3.2) , nalazimo da je faktor proporcionalnosti

$$f = \frac{4\pi^2 a^3}{(M+m)T^2} \quad \text{atr}\, f = M^{-1}L^3T^{-2}, \tag{3.3}$$

bez obzira na to da li je masa planete mala veličina u odnosu na masu Sunca. Taj oblik veličine f važi za bilo koja dva tela masa m_1 i m_2, tj.

$$f = \frac{4\pi^2 a^3}{(m_1+m_2)T^2} = \frac{\mu}{m_1+m_2},, \tag{3.4}$$

gde je μ poznato u literaturi pod nazivom *Gausova konstanta*, čije je svojstvo

$$\text{atr}\,\mu = L^3T^{-2}.$$

To dovoljno jasno pokazuje da f nije jedan te isti broj za celu vasionu, kao ni za Sunčev planetarni sistem. Logičniji je zaključak da f zavisi od Keplerove konstante K, mase Sunca i masa planeta. Keplerova konstanta jeste treći Keplerov zakon, koji se vrednuje za srednja rastojanja planete od Sunca. Ne može se mimoići činjenica da se f menja od planete do planete. To ubedljivije pokazuju bojni tablični rezultati ([3], str. 73).

Navedeni podaci opovrgavaju jednu te istu tabulisanu brojevnu vrednost gravitacione konstante,

$$f = k^2 = 6,67 \times 10^{-11} kg^{-1}m^3s^{-2}.$$

Ako faktor f iz jednačine (3.4) zamenim u diferencijalnu jednačinu kretanja (3.1) dobija se diferencijalna jednačina kretanja planete, mase m, oko Sunca u obliku

$$m\frac{d^2\mathbf{r}}{dt} = -\mu\frac{m}{r^3}\mathbf{r}. \tag{3.5}$$

a veličina njutnovske sile gravitacije, u obliku

$$F = -\mu\frac{m}{r^2}. \tag{3.6}$$

Dakle, umesto jednačine (3.1) može se pisati takodje njutnovska jednačina (3.5) za sve planete u obliku (3,5), odnosno tačnije po formuli (20).

Čitajući Njutnovo delo više puta, pisac ovih redova nije mogao da zaključi da je Njutn lično ustanovio naziv *zakon univerzalne gravitacije*, predstavljen formulom (2.21), gde je k^2 "univerzalna konstanta gravitacije" kao jedan te isti broj za celu vasionu. Veći broj školaca naučili su da je to "univerzalni zakon prirode", što nije čak ni po Njutnu. Reč *zakon* Njutn je upotrebio kao aksiom, koji ne podležu dokazima, nego predstavljaju osnovni logički stav koji je saglasan sa pojavama u prirodi i ljudskoj praksi. Formula (2.21) je matematički izraz teoreme *VII* (III knjiga) znamenitog Njutnovog dela, koja se dokazuje na osnovu aksioma i prethodnih teorema.

Njutn pretpostavlja da Sunce miruje ili se kreće jednoliko, što već znamo da je to pretpostavka.

Primetimo još da konstanta k^2 u formuli (2.21) sadrži, kao što se vidi na prvi pogled, Keplerovu konstantu $K = a^3/T^2$, u kojem je a velika poluosa elipse, kao srednje rastojanje izmedju planete i Sunca. To znači da se kretanje posmatra po kružnoj liniji poluprečnika $\rho = a = const.$.

Značajna modifikacija (20) njutnovske formule (21) odražava se i na tačnijem odredjivanju sfera gravitacije planeta.

Na sličan način rešavanja problema paradoksa Mesečevog kretanja dobija se da je poluprečnik sfere gravitacije Zemlje daleko veći nego što to proizilai iz njutnovske formule (21). Po njutnovskoj formuli poluprečnik sfere gravitacije Zemlje približno iznosi 216000 km. Tu konstataciju opovrgava kretanje Meseca oko Zemlje na razdaljini od 384400

km. Po istraživanjima i proračunu Tisseranda ♯ taj poluprečnik iznosi približno 917 000 km. Medjutim po formuli (21) tj (26) nalazimo da je poluprečnik sfere gravitacije Zemlje približno jednak

$$\rho \approx 1\,400\,000 km.$$

References

[1] Is.Newton Is., Matematicheskie nachala natural'noj filosofii, "Nauka", Moskva, (1989), pp. 689; Translated by Krylov A.N. from Isaaco Newton, Philosophia naturalis principia mathematica, Editio tretio, Londini, *MDCCXXVI*.

[2] MOND-Modification Newton's Dynamic, WIKIPEDIA, the free encyclopedia - Mordehai Milgrom, (1983), Weizmann Institute, Izrael.

[3] V. Vujičić, Preprinciples of mechanics, Mathematical Institute SANU, (1999), p. 227.

[4] V.Vujičić, Action of force - Formality or Essence, Facta Universitatis, Series: Mechanics, Automatic Control and Robotics, V. 2, No 10, pp 489-495, (2000).

[5] Andre Deprit, Dviženie Luni v prostranstve, Physics and Astronomy, Sekond Edition, Edited by Zdenek Kopal, Department of Astronomy University of Manchester, Manchester, England, Academic Pres, New york and London, 1971; Prevod na ruski, pod redakcijom G.A. Lejkina, Izdavač "MIR", Moskva (1973).

[6] S.I. Seleshnikov, Astronomija i Kosmonautika, Kijev, (1967).

[7] M. Milanković, Osnovi nebeske mehanike, drugo izdanje, glava druga, paragraf 5, str. 23., "Naučna knjiga", Beograd, (1955).

[8] V. Vujnović, Astronomija, 1, školska knjiga, Zagreb, (1989), p. 149.

[9] V.A. Vujičić. Modification of the characteristic gravitational constants, Astronomical and Astrophysical Transaction, **24**, 6, (2005).

[10] T.P. Andjelich and R. Stojanović, Racionalna mehanika, Zavod za udžbenike, Beograd (1965).

[11] The Astronomical Almanac for the Year 2000, U.S. Government Printing Office, Washington, D.C. (2000).

[12] Y.A. Perel'man, Zanimatel'naya astronomiya, izdanie 9-e, Fiz. Mat. Lit., Moscow (1958).

[13] V.A. Vujičić, Prikl.Mekh 40,136 (2004) (Engl.transl. Int. Appl. Mech. 40 (2004) It should be...[18] V.A. Vujičić, Prikladnaya Mechanika, Vol 40, No. 3, (2004) pp.136-144, Engl. transl. Int. Appl. Mech. Vol.**40**, No. 3, (2004), pp. 351-359.

[14] .A. Vujičić , On a generalization of Kepler's third law, Astronomical and Astrophysical Transactions, Taylor-Francis, Vol. 24, Number 06, (2005), p. 489-495.

[15] .A. Vujičić, Dynamical Paradox in Theory of Lunar Motion. International Journal of Nonlinear Sciences & Numerical Simulation, 10(xx):xxx, (2009).

♯ Tisserand, Treté de mécanique celeste, IV. i T.P. Andjelić i R Stojanović, Racionalna mehanika.

MULTI-OBJECTIVE OPTIMIZATION OF PIEZOELECTRIC SENSOR AND ACTUATOR PLACEMENT AND SIZING FOR ACTIVE VIBRATION CONTROL

N. Zorić, Z. Mitrović, A. Simonović

Faculty of Mechanical Engineering,
The University of Belgrade, Kraljice Marije 16, 11120 Belgrade 35
e-mail: nzoric@mas.bg.ac.rs , zmitrovic@mas.bg.ac.rs , asimonovic@mas.bg.ac.rs

Abstract. Piezoelectric sensors and actuators have wide range of applications in suppression of vibrations and shape control. Design of thin-walled composite structures with integrated piezoelectric sensors and actuators is complex process, and it requires taking into account various design variables. The placement and sizing of the actuators and sensors are based on control effectiveness and observability, but these piezoelectric patches affect the host structure's mass and original dynamics properties and in the case of failure of active system, this change of dynamics properties becomes significant. This paper deals with optimal placement and sizing of piezoelectric sensor and actuator on composite beam for maximum active vibration control effectiveness and observability considering residual modes to limit spill-over effects with minimal change in original system dynamics. The problem is formulated using finite element method (FEM) based on third-order shear deformation theory (TSDT). Particle swarm optimization method is used to find optimal configuration. Numerical example is presented for cantilever beam.

1. Introduction

Active vibration control of thin-walled structures is an important subject of research in mechanical and aerospace engineering. Vibration control can be passive, with passive constrained layer damping and active with active damping and active constrained layer damping. In active vibration control, the use of piezoelectric sensors and actuators has significant research interests. The original approach of analysis of active vibration control with piezoelectric patches is presented in [1], where polyvinylidene fluoride (PVDF) was used for vibration control of cantilever beam.

Optimization of sizing and placement piezoelectric sensors and actuators has been shown as the most important issue in design of active structures. An exhaustive review of optimization problems until 2001 is presented in [2], and review of various optimization criteria is presented in [3]. The optimization problem can be divided in two approaches. The first approach consists of combination of optimal location and size of sensors and actuators and controller parameters. A few studies [4,5,6] propose a quadratic cost function which is used to taking into account the measurement error and control energy. The second approach deals with optimal location and size of sensors and actuators independently of controller definition. Optimization using objective function based on grammian matrix is presented in [7,8]. Ref. [9] presents an optimal placement method using H_2. In [10] modal controllability index based on singular value analysis of control vector was developed.

It can be seen that the main focus of these investigations is sizing and location of piezoelectric actuators and sensors for maximum controllability and observabillity. But, these piezoelectric patch cause modification of dynamics properties of host structures changing natural frequencies and in the case of failure of active system, this change of dynamics properties becomes significant. In [11], change of natural frequencies has been considered through objective function in multi-objective optimization.

Many times, an active structure is discretized into finite number of elements for vibration analysis and control. For practical implementation, this model needs to be truncated, where only first few modes are taken into account. But, state feedback control law can based on reduced model may excite the residual modes which results into spillover instability for even simple beam problem [12]. Ref. [13] takes into account the residuals modes in optimization problem.

This paper deals with optimal placement and sizing of collocated piezoelectric sensors and actuators on cantilever composite beam for maximum active vibration control effectiveness and observability considering residual modes to limit spillover effects with minimal change in original system dynamics. The problem is formulated using finite element method (FEM) based on third-order shear deformation theory (TSDT). Due to complexity of the problem, classical optimization methods which apply gradient-based search techniques can not be used. Because of that, stochastic optimization method is used: Particle Swarm Optimization. Maximizations of controllability and observability, as minimization of spillover effects are involved through objective functions, and changes of natural frequencies are involved through constraint functions.

2. Finite element model

A laminated composite beam with integrated piezoelectric sensors and actuators is considered (Fig. 1.).

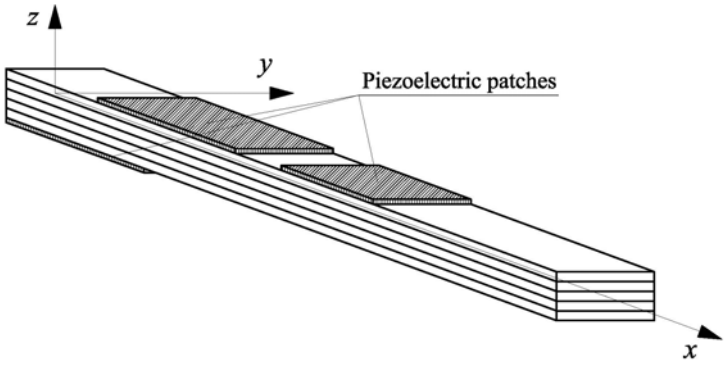

Figure 1. Laminated composite beam with piezoelectric sensors and actuators

The coordinate x is coincident with the beam axis, the $x-y$ plane coincides with mid-plane of the beam and z axis is defined as normal to the mid-plane according to the right-

hand rule. Both elastic and piezoelectric layers are supposed to be thin, such that a plane stress state can be assumed. The sensors and actuators are perfectly bonded on upper and lower surfaces at different locations along the length of beam. It is assumed that they span the entire width of beam. Elastic layers are obtained by setting their piezoelectric coefficients to zero. The equivalent single layer theory is used, so the same displacement field is considered for all layers of beam. The formulation results in a coupled finite element model with mechanical (displacement) and electrical (potentials of piezoelectric patches) degrees of freedom. Also, only specially orthotropic layers are considered.

2.1. Mechanical displacements and strains

The displacement field based on third-order shear deformation theory of Reddy [14] is given

$$\begin{aligned} u(x,z,t) &= u_0(x,t) + z\phi_x(x,t) - c_1 z^3\left(\phi_x + \frac{\partial w_0}{\partial x}\right) \\ w(x,z,t) &= w_0(x,t) \end{aligned} \tag{1}$$

where u and w are displacement components in the x and z directions respectively, u_0, w_0 are mid-plane ($z=0$) displacement and ϕ_x is bending rotation of mid-plane, $c_1 = 4/(3h^2)$, where h is total thickness of the beam. The strains associated with above displacement field are

$$\begin{aligned} \varepsilon_{xx} &= \varepsilon_{xx}^0 + z\varepsilon_{xx}^1 - c_1 z^3 \varepsilon_{xx}^3 \\ \gamma_{xz} &= \gamma_{xz}^0 - c_2 z^2 \gamma_{xz}^2 \end{aligned} \tag{2}$$

where

$$\begin{aligned} &\varepsilon_{xx}^0 = \frac{\partial u_0}{\partial x} \quad \varepsilon_{xx}^1 = \frac{\partial \phi_x}{\partial x} \quad \varepsilon_{xx}^3 = \frac{\partial \phi_x}{\partial x} + \frac{\partial^2 w_0}{\partial x^2} \\ &\gamma_{xz}^0 = \gamma_{xz}^2 = \phi_x + \frac{\partial w_0}{\partial x} \end{aligned} \tag{3}$$

and

$$c_2 = \frac{4}{h^2}. \tag{4}$$

2.2. Piezoelectric constitutive equations

Specific electric enthalpy density of a piezoelectric layer is given in [15]

$$h=\frac{1}{2}\{\varepsilon\}^T[Q]\{\varepsilon\}-\{\varepsilon\}^T[e]\{E\}-\frac{1}{2}\{E\}^T[k]\{E\}, \tag{5}$$

where $[Q]$ is the elastic stiffness matrix, $\{\varepsilon\}$ is the strain vector, $[e]$ is the piezoelectric constant matrix, $\{E\}$ is the electric field vector and $\{k\}$ is the permittivity matrix. The constitutive equations for each piezoelectric layer can be obtained

$$\begin{aligned}\{\sigma\}&=\frac{\partial h}{\partial\{\varepsilon\}}=[Q]\{\varepsilon\}-[e]^T\{E\}\\ \{D\}&=-\frac{\partial h}{\partial\{E\}}=[e]\{\varepsilon\}+[k]\{E\}\end{aligned} \tag{6}$$

where $\{\sigma\}$ is the stress vector and $\{D\}$ is the electric displacement vector. For a one-dimensional composite beam, the width (y-direction) is free of stresses. Therefore $\sigma_y=\sigma_{yz}=\sigma_{xy}=0$ while $\varepsilon_y\neq\gamma_{yz}\neq\gamma_{xy}\neq 0$. Using the above constraints, assuming that $E_1=E_2=0$ and taking into account orthotropic lamina, equation (6) can be written in following form

$$\begin{Bmatrix}\sigma_{xx}\\ \sigma_{xz}\\ D_3\end{Bmatrix}^{(k)}=\begin{bmatrix}\overline{Q}_{11} & 0 & -\overline{e}_{31}\\ 0 & \overline{Q}_{55} & 0\\ -\overline{e}_{31} & 0 & \overline{k}_{33}\end{bmatrix}^{(k)}\begin{Bmatrix}\varepsilon_{xx}\\ \gamma_{xz}\\ E_3\end{Bmatrix}^{(k)} \tag{7}$$

where superscript k denotes number of layer, and material constants are expressed in principal directions. Relations between material constants expressed in principal directions and material directions for orthotropic lamina are

$$\begin{aligned}\overline{Q}_{11}&=Q_{11}\cos^4\Theta+Q_{22}\sin^4\Theta\\ \overline{Q}_{55}&=Q_{55}\cos^2\Theta+Q_{44}\sin^2\Theta\\ \overline{e}_{31}&=e_{31}\cos^2\Theta+e_{32}\sin^2\Theta\\ \overline{k}_{33}&=k_{33},\end{aligned} \tag{8}$$

where Θ presents angle between material directions of layer and principal direction of lamina.

2.3. Variational formulation

The governing equations of motions are derived using Hamilton's principle

$$\int_{t_1}^{t_2}(\delta T-\delta H+\delta W)dt=0, \tag{9}$$

where t_1 and t_2 are two arbitrary time instants, δT is variation of kinetic energy, δH is variation of electric enthalpy and δW is variation of work done by external forces. According to the equation (5), variation of electric enthalpy can be written in following form

$$\delta H = \int_V \delta h dV = \delta H_m - \delta H_{me} - \delta H_{em} - \delta H_e , \tag{10}$$

where

$$\begin{aligned} \delta H_m &= \int_V \delta\{\varepsilon\}^T [\bar{Q}]\{\varepsilon\} dV \\ \delta H_{me} &= \int_V \delta\{\varepsilon\}^T [\bar{e}]^T \{E\} dV \\ \delta H_{em} &= \int_V \delta\{E\}^T [\bar{e}]\{\varepsilon\} dV \\ \delta H_e &= \int_V \delta\{E\}^T [\bar{k}]\{E\} dV. \end{aligned} \tag{11}$$

The variation of kinetic energy, written in terms of mechanical displacements, is

$$\delta T = \int_V \rho \delta\{\dot{u}\}^T \{\dot{u}\} dV , \tag{12}$$

where $\{\dot{u}\}$ is velocity vector, and ρ is density of layer.

2.4. Finite element discretization and coupled equations of motions

After finite element discretization [16,17,18], assembling obtained equations into Hamilton's principle (11), it can be obtain global equations of motions written in terms of the nodal mechanical and electrical degrees of freedom

$$\begin{aligned} &[M]\{\ddot{u}\} + [K_m]\{u\} + [K_{me}]_A \{\phi\}_A + [K_{me}]_S \{\phi\}_S = \{F_m\} \\ &[K_{me}]_A^T \{u\} - [K_e]_A \{\phi\}_A = [K_e]_A \{\phi\}_{AA} \\ &[K_{me}]_S^T \{u\} - [K_e]_S \{\phi\}_S = 0, \end{aligned} \tag{13}$$

where $[M]$ presents mass matrix, $[K_m]$ presents elastic stiffness matrix, $[K_{me}]_A$ and $[K_{me}]_S$ are piezoelectric stiffness matrices of actuator and sensor, respectively, $[K_e]_A$ and $[K_e]_S$ are dielectric stiffness matrices of actuator and sensor, respectively, $\{u\}$ presents vector of mechanical nodal variables, $\{\phi\}_A$ and $\{\phi\}_S$ are electric potentials on actuators and sensors, respectively and $\{\phi\}_{AA}$ is vector of external applied electric potentials on actuators. Replacing electric potentials of actuators and sensors expressed form last two equation of (13) in first one, it can be obtained following equation of motion

$$[M]\{\ddot{u}\} + [K^*]\{u\} = \{F_m\} + [K_{me}]_A \{\phi\}_{AA}, \tag{14}$$

where

$$\left[K^*\right] = \left[K_m\right] + \left[K_{me}\right]_A \left[K_e\right]_A^{-1} \left[K_{me}\right]_A^T + \left[K_{me}\right]_S \left[K_e\right]_S^{-1} \left[K_{me}\right]_S^T . \tag{15}$$

Equations of motion in modal coordinates. The equation (16) can be converted to modal-space as

$$\left\{\ddot{\eta}\right\} + \left[\omega^2\right]\left\{\eta\right\} = \left[\Psi\right]^T \left\{F_m\right\} + \left[\Psi\right]^T \left[K_{me}\right]_A \left\{\phi\right\}_{AA}, \tag{16}$$

where $\left[\Psi\right]$ presents modal matrix which has been normalized with respect to mass, $\left\{\eta\right\}$ vector of modal coordinates and $\left[\omega^2\right]$ diagonal matrix of squares natural frequencies obtained as following way

$$\left[\omega^2\right] = \left[\Psi\right]^T \left[K^*\right]\left[\Psi\right]. \tag{17}$$

State-space representation. Lower ordered modes are the most easily excitable because they have lower energy associated. Due to that, controller has been designed for active control only first few modes. Thus, equation (16), expressed in truncated modal-space, becomes

$$\left\{\ddot{\eta}\right\} + \left[\omega^2\right]_{Tr} \left\{\eta\right\} = \left[\Psi\right]_{Tr}^T \left\{F_m\right\} + \left[\Psi\right]_{Tr}^T \left[K_{me}\right]_A \left\{\phi\right\}_{AA}, \tag{18}$$

where matrix $\left[\omega^2\right]_{Tr}$ is consisted of first few controllable eigen-modes. For residual modes, equation (17) becomes

$$\left\{\ddot{\eta}\right\} + \left[\omega^2\right]_{\mathrm{Re}z} \left\{\eta\right\} = \left[\Psi\right]_{\mathrm{Re}z}^T \left\{F_m\right\} + \left[\Psi\right]_{\mathrm{Re}z}^T \left[K_{me}\right]_A \left\{\phi\right\}_{AA} . \tag{19}$$

Equations (18) and (19) can be presented in state-space form as

$$\left\{\dot{X}\right\} = \left[A\right]\left\{X\right\} + \left[B\right]\left\{\phi\right\}_{AA} + \left\{d\right\}, \tag{20}$$

where

$$\left\{X\right\} = \begin{Bmatrix} \left\{\eta\right\} \\ \left\{\dot{\eta}\right\} \end{Bmatrix} \tag{21}$$

present state vector,

$$\left[A\right] = \begin{bmatrix} \left[0\right] & \left[0\right] & \left[I\right] & \left[0\right] \\ \left[0\right] & \left[0\right] & \left[0\right] & \left[I\right] \\ -\left[\omega^2\right]_{Tr} & \left[0\right] & \left[0\right] & \left[0\right] \\ \left[0\right] & -\left[\omega^2\right]_{\mathrm{Re}z} & \left[0\right] & \left[0\right] \end{bmatrix} \tag{22}$$

present state matrix,

$$[B]=\begin{bmatrix}[0]\\[0]\\[B]_{tr}\\[B]_{\mathrm{Re}z}\end{bmatrix}=\begin{bmatrix}[0]\\[0]\\[\psi]_{Tr}^{T}[K_{me}]_{A}\\[\psi]_{\mathrm{Re}z}^{T}[K_{me}]_{A}\end{bmatrix} \tag{23}$$

present control matrix, and

$$\{d\}=\begin{Bmatrix}\{0\}\\\{0\}\\[\psi]_{Tr}^{T}\{F_m\}\\[\psi]_{\mathrm{Re}z}^{T}\{F_m\}\end{Bmatrix} \tag{24}$$

is disturbance vector. From third equation in (13) it can be expressed sensor output in state-space form

$$\{Y\}=[C]\{X\}, \tag{25}$$

where $[C]$ presents output matrix given as

$$[C]=[[C]_{Tr}\quad[C]_{\mathrm{Re}z}\quad[0]\quad[0]]=\left[[K_{me}]_{S}^{T}[\Psi]_{Tr}\quad[K_{me}]_{S}^{T}[\Psi]_{\mathrm{Re}z}\quad[0]\quad[0]\right]. \tag{26}$$

3. Optimization criteria for piezoelectric actuators and sensors sizing and location

In [10], a controllability index for actuator is proposed, which is obtained by maximizing global control force. The modal control force applied to the system can be written as

$$\{f_C\}=[B]\{\phi\}_{AA}. \tag{27}$$

It follows from (27) that

$$\{f_C\}^{T}\{f_C\}=\{\phi\}_{AA}^{T}[B]^{T}[B]\{\phi\}_{AA}. \tag{28}$$

Using singular value analysis, $[B]$ can be written as $[B]=[M][S][N]^{T}$, where $[M]^{T}[M]=[I]$, $[N]^{T}[N]=[I]$ and

$$[S]=\begin{bmatrix}\sigma_1 & 0 & \cdots & 0\\ 0 & \sigma_2 & & 0\\ \vdots & & \ddots & \vdots\\ 0 & 0 & \cdots & \sigma_{Na}\\ \vdots & \vdots & & \vdots\\ 0 & 0 & \cdots & 0\end{bmatrix} \tag{29}$$

where N_a presents number of actuators. Equation (29) can be written as

$$\{f_C\}^T\{f_C\} = \{\phi\}_{AA}^T[N][S]^T[S][N]^T\{\phi\}_{AA}, \tag{30}$$

or

$$\|f_C\|^2 = \|\{\phi\}_{AA}\|^2\|S\|^2. \tag{31}$$

Thus, maximizing this norm independently of the applied voltage $\{\phi\}_{AA}$ induces maximizing $\|S\|^2$. The magnitude of σ_i is a function of location and size of piezoelectric actuator. In [10] is proposed controllability index which is defined by

$$\Omega_C = \prod_{i=1}^{Na}\sigma_i . \tag{32}$$

The higher controllability index indices the smaller electrical potential will be required for control. The observabillity index can be obtained on similar way

$$\Omega_O = \prod_{i=1}^{Ns}\sigma_i , \tag{33}$$

Controllability index can be obtained in more suitable form for models based on finite element, where, instead of maximizing the norm $\|S\|^2$, applied force for each mode have been maximized independently of $\{\phi\}_{AA}$. According to the (23), controllability index can be written on following way

$$\bar{\sigma}_{Ci}^2 = (B_i)_{Tr}(B_i)_{Tr}^T \tag{34}$$

for controlled mode, and

$$\left(\bar{\sigma}_{Ci}^{\mathrm{Rez}}\right)^2 = (B_i)_{\mathrm{Rez}}(B_i)_{\mathrm{Rez}}^T \tag{35}$$

for residual mode. $(B_i)_{Tr}$ and $(B_i)_{\mathrm{Rez}}$ present i-th row of matrices $[B]_{Tr}$ and $[B]_{\mathrm{Rez}}$, respectively. Simillary, observabillity index is

$$\bar{\sigma}_{Oi}^2 = \{C_i\}_{Tr}^T\{C_i\}_{Tr} \tag{36}$$

for observable mode, and

$$\left(\bar{\sigma}_{Oi}^{\mathrm{Rez}}\right)^2 = \{C_i\}_{\mathrm{Rez}}^T\{C_i\}_{\mathrm{Rez}} \tag{37}$$

where $\{C_i\}_{Tr}$ and $\{C_i\}_{\mathrm{Rez}}$ present i-th column of matrices $[C]_{Tr}$ and $[C]_{\mathrm{Rez}}$, respectively.

4. Optimization implementation using particle swarm optimization

The particle swarm optimization (PSO) has been inspired by the social behavior of animals such as fish schooling, insect swarming and birds flocking. It was first introduced in [19]. The system is initialized with a population of random solutions (called particle position in

PSO). Every particle is affected by three factors: its own velocity, the best position it has achieved (best local position) which is determined by the highest value of the objective function encountered by this particle in all previous iteration and overall best position achieved by all particles (best global position), which is determined by the highest value of the objective function encountered in all the previous iteration. A particle changes its velocity (v) and position (p) on following way

$$v_{id}^{k+1} = wv_{id}^{k} + c_1 r_1 \left(plbest_{id} - p_{id}^{k} \right) + c_2 r_2 \left(pgbest_{d} - p_{id}^{k} \right), \tag{38}$$

$$p_{id}^{k+1} = p_{id}^{k} + v_{id}^{k+1}, \quad i = 1,..,n \quad d = 1,...,m \tag{39}$$

where w is inertia weight, c_1 is cognition factor, c_2 is social learning factor, r_1 and r_2 are random numbers between 0 and 1, the superscript k denotes iterative generation, n is population size, m is particle's dimension, $plbest_{id}$ and $pgbest_{d}$ are best local and global position. Cognition factor and social learning factor are usually set as $c_1 = c_2 = 1.5$. Upper and lower limits of inertia weight for structural design are given in [20].

In this work, beam is discretized in finite elements. Each piezoelectric patch is determined with two coordinates: left node, which defines position and number of elements covered by this patch which defines size of piezoelectric patch (Fig. 2), so, dimension of particle is twice then number of piezoelectric patches.

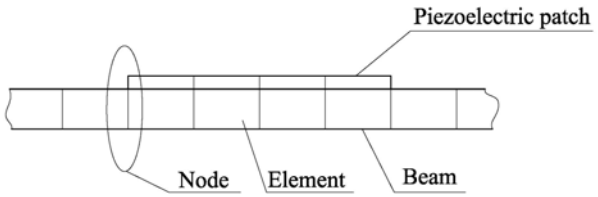

Figure 2.

It is obvious that coordinates of particle and corresponding velocity are integer number. Because of that, discrete method must be used. According to the [21], velocity is updated by following equation on every iteration

$$v_{id}^{k+1} = \mathrm{int}\left(wv_{id}^{k} + c_1 r_1 \left(plbest_{id} - p_{id}^{k} \right) + c_2 r_2 \left(pgbest_{d} - p_{id}^{k} \right) \right), \tag{40}$$

in which $\mathrm{int}(f)$ is getting integer part of f .

4.1. Objective functions

As mentioned earlier, the piezoelectric patches sizing and location should be such that those should give good controllability and observability with minimization of spillover effects. According to the (34-37), objective functions can be written as

$$\text{maximize} \quad f_i = \frac{\overline{\sigma}_{Ci}^2}{\overline{\sigma}_{Ci\max}^2} \cdot 100 \quad i = 1,.., N_{TrA}, \tag{41}$$

$$\text{minimize} \quad f_i = \frac{\left(\overline{\sigma}_{Ci}^{\mathrm{Re}z}\right)^2}{\left(\overline{\sigma}_{Ci\max}^{\mathrm{Re}z}\right)^2} \cdot 100 \quad i = 1,.., N_{\mathrm{Re}zA}, \tag{42}$$

$$\text{maximize} \quad f_i = \frac{\overline{\sigma}_{Oi}^2}{\overline{\sigma}_{Oi\max}^2} \cdot 100 \quad i = 1,.., N_{TrS}, \tag{43}$$

$$\text{minimize} \quad f_i = \frac{\left(\overline{\sigma}_{Oi}^{\mathrm{Re}z}\right)^2}{\left(\overline{\sigma}_{Oi\max}^{\mathrm{Re}z}\right)^2} \cdot 100 \quad i = 1,.., N_{\mathrm{Re}zS}, \tag{44}$$

where $\overline{\sigma}_{Ci\max}$, $\overline{\sigma}_{Ci\max}^{\mathrm{Re}z}$, denote maximum controllability index of controlled modes and residual modes and $\overline{\sigma}_{Oi\max}$, $\overline{\sigma}_{Oi\max}^{\mathrm{Re}z}$ denote maximum observability index of observed modes and residual modes. These functions are called degree of controllability and observability. It can be seen that there are $N_{TrA} + N_{\mathrm{Re}zA} + N_{TrS} + N_{\mathrm{Re}zS}$ objective functions. In this work, only collocated sensors and actuators will be considered. Actuator and its corresponding sensor have the equal length and they are set symmetrically: sensor at the bottom surface, and actuator on the top surface of the beam. In [22] states that it is not necessary to search for maximum controllability and observability index separately. The same result can be obtained by maximizing only one index. According to that, only equations (41) and (42) will be considered. $N_{TrA} + N_{\mathrm{Re}zA}$ objective functions (41) and (42) can be transformed in two objective functions using weighted aggregation approaches

$$\text{maximize} \quad f_{Tr} = \sum_{i=1}^{N_{TrA}} w_i^{Tr} \frac{\overline{\sigma}_{Ci}^2}{\overline{\sigma}_{Ci\max}^2} \cdot 100 \tag{45}$$

and

$$\text{minimize} \quad f_{\mathrm{Re}z} = \sum_{j=1}^{N_{\mathrm{Re}zA}} w_j^{\mathrm{Re}z} \frac{\overline{\sigma}_{Cj}^2}{\overline{\sigma}_{Cj\max}^2} \cdot 100, \tag{46}$$

where w_i^{Tr} and $w_j^{\mathrm{Re}z}$ are the weighting coefficients which express the relative importance of the objective function. Two obtained objective functions can be transformed in one objective function in following way

$$\textit{maximize} \quad f = f_{Tr} - \gamma f_{\mathrm{Re}z} \tag{47}$$

where γ denotes weighting constant which expresses relative importance of minimization controllability of residual modes related to maximization of controllability of controlled modes. So, multi-objective optimization problem which consist of $N_{TrA} + N_{\mathrm{Re}zA} + N_{TrS} + N_{\mathrm{Re}zS}$ objective functions are transformed in single-objective problem.

4.2. Constraints

The first type of constraint used in optimization problem in this work is related to the geometry of the piezoelectric patches. These geometric constraints are

1. no one of the coordinate of the particle must not be nonpositive number
2. minimum distance between two patches is 1
3. last piezoelectric patch must not to be outside of beam

The problem of violation of geometric constraint is solved on following way:

1. generate given number of particles in feasible space which every of them is placed between the particle in previous iteration, which is placed in feasible space, and obtained particle in current iteration, which is placed in nonfeasible space.
2. calculate Euclidian distances between generated particles and particle in current iteration
3. new particle is one which distance is minimum
4. modify velocity on following way

$$v_{id}^{k+1} = p_{id}^{k+1*} - p_{id}^{k}, \tag{48}$$

where p_{id}^{k+1*} is particle obtained in 3.

Second type of constraints are related to change of natural frequencies. It can be written on following

$$\left|\omega_i^{New} - \omega_i^{Old}\right| / \omega_i^{Old} < \varepsilon_i \quad i = 1,.., N_{\mathrm{mod}\, s}, \tag{49}$$

where ω_i^{New} denotes natural frequency of i-th mode of the beam with piezoelectric patches, ω_i^{Old} denotes natural frequency of i-th mode of the beam without piezoelectric patches and i-th ε_i is tolerance. These constraints will be treated with penalty function technique, so objective function to be maximized is modified to

$$maximize \quad f' = f - k \cdot |f| \cdot g_j / g \tag{50}$$

where

$$g_j = \sum_{i=1}^{N_{\mathrm{mod}\, s}} \left[\left|\omega_{ij}^{New} - \omega_{ij}^{Old}\right| / \omega_{ij}^{Old} - \varepsilon_{ij}\right], \tag{51}$$

presents constraint violation of j-th particle which left feasible design space, g is average of all g_j in current iteration and k presents number of current iteration.

5. Numerical example

In the example, cantilever beam is considered. The length of beam is $L = 0.5m$, and its width is $b = 0.025m$. Laminated layers are made of Graphite-Epoxy. Their thicknesses is given as $h = [0.0005 \quad 0.001 \quad 0.002]$, and its orientations are $\Theta = [90 \quad 0 \quad 90]$. Piezoelectric sensors and actuators are made of PZT. Their thickness is $0.35mm$. Material properties of Graphite-Epoxy and PZT are given in Table 1.

Material properties	Graphite-Epoxy	PZT
$E_1(GPa)$	174	63
$E_2(GPa)$	10.3	63
$G_{13}(GPa)$	7.17	24.6
$G_{23}(GPa)$	6.21	24.6
ν_{12}	0.25	0.28
$\rho(kg/m^3)$	1389.23	7600
$e_{31}(C/m^2)$	/	10.62
$k_{33}(F/m)$	/	0.1555

Table 1. Material properties of Graphite-Epoxy and PZT.

In the example are involved three sensors and actuators. The objective is good controllability the 4 first modes ($N_{Tr} = 4$) and less controllability the of the 5th to 8th modes ($N_{\mathrm{Re}z} = 4$). The constraint is that changes of the four first modes are less then 10%. The beam is divided into 50 finite elements. Cognition factor and social learning factor are set as $c_1 = c_2 = 1.5$, and inertia weight are linearly varied form 1 to 0.5, number of population is 20 particles, and number of iteration is 50. Weighting coefficients are given as follows: $w^{Tr} = (0.25 \quad 0.25 \quad 0.25 \quad 0.25)$ and $w^{\mathrm{Re}z} = (0.25 \quad 0.25 \quad 0.25 \quad 0.25)$.

5.1. First case - $\gamma = 0$ (residual modes are neglected)

The optimal solution of this case is given as $pgbest = (6 \quad 14 \quad 24 \quad 16 \quad 48 \quad 3)$. Model of the beam with piezoelectric patches which corresponds to the optimal solution is presented at Fig. 3. Fig. 4 presents convergence of objective functions. Changes of natural frequencies and degree of controllability of each controlled and residual mode are presented in Table 2 and Table 3.

Mode	$\omega^{Old}(rad/s)$	$\omega^{New}(rad/s)$	NF change(%)	Deg. of Cont. (%)
1	52.36	55.23	5.48	13.81
2	328.18	348.56	6.09	20.64
3	919.11	1008.28	9.7	29.28
4	1801.67	1978.09	9.79	33.38

Table 2.

Res. mode	$\omega^{Old}(rad/s)$	$\omega^{New}(rad/s)$	NF Change(%)	Deg. of Cont. (%)
1	2979.53	3367.66	13.03	36.07
2	4453.2	5303	19.08	43.31
3	6223.58	7216.81	15.96	34.61
4	8291.74	9611	15.91	36.71

Table 3.

Figure 3. Beam with piezoelectric sensors and actuators which corresponds to the first case

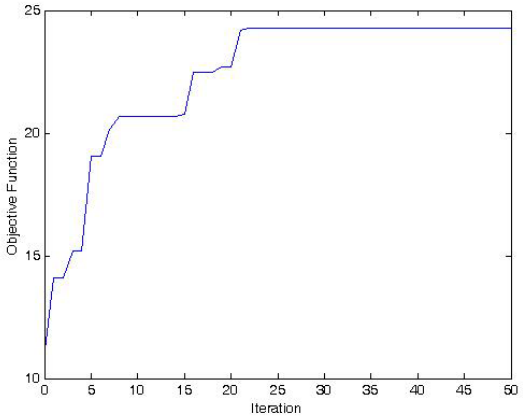

Figure 4. Convergence of objective function

5.2. Second case - $\gamma = 1$

The optimal solution of this case is given as $pgbest = (2 \quad 4 \quad 35 \quad 1 \quad 40 \quad 2)$. Beam with piezoelectric patches which corresponds to the optimal solution is presented at Fig. 5. Fig. 6 presents convergence of objective functions. Changes of natural frequencies and degree of controllability of each controlled and residual mode are presented in Table 4 and Table 5.

Mode	$\omega^{Old}(rad/s)$	$\omega^{New}(rad/s)$	NF change(%)	Deg. of Cont. (%)
1	52.36	55.46	5.92	4.13
2	328.18	360.81	9.94	4.44
3	919.11	988.97	7.49	4.24
4	1801.67	1873.68	4	3.08

Table 4.

Res. mode	$\omega^{Old}(rad/s)$	$\omega^{New}(rad/s)$	NF Change(%)	Deg. of Cont. (%)
1	2979.53	3004	0.79	1.73
2	4453.2	4403.64	1.11	1
3	6223.58	6138.47	1.37	0.92
4	8291.74	8247.69	0.54	1.98

Table 5.

Figure 5. Beam with piezoelectric sensors and actuators which corresponds to the second case

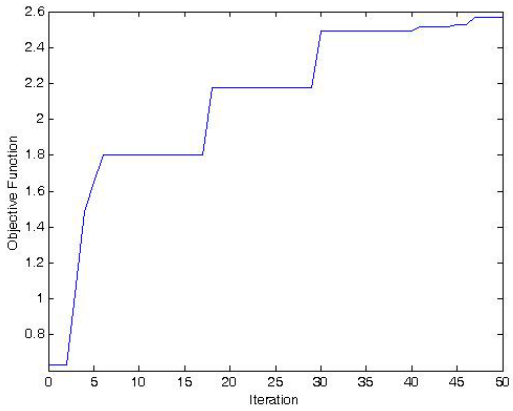

Figure 6. Convergence of objective function

6. Conclusion

In this paper, the problem of sensors and actuators sizing and placement on laminated beam with minimum changes of original dynamics properties is considered. Multi-objective problem is transformed into single-objective using weighted aggregation approach. Optimization problem is solved using Particle swarm optimization which is shown up as suitable algorithm for this case of optimization. Several applications presented in the case of cantilever beam using three collocated sensors and actuators. In the first case, residual modes are neglected. The degree of controllability of residual modes is higher compared to the controlled modes. Minimizing of degrees of controllability of residual modes affects on degrees of controllability of controlled modes, causing their reduction, which can be seen for second and third case. One of solution for avoiding this problem is placing large number of smaller sensors and actuators [8].

Acknowledgement. This work is supported by the Ministry of Science and Technological Development of Republic of Serbia as Technological Development Projects No. 35035 and No. 35006.

References

[1] Bailey T, Hubbard J E (1985) Distributed piezoelectric-polymer active vibration control of a cantilever beam, *journal of Guidance control and Dynamics*, **8**, pp. 605-611.
[2] Frecker M (2003) Recent Advances in Optimization of Smart Structures and Actuators, *Journal of Intelligent Material Systems and Structures*, **14**, pp. 207-215.
[3] Gupta V, Sharma M and Thakur N (2010) Optimization Criteria for Optimal Placement of Piezoelectric Sensors and Actuators on a Smart Structure: A Technical Review, *Journal of Intelligent Material Systems and Structures*, **0**, pp. 1-17.
[4] Bruant I, Coffignal G, Lene F and Verge M (2001) A methodology for determination of piezoelectric actuator and sensor location of piezoelectric actuator and sensor location on beam structures, *Journal of Sound and Vibration*, **243(5),** pp. 862-882.
[5] Kumar K R and Narayanan S (2008) Active vibrations control of beams with optimal placement of piezoelectric sensors/actuators pairs, *Smart Materials and Structures*, **17.**
[6] Tarapada R and Chakraborty D (2009) Optimal vibration control of smart fiber reinforced composite shell structures using improved genetic algorithm, *Journal of Sound and Vibration*, **319**, pp. 15-40.
[7] 7. Hac A and Liu L (1993) Sensor and Actuator location in motion of flexible structures, *Journal of Sound and Vibration*, **167(2)**, pp. 239-261.
[8] Bruant I, Gallimard L and Nikoukar S (2010) Optimal piezoelectric actuator and sensor location for active vibration control, using genetic algorithm, *Journal of Sound and Vibration*, **329**, pp. 1615-1635.
[9] Qiu Z, Zhang X, Wu H and Zhang H (2007) Optimal placement and active vibration control for piezoelectric smart flexible cantilever plate, *Journal of Sound and Vibration*, **301**, pp. 521-543.
[10] Wang Q and Wang C M (2001) A controllability index for optimal design of piezoelectric actuators in vibration control of beam structures, *Journal of Sound and Vibration*, **242(2)**, pp. 507-518.
[11] Dhuri K D and Seshu P (2006) Piezo actuator placement and sizing for good control effectiveness and minimal change in original system dynamics, *Smart Materials and Structures*, **15**, pp. 1661-1672.
[12] Preumont A (2002) *Vibration control of Active Structures: An Introduction*, 2nd edn, Kluwer Academic Publisher, USA.
[13] Bruant I and Poisler L (2005) Optimal Location of Actuators and Sensors in Active Vibration Control, *Journal of Intelligent Material Systems and Structures*, **16**, pp. 197-206.
[14] Heyliger N D and Reddy N (1985) A higher order beam finite elements for bending and vibration problem, *Journal of Sound and Vibration*, **126**, pp. 309-326.
[15] Ballas P G (2007) *Piezoelectric Multilayer Beam Bending Actuators*, Springer-Verlag Berlin Heidelberg
[16] Jiang J P and Li D X (2007) A new finite element model for piezothermoelastic composite beam, *Journal of Sound and Vibration*, **306**, pp. 849-864.
[17] Peng X Q, Lam K Y and Liu G R (1998) Active vibration control of composite beams with piezoelectrics: a finite element model with third order theory, *Journal of Sound and Vibration*, **209**(4), pp. 635-650
[18] Moita J M S, Soares C M M, Soares C A M (2005) Active control of forced vibrations in adaptive structures using a higher order model, *Composite Structures*, **71**, pp. 349-355.
[19] Kennedy J and Everhart R C (1995) Particle swarm optimization, *Proceedings of the IEEE international conference on neural networks*, **4,** pp. 1942-1948.
[20] Perez R E and Behdinan K (2007) Particle swarm approach for structural design optimization, *Computers and Structures*, **85**, pp. 1579-1588.
[21] Jin Y-X, Cheng H-Z, Yan J-Y and Zhang L (2007), New discrete method for particle swarm optimization and its application in transmission network expansion planning, *Electric Power Systems Research*, **77**, pp. 227-233.
[22] Mandal S (2010) *Optimal Placement of Collocated Sensors and Actuators in FRP Composites Substrate*, Bachelor Thesis, Department of Mechanical Engineering, National Institute of Technology, Rourkela, Odisha.

CONTROL FORCE FOR SCLERONOMIC MECHANICAL SYSTEM IN DECOMPOSITION MODE

Miloš Živanović

Faculty of Mechanical Engineering, The University of Belgrade, Kraljice Marije 16, 11120 Belgrade 35
e-mail: milanzi@sbb.rs

Abstract.

To bring a scleronomic, holonomic mechanical system into the decomposition mode, the switching control force with corresponding switching amplitude must act on it. In the decomposition mode, the mechanical system "slides" along the sliding surface which represents a set of discontinuities (switching surface) of the control force. The control force is defined out of the switching surface, but its values on it should be determined. In this paper, how the control force must act on the mechanical system in the decomposition mode is determined and simulation results in relation to the motion of a three-degree-of-freedom robotic manipulator coming into and moving in the decomposition mode are presented and discussed.

1. Introduction

The problem of determination of the control force in the decomposition mode is a partial case of the problem of determination of the right-hand discontinuous function on the set of its discontinuities in differential equations with discontinuous right-hand side [5], [1], [11], [7]. This problem is specific because the mechanical system is under the action of unpredictable disturbance forces, so that the right-hand side of the differential equations of motion is unknown. Nevertheless, the problem can be solved theoretically using the method of equivalent control [11].

Firstly, the switching and sliding surfaces of the mechanical system are defined and determined and corresponding illustrations of them in different spaces are presented. Then, the method of equivalent control is applied to determine the control force in the decomposition mode. Finally, the results of simulation of motion of a three-degree-of-freedom robotic manipulator are presented to show the motion of the mechanical system and action of the control force before and after the moment of entering the decomposition mode. Notation used in the paper is given in the last section.

1.1. Mathematical model of scleronomic holonomic mechanical systems

Let $\mathscr{M}$ be the n-dimensional, at least $\mathscr{C}^2$-differentiable configuration manifold [2, 10, 3] of the mechanical system (MS). Restrict, if necessary, the movements of the system to the open, bounded and connected manifold $\mathscr{M}'$ such that a bounded chart $\underline{q}(\cdot)_{\mathscr{M}'} \subset \mathscr{M} \times \Re^n_{\underline{q}}$

exists. The mathematical model of a scleronomic holonomic mechanical system expressed in coordinates $\underline{q}$, [12], is

$$\underline{M}(\underline{q})\ddot{\underline{q}} + \underline{c}(\underline{q},\dot{\underline{q}}) = \underline{f}^{\mathrm{d}}(\underline{q},\dot{\underline{q}},t) + \underline{f}^{\mathrm{c}}, \tag{1}$$

where $\underline{q} \in_{\mathrm{v}} \mathscr{Q} \subset \underline{q}(\mathscr{M}') \subset \Re^{\mathrm{n}}_{\underline{\mathrm{q}}}$, $\dot{\underline{q}} \in_{\mathrm{v}} \mathscr{Q}^1 \subset \Re^{\mathrm{n}}_{\dot{\underline{\mathrm{q}}}}$ and $\ddot{\underline{q}} \in_{\mathrm{v}} \Re^{\mathrm{n}}_{\ddot{\underline{\mathrm{q}}}}$ are referred to as position, velocity and acceleration of the MS, respectively. $t \in_{\mathrm{v}} \mathscr{T}_\infty \subset \Re_{\mathrm{t}}$ is a time variable; $\mathscr{T}_\infty = (\mathrm{t_i}, \infty\mathrm{s})$ where $\mathrm{t_i} < \infty\mathrm{s}$ is the initial instant, $\underline{M} = [M_{ij}]_{\mathrm{n}\times\mathrm{n}} \in_{\mathrm{v}} \Re^{\mathrm{n}\times\mathrm{n}}_{\underline{\mathrm{M}}}$ is the inertia or mass matrix, while $\underline{M}(\cdot)_{\underline{q}(\mathscr{M}')}$ is a continuously differentiable function, $\underline{f}^{\mathrm{d}} \in_{\mathrm{v}} \mathscr{F}^{\mathrm{d}} \subset \Re^{\mathrm{n}}_{\underline{\mathrm{f}}^{\mathrm{d}}}$ is the disturbance force, $\underline{f}^{\mathrm{c}} \in_{\mathrm{v}} \mathscr{F}^{\mathrm{c}} \subset \Re^{\mathrm{n}}_{\underline{\mathrm{f}}^{\mathrm{c}}}$ is the control force. The elements c_i of the vector $\underline{c} = [c_i]_{\mathrm{n}\times 1} \in_{\mathrm{v}} \Re^{\mathrm{n}}_{\underline{\mathrm{c}}}$ have the form

$$c_i = C_{jk,i}\,\dot{q}^j\dot{q}^k, \quad C_{jk,i} = \frac{1}{2}\left(\frac{\partial M_{ij}}{\partial q^k} + \frac{\partial M_{ik}}{\partial q^j} - \frac{\partial M_{jk}}{\partial q^i}\right), \quad i,j,k = 1,\ldots,n, \tag{2}$$

where $C_{jk,i}$ are Christoffel's symbols of the first kind, and Einstein's summation convention is used. The given sets $\mathscr{Q}$, $\mathscr{Q}^1$, $\mathscr{F}^{\mathrm{d}}$ and $\mathscr{F}^{\mathrm{c}}$ are bounded, connected and open in corresponding spaces $\Re^{\mathrm{n}}_{\underline{\mathrm{q}}}$, $\Re^{\mathrm{n}}_{\dot{\underline{\mathrm{q}}}}$, $\Re^{\mathrm{n}}_{\underline{\mathrm{f}}^{\mathrm{d}}}$, and $\Re^{\mathrm{n}}_{\underline{\mathrm{f}}^{\mathrm{c}}}$. Every continuously differentiable function $\underline{q}(\cdot)_{\mathscr{T}_\infty}$ that is a solution of differential equation (1) is a motion of the MS.

1.2. Problem formulation

Suppose MS ought to track the nominal motion $\underline{q}_{\mathrm{n}}(\cdot)_{\mathscr{T}_\infty}$ [12], for which $\underline{q}_{\mathrm{n}}(\mathscr{T}_\infty) \subset \mathscr{Q}$, $\dot{\underline{q}}_{\mathrm{n}}(\mathscr{T}_\infty) \subset \mathscr{Q}^1$, and $\ddot{\underline{q}}_{\mathrm{n}}(\cdot)_{\mathscr{T}_\infty}$ is bounded and continuous. Introduce the position and velocity deviation as

$$\underline{x} = \underline{q} - \underline{q}_{\mathrm{n}} \quad \text{and} \quad \dot{\underline{x}} = \dot{\underline{q}} - \dot{\underline{q}}_{\mathrm{n}}, \tag{3}$$

and let the control force

$$\underline{f}^{\mathrm{c}} = -\mathrm{f^c} \cdot \underline{s}_{\mathrm{gn}}(\dot{\underline{x}}), \qquad \mathrm{f^c} > 0\mathrm{N}, \quad \dot{\underline{x}} \neq \underline{0}\,\tfrac{\mathrm{m}}{\mathrm{s}}, \tag{4}$$

acts on the system. If the control force parameter $\mathrm{f^c}$ is large enough, it can be shown [12] that the MS, starting motion from certain initial states, tracks ideally the nominal velocity $\dot{\underline{q}}_{\mathrm{n}}(t)$ after certain moment $\mathrm{t_d}$. Mathematically, $\dot{\underline{x}}(t) = \underline{0}\,\frac{\mathrm{m}}{\mathrm{s}}$, $t \geq \mathrm{t_d}$, which means the MS is in the decomposition mode. The tracking is achieved even though the control force is not defined for $\dot{\underline{x}}(t) = \underline{0}\,\frac{\mathrm{m}}{\mathrm{s}}$. However, the control force function must take values on the sets where it is not defined if the velocity error $\dot{\underline{x}}$ might pass through those sets. Also, control force function must be determined on the sets where it is defined but not determined.

The problem is to find the switching and sliding surfaces of the MS and to determine how the control force acts on the MS in the decomposition mode.

2. Switching and sliding surfaces of mechanical system

The switching and sliding surfaces are determined by the set of discontinuities of the generalized force which acts on the mechanical system.

Definition 1 *The switching surface of the MS is the set of all simple discontinuities of the generalized force which acts on the MS.*

It is assumed that the generalize force function does not have other discontinuities save simple ones because the other discontinuities assume unboundedness or infinitely fast oscillations. The generalized force need not be defined on the switching surface, but if the MS can "pass" through the switching surface, the generalized force must exist and should be determined. Hence, it can be said that the switching surface is a subset of the domain of the generalized force function.

Definition 2 *The sliding surface of the MS is the set of discontinuities of the generalized force where conditions for the sliding mode are satisfied.*

Therefore, the sliding surface is a subset of the switching surface.

It is assumed here that disturbance force function $\underline{f}^{\mathrm{d}}(\cdot)_{\mathscr{Q}\times\dot{\mathscr{Q}}^{1}\times\mathscr{T}_{\infty}}$ are continuous, so that the set of discontinuities of the generalized force is the set of discontinuities of the control force. Since the control force directly depends on the velocity deviation $\underline{\dot{x}}$, the switching and sliding surfaces will be determined in the space $\mathfrak{R}^{\mathrm{n}}_{\underline{\dot{\mathrm{x}}}} = \mathfrak{R}_{\dot{\mathrm{x}}^{1}} \times \cdots \times \mathfrak{R}_{\dot{\mathrm{x}}^{\mathrm{n}}}$, where $\mathfrak{R}_{\dot{\mathrm{x}}^{i}}$, $i = 1,\ldots,n$ are one-dimensional subspaces of $\mathfrak{R}^{\mathrm{n}}_{\underline{\dot{\mathrm{x}}}}$ and represent coordinate lines of the coordinates $\dot{x}^{i}$.

According to (4), the switching surface $\mathscr{S}_{\mathrm{w}}$ is determined as

$$\mathscr{S}_{\mathrm{w}} = \bigcup_{i=1}^{\mathrm{n}} \mathscr{S}_{\mathrm{w}i}, \tag{5}$$

where the $(n-1)$-dimensional plain $\mathscr{S}_{\mathrm{w}i} = \mathfrak{R}_{\dot{\mathrm{x}}^{1}} \times \cdots \times \mathfrak{R}_{\dot{\mathrm{x}}^{i-1}} \times \{0\frac{\mathrm{m}}{\mathrm{s}}\} \times \mathfrak{R}_{\dot{\mathrm{x}}^{i+1}} \times \cdots \times \mathfrak{R}_{\dot{\mathrm{x}}^{\mathrm{n}}}$ represents the coordinate surface of the coordinate $\dot{x}^{i}$ for $\dot{x}^{i} = 0\frac{\mathrm{m}}{\mathrm{s}}$.

In order to determine the sliding surface, we ought to know what the conditions for sliding mode are and where on the switching surface they are satisfied. Sufficient conditions for decomposition mode are given in the paper [12], in which case the point $\underline{\dot{\mathrm{x}}} = \underline{0}\frac{\mathrm{m}}{\mathrm{s}}$ certainly belongs to the sliding surface. Whether this point is the only point of the sliding surface stays unknown since there is no conditions that guarantees that some other points of the switching surface belong to the sliding surface, which does not mean that such points do not exist. Moreover, if such points exist they need not be fixed, they may appear and disappear as points of the sliding surface. It usually happens when disturbance forces change their magnitudes and directions. Even more, the point $\underline{\dot{\mathrm{x}}} = \underline{0}\frac{\mathrm{m}}{\mathrm{s}}$ may disappear as point of the sliding surface if conditions for decomposition mode are violated [12, p. 12]. Therefore, the sliding surface is not a fixed surface, but may move and change its shape along the switching surface.

The sliding surface $\mathscr{S}_{\mathrm{ld}}$ of the decomposition mode degenerates to the point $\mathscr{S}_{\mathrm{ld}} = \{\underline{0}\frac{\mathrm{m}}{\mathrm{s}}\}$ in the space $\mathfrak{R}^{\mathrm{n}}_{\underline{\dot{\mathrm{x}}}}$. It can be expressed as

$$\mathscr{S}_{\mathrm{ld}} = \bigcap_{i=1}^{\mathrm{n}} \mathscr{S}_{\mathrm{w}i} = \underline{0}\frac{\mathrm{m}}{\mathrm{s}}. \tag{6}$$

Coming at the point $\mathscr{S}_{\mathrm{ld}}$, the velocity error stays zero all the time. To always see sliding, it is appropriate to present the sliding surface in the space $\mathfrak{R}^{\mathrm{n}}_{\underline{\dot{\mathrm{x}}}} \times \mathfrak{R}_{\mathrm{t}}$. In this space, the sliding surface of the decomposition mode $\mathscr{S}_{\mathrm{ld}}$ becomes a sliding line $\mathscr{S}^{\mathrm{t}}_{\mathrm{ld}} = \mathscr{S}_{\mathrm{ld}} \times \mathscr{T}_{\infty} = \{\underline{0}\frac{\mathrm{m}}{\mathrm{s}}\} \times \mathscr{T}_{\infty}$ and the point $(\underline{0}\frac{\mathrm{m}}{\mathrm{s}}, t)$ slides along the sliding line as fast as fast time passes.

The sliding line can also be presented in the spaces of absolute quantities $\underline{\dot{q}}$ and $\underline{\dot{q}}_{\mathrm{n}}$. For that purpose, consider the function $\underline{\dot{x}}(\cdot)_{\mathfrak{R}^{\mathrm{n}}_{\underline{\dot{\mathrm{q}}}}\times\mathfrak{R}^{\mathrm{n}}_{\underline{\dot{\mathrm{q}}}_{\mathrm{n}}}}$ determined by $\underline{\dot{x}} = \underline{\dot{q}} - \underline{\dot{q}}_{\mathrm{n}}$ and the function $\underline{\dot{q}}(\cdot)_{\underline{\dot{q}}_{\mathrm{n}}(\mathscr{T}_{\infty})}$ determined by $\underline{0}\frac{\mathrm{m}}{\mathrm{s}} = \underline{\dot{q}} - \underline{\dot{q}}_{\mathrm{n}}$. Then, the sliding line in the space $\mathfrak{R}_{\underline{\dot{\mathrm{x}}}} \times \mathfrak{R}_{\underline{\dot{\mathrm{q}}}} \times \mathfrak{R}_{\underline{\dot{\mathrm{q}}}_{\mathrm{n}}}$

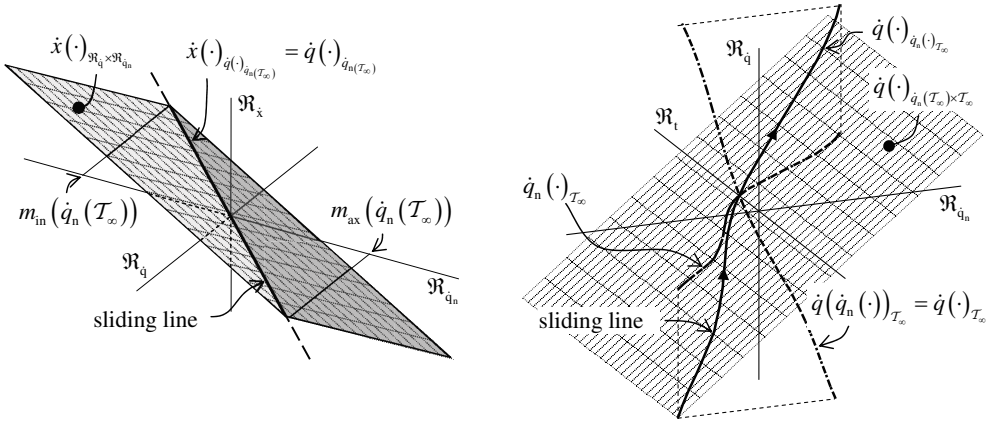

Figure 1. The sliding line in the spaces $\Re_{\underline{\dot{x}}} \times \Re_{\underline{\dot{q}}} \times \Re_{\underline{\dot{q}}_n}$ (left) and $\Re^n_{\underline{\dot{q}}} \times \Re_{\underline{\dot{q}}_n} \times \Re_t$ (right); an illustration for one-dimensional case.

is the function $\underline{\dot{x}}(\cdot)_{\underline{\dot{q}}(\cdot)_{\underline{\dot{q}}_n(\mathcal{T}_\infty)}}$, which geometrically coincides with the function $\underline{\dot{q}}(\cdot)_{\underline{\dot{q}}(\mathcal{T}_\infty)}$ as is illustrated in Figure 1 (left) for one-dimensional case. Namely, $\underline{\dot{x}}(\cdot)_{\underline{\dot{q}}(\cdot)_{\underline{\dot{q}}_n(\mathcal{T}_\infty)}} = \{\underline{0}\frac{m}{s}\} \times \underline{\dot{q}}(\cdot)_{\underline{\dot{q}}_n(\mathcal{T}_\infty)}$ which can be identified with $\underline{\dot{q}}(\cdot)_{\underline{\dot{q}}_n(\mathcal{T}_\infty)}$ if $\underline{0}\frac{m}{s}$ is considered as empty set‡.

The sliding line, observed from the space $\Re^n_{\underline{\dot{q}}} \times \Re_{\underline{\dot{q}}_n} \times \Re_t$, lies on the function $\underline{\dot{q}}(\cdot)_{\underline{\dot{q}}_n(\mathcal{T}_\infty)\times\mathcal{T}_\infty}$ extruded from the function $\underline{\dot{q}}(\cdot)_{\underline{\dot{q}}_n(\mathcal{T}_\infty)}$, $\underline{\dot{q}} = \underline{\dot{q}}_n$ on the set $\mathcal{T}_\infty$, Figure 1 (right). In this case, the sliding line is the function $\underline{\dot{q}}(\cdot)_{\underline{\dot{q}}_n(\mathcal{T}_\infty)\times\mathcal{T}_\infty}$ along the nominal velocity function $\underline{\dot{q}}_n(\cdot)_{\mathcal{T}_\infty}$, that is, the function $\underline{\dot{q}}(\cdot)_{\underline{\dot{q}}_n(\cdot)_{\mathcal{T}_\infty}}$. Its projection on the space $\Re^n_{\underline{\dot{q}}} \times \Re_t$ is the velocity function $\underline{\dot{q}}(\cdot)_{\mathcal{T}_\infty}$ as if the MS is in the decomposition mode from the initial instant or, in other words, as if the initial velocity of the MS is nominal and conditions for the decomposition mode are satisfied.

3. Control force in decomposition mode

In order to determine the control force in decomposition mode, the method of equivalent control [11] is applied.

Let the decomposition mode arise at the instant $t_d \geq t_i$. Then,

$$\underline{\dot{x}} = \underline{0}\frac{m}{s} \Leftrightarrow \underline{\dot{q}}_n(t) = \underline{\dot{q}}(t), \quad \forall t \geq t_d, \tag{7}$$

which implies

$$\underline{x}(t) = \underline{x}_d \Leftrightarrow \underline{q}(t) = \underline{q}_n(t) + \underline{x}_d \quad \wedge \quad \underline{\ddot{q}}(t) = \underline{\ddot{q}}_n(t), \quad \forall t \geq t_d. \tag{8}$$

‡ In addition to arbitrary direction, it is convenient to adopt that the zero vector can have arbitrary dimension and arbitrary measurement unit. The zero vector or zero of something should be considered as empty set or nothing. In that case any two vector spaces have the same zero vector $\emptyset$ and the intersection of any two vector spaces is the point $\{\emptyset\}$. This makes it possible to construct affine spaces from different vector spaces having the same common point - the zero vector.

The control force must always satisfy the equation 1, so must in the decomposition mode, in which

$$\underline{f}^{\mathrm{c}}(t) = \underline{M}\left(\underline{q}_{\mathrm{n}}(t) + \underline{\mathrm{x}}_{\mathrm{d}}\right)\ddot{\underline{q}}_{\mathrm{n}}(t) + \underline{c}\left(\underline{q}_{\mathrm{n}}(t) + \underline{\mathrm{x}}_{\mathrm{d}}, \dot{\underline{q}}_{\mathrm{n}}(t)\right) - \underline{f}^{\mathrm{d}}\left(\underline{q}_{\mathrm{n}}(t) + \underline{\mathrm{x}}_{\mathrm{d}}, \dot{\underline{q}}_{\mathrm{n}}(t), t\right) \qquad (9)$$

holds for all $t \geq \mathrm{t_d} \geq \mathrm{t_i}$. Since $\underline{M}(\cdot)_{\mathscr{Q}}$ and $\dot{\underline{q}}_{\mathrm{n}}(\cdot)_{\mathscr{T}_\infty}$ are continuously differentiable and $\underline{f}^{\mathrm{d}}(\cdot)_{\mathscr{Q}\times\mathscr{Q}^1\times\mathscr{T}_\infty}$ is continuous, the control force function $\underline{f}^{\mathrm{c}}(\cdot)_{[\mathrm{t_d},\infty\mathrm{s})}$ is a continuous function, too. However, the function $\underline{f}^{\mathrm{c}}(\cdot)_{(\mathrm{t_d}-\varepsilon,\infty\mathrm{s})}$ has, in general, a discontinuity of the first kind at $\mathrm{t_d}$ for any small $\varepsilon > 0\mathrm{s}$.

The system that realizes the control force $\underline{f}^{\mathrm{c}}$ need not realize it in the decomposition mode. In the decomposition mode the control force is forced to be realized by itself exactly in the way defined by equation (9). It is forced by the force field around the sliding surface and by nature of the MS described by differential equation (1). Mathematically, determination of the control force on a sliding surface and determination of the reaction force on a holonomic constraint [6, p. 19] are similar. In both cases the force is to be determined in such a way that equations of motion are satisfied. However, "sliding" on the sliding surface is physically realized differently with respect to "sliding" along the holonomic constraint. In the first case, the system is kept on the sliding surface by the force field surrounding it, and in the latter case, the holonomic constraint itself keeps the system on it. Both holonomic constraints and sliding modes do not exist in practice but may serve as a tool for describing and better understanding of natural phenomena.

4. Example

Motion of a three-degree-of-freedom robotic manipulator, Fig. 2, was simulated to illustrate coming to and moving in the decomposition mode with determined control force on the sliding surface.

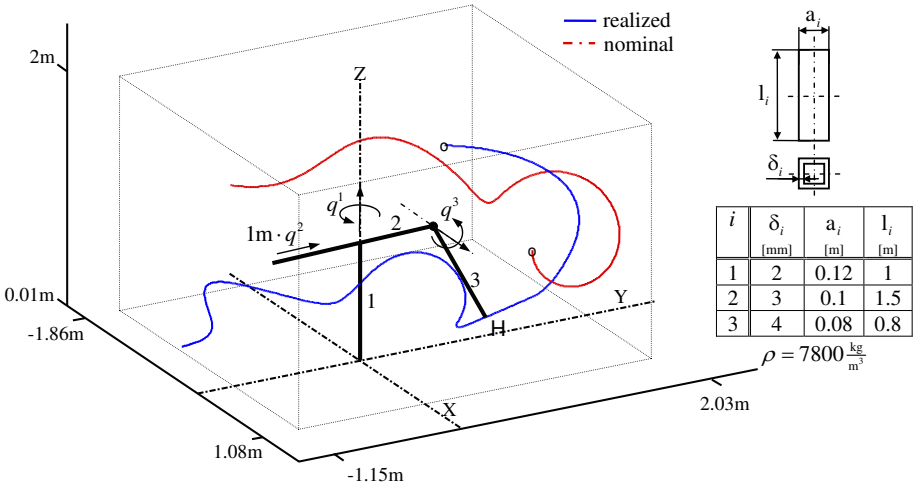

i	δ_i [mm]	a_i [m]	l_i [m]
1	2	0.12	1
2	3	0.1	1.5
3	4	0.08	0.8

Figure 2. A three-degree-of-freedom manipulator with its inertio-geometrical characteristics

The manipulator is in a constant gravitational field

$$\underline{g} = \begin{bmatrix} 0 & 0 & -9.81 \end{bmatrix}^{\mathrm{T}} \frac{\mathrm{m}}{\mathrm{s}^2}, \tag{10}$$

and the disturbance force

$$\underline{f}^{\mathrm{d}} = \begin{bmatrix} 20\sin(1.8t)+40 & 20\sin t+60 & 10\sin(3t)-80 \end{bmatrix}^{\mathrm{T}} \mathrm{Nm} + \underline{f}^{\mathrm{d}}_{\mathrm{g}}, \quad t \in \mathscr{T}_{\infty} \tag{11}$$

acts on the MS, where $\underline{f}^{\mathrm{d}}_{\mathrm{g}}$ is the disturbance force due to gravity.

The nominal motion $\underline{q}_{\mathrm{n}}(\cdot)_{\mathscr{T}_{\infty}}$ was indirectly defined by defining a motion of the manipulator gripper tip H. The motion of the tip was defined by its trajectory given in the cylindrical coordinates with respect to the X-axis

$$\begin{array}{l} r_{\mathrm{H}} = 0.5\mathrm{m} \cdot s_{\mathrm{in}}(0.3p) \cdot e_{\mathrm{xp}}(-0.02p) + 1.8\mathrm{m} \\ \varphi_{\mathrm{H}} = 0.05\,\mathrm{rad} \cdot p \\ Z_{\mathrm{H}} = 0.5\mathrm{m} \cdot s_{\mathrm{in}}\left(0.3p - \frac{\pi}{2}\right) \cdot e_{\mathrm{xp}}(-0.02p) + 1\mathrm{m} \end{array} \quad , \quad p(\mathrm{t_i}) = 0 \ , \tag{12}$$

and the speed along the trajectory

$$V_{\mathrm{H}} = 0.95 \cdot e_{\mathrm{xp}}\left(0.5 \cdot s_{\mathrm{in}}(t)\right) \frac{\mathrm{m}}{\mathrm{s}}, \quad t \in \mathscr{T}_{\infty}. \tag{13}$$

The manipulator starts to move at the initial moment $\mathrm{t_i} = 1\mathrm{s}$ from the initial state

$$\underline{q}_{\mathrm{i}} = \begin{bmatrix} 0.5 & 0.6 & \pi/2 \end{bmatrix}^{\mathrm{T}} \mathrm{rad} \qquad \underline{\dot{q}}_{\mathrm{i}} = \begin{bmatrix} 5 & -1 & -8 \end{bmatrix}^{\mathrm{T}} \frac{\mathrm{rad}}{\mathrm{s}}. \tag{14}$$

The simulation was done in two steps. Firstly, coming to the decomposition mode had been simulated, and then, moving in the decomposition mode using calculated control force (9). The fourth-order Runge-Kutta continuous solver with fixed step 0.001s was used in both cases. Both simulations were compiled into one to obtain entire motion of the manipulator. In coming to the decomposition mode the control force was defined by

$$\underline{f}^{\mathrm{c}} = -110 \cdot s_{\mathrm{ign}}(\underline{\dot{q}} - \underline{\dot{q}}_{\mathrm{n}}))\mathrm{Nm}, \tag{15}$$

while in the decomposition mode the control force was determined by equation (9). The simulation results are presented in Figures 3 and 4.

The manipulator enters the decomposition mode at the instant $\mathrm{t_d} = 1.758\mathrm{s}$ in which the position deviation is

$$\underline{\mathrm{x}}_{\mathrm{d}} = [0.876749 \quad 0.244765 \quad -1.134695]^{\mathrm{T}}\mathrm{rad}. \tag{16}$$

As can be seen in the Figures, switching arises before the decomposition mode. To better see what was going on around the instant of entering the decomposition mode, the results were zoomed around that instant and presented in Figures 5 and 6.

The first contact with the switching surface after the instant t=1.3s is realized at the point A on the switching plane $\Re_{\dot{\mathrm{x}}^2} \times \Re_{\dot{\mathrm{x}}^3}$, see Figure 6. After that instant chattering of the first coordinate of the velocity deviation arises as well as switching of the first coordinate of the control force due to fixed-step integration. This indicates that conditions for sliding mode are probably fulfilled along the hodograph of the velocity deviation on the switching plane $\Re_{\dot{\mathrm{x}}^2} \times \Re_{\dot{\mathrm{x}}^3}$ from the point A. This means that, in this case, the manipulator had entered a

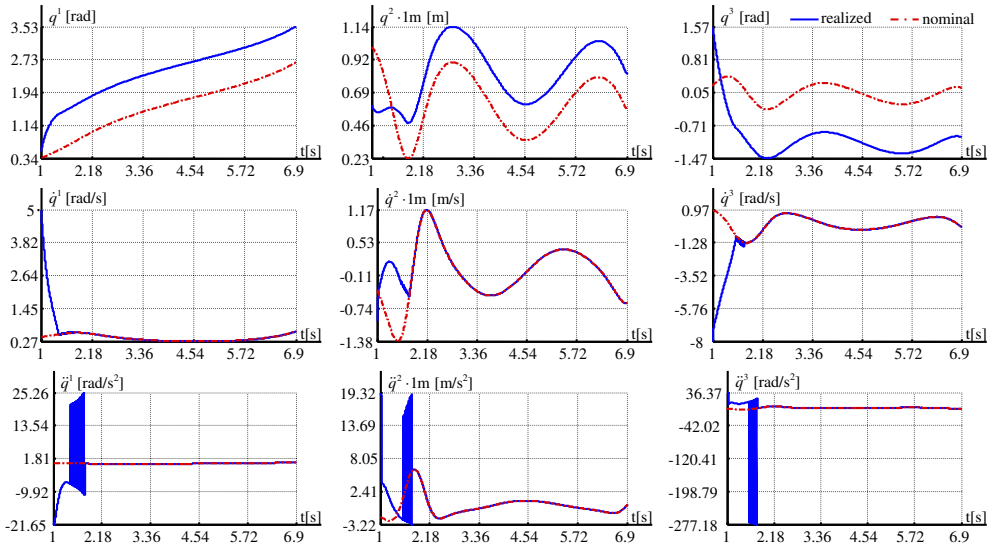

Figure 3. The time histories of the coordinates of the position $\underline{q}$, velocity $\underline{\dot{q}}$ and acceleration $\underline{\ddot{q}}$ of the MS coming to and moving in the decomposition mode

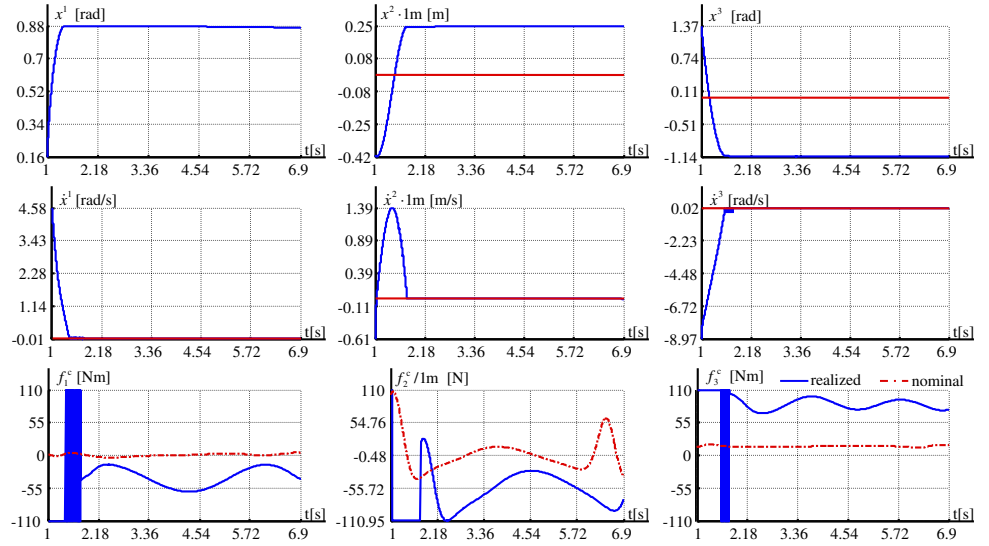

Figure 4. The time histories of the coordinates of the position deviation $\underline{x}$, velocity deviation $\underline{\dot{x}}$ and control force $\underline{f}^c$

sliding mode before it entered the decomposition mode, which means that the zero velocity deviation is not the only point of the sliding surface. At the point B, the velocity deviation reaches the switching plane $\Re_{\dot{x}^1} \times \Re_{\dot{x}^2}$ and chattering of the third coordinate of the velocity deviation arises additionally which indicates that the segment $\overline{BO}$ is the sliding segment,

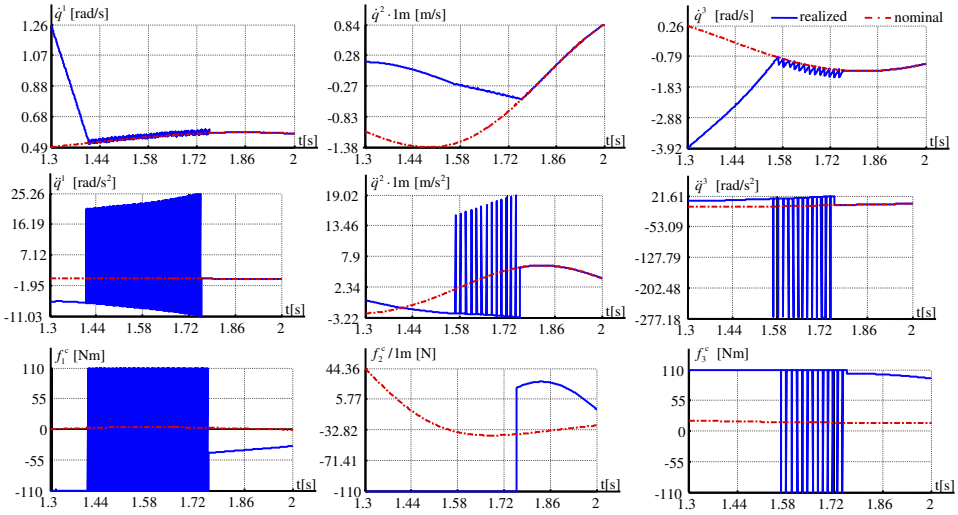

Figure 5. The time histories of the coordinates of the velocity $\dot{\underline{q}}$, acceleration $\ddot{\underline{q}}$ and control force $\underline{f}^{\mathrm{c}}$ around the instant of entering the decomposition mode

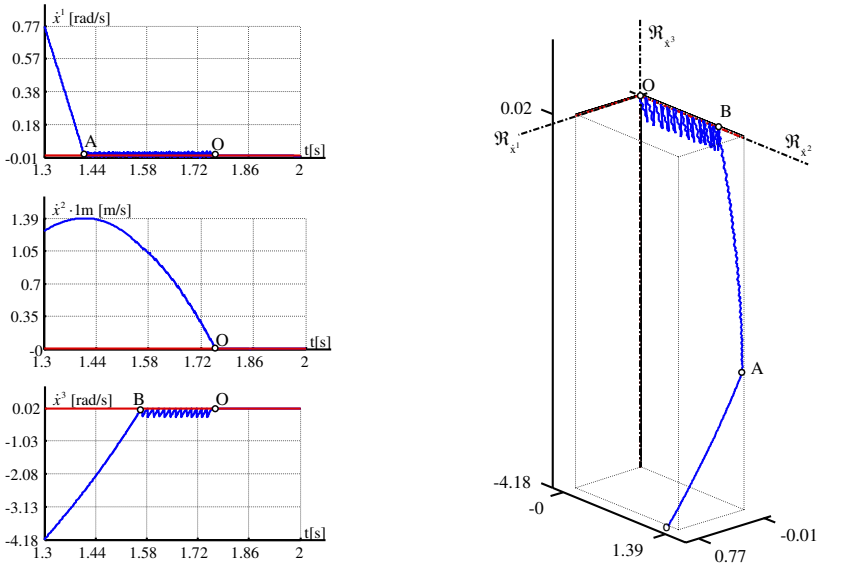

Figure 6. The change of the coordinates of the velocity deviation $\underline{\dot{x}}$ in the spaces $\mathfrak{R}_{\dot{x}^i} \times \mathfrak{R}_{\mathrm{t}}$, $i = 1,2,3$ (left) and $\mathfrak{R}^3_{\underline{\dot{x}}}$ (right)

Figure 6 right. Finally, the manipulator enters the decomposition mode at the point O and chattering disappears because the control force has a continuous change after that instant according to (9).

5. Conclusion

The switching and sliding surfaces of the mechanical system have been defined and determined. In the decomposition mode, the sliding surface degenerates to a point in the space of the velocity deviation. However, the decomposition mode need not be the only sliding mode of the mechanical system. The mechanical system can "slide" out of the decomposition mode along the sliding surface which can change its position and shape on the switching surface.

The control force, which acts on the mechanical system in the decomposition mode, has been determined by using the method of equivalent control. According to this method the control force is determined from the equations of motion of the mechanical system and conditions which relates to the restriction of motion of the mechanical system on the sliding surface. In that sense, determination of the control force in the decomposition mode is equivalent to determination of the reaction force on a holonomic constraint. However, motion on a sliding surface and motion on the holonomic constraint are physically different. In the first case, the mechanical system is kept on the sliding surface by the force field surrounding the surface, while, in the latter case, the holonomic constraint keeps the mechanical system on the constraint.

Although the control force is not determined on the sliding surface, the force field around the sliding surface forces the control force to take exactly those values such that the motion of the mechanical system is on the sliding surface and the differential equation of motion is satisfied. Assuming the discontinuities originate only from the control force, the control force function is continuous in the decomposition mode even though it is discontinuous out of the decomposition mode. When the disturbances are present, the force field around the sliding surface changes and, in some cases, conditions for sliding mode may be violated allowing the mechanical system to leave the sliding surface. In other cases, they may so strengthen the force field around the switching surface that conditions for sliding mode are satisfied and sliding may arise if the system is near the switching surface.

6. Notation

$\Re$ is the set of all real numbers. Italics denote variables, for instance, $a, b, \underline{a}, \underline{b}, \underline{A}, \underline{B}, \ldots$. Regular letters denote constants, symbols or abbreviations, for instance, $\mathrm{a}, \underline{\mathrm{a}}, \underline{\mathrm{A}}, s_{\mathrm{ign}}, s_{\mathrm{in}}, q_{\mathrm{n}}, \lambda_{\max}, \ldots$. $\mathscr{A}, \mathscr{B}, \mathscr{C}, \ldots$ are sets. $\bar{\mathscr{A}}$ is the closure of a metric space $\mathscr{A}$, $\mathscr{A}^{\circ}$ is its interior, and $\partial\mathscr{A}$ is its boundary. Underlined small letters denote column matrices, which are called vectors, $\underline{a} = [a^1, \ldots, a^{\mathrm{n}}]^{\mathrm{T}}, \underline{b} = [b_i]_{\mathrm{n}\times 1}, \underline{\mathrm{a}}, \underline{\alpha}, \ldots$. Underlined capital letters denote square matrices, $\underline{\mathrm{A}} = [\mathrm{A}_{ij}]_{\mathrm{n}\times\mathrm{n}}, \underline{A}, \underline{B}, \ldots$.

The *space of a matrix variable a* with n elements is the real, n-dimensional, metric vector space $\Re_{\mathrm{a}}^{\mathrm{n}}$ in which the variable a takes values.

Only the matrix variables each having the elements of the same measurement unit shall be considered; thus metrization of spaces of such variables makes physical sense. The *measurement unit of a matrix variable* is the measurement unit of one of its elements.

It is said that two matrix variables $a \in \Re_{\mathrm{a}}^{\mathrm{n}}$ and $b \in \Re_{\mathrm{b}}^{\mathrm{m}}$ are *of the same nature* if they have the same measurement unit; subsequently, such are their spaces $\Re_{\mathrm{a}}^{\mathrm{n}}$ and $\Re_{\mathrm{b}}^{\mathrm{m}}$.

Two variables are *identical* if they measure quantity of the same quality of the same thing and have the same measurement unit; otherwise, they are different.

It is said that two spaces are *disjoint in variable* if they are the spaces of two different variables.

If two spaces are disjoint in variable then they need not be disjoint if they are of the same nature. If they are identical in variable, then they are identical. A mathematical operation "$*$" with the subscript "v" shall be used to emphasize the restriction of the mathematical operation to a certain variable.

Example. Two forces $\vec{F}_1$ and $\vec{F}_2$, whose coordinates with respect to some frame of reference are $\underline{F}_1$ and $\underline{F}_2$, act on a material point. The variables $\underline{F}_1$ and $\underline{F}_2$ induce the spaces $\mathfrak{R}^3_{\underline{F}_1}$ and $\mathfrak{R}^3_{\underline{F}_2}$, which are of the same nature, identical and disjoint in variable, that is, $\underline{F}_1, \underline{F}_2 \in \mathfrak{R}^3_{\underline{F}_1} \equiv \mathfrak{R}^3_{\underline{F}_2}$ and $\underline{F}_1 \in_{\mathrm{v}} \mathfrak{R}^3_{\underline{F}_1}$, $\underline{F}_2 \in_{\mathrm{v}} \mathfrak{R}^3_{\underline{F}_2}$, but $\underline{F}_1 \notin_{\mathrm{v}} \mathfrak{R}^3_{\underline{F}_2}$, $\underline{F}_2 \notin_{\mathrm{v}} \mathfrak{R}^3_{\underline{F}_1}$, $\mathfrak{R}^3_{\underline{F}_1} \not\equiv_{\mathrm{v}} \mathfrak{R}^3_{\underline{F}_2}$ and $\mathfrak{R}^3_{\underline{F}_1} \cap_{\mathrm{v}} \mathfrak{R}^3_{\underline{F}_2} = \emptyset$.

Definition 3 *A pair* (a,b) *is* $(a,b) \stackrel{\text{def}}{=} \begin{cases} \{a\} \cup \{b\}, & \text{if } a \text{ and } b \text{ are not sets.} \\ a \cup \{b\}, & \text{if } a \text{ is a nonempty set and } b \text{ is not a set.} \\ b, & \text{if } a \text{ is the empty set and } b \text{ is not a set.} \\ \{a\} \cup b, & \text{if } a \text{ is not a set and } b \text{ is a nonempty set.} \\ a, & \text{if } a \text{ is not a set and } b \text{ is the empty set.} \\ a \cup b, & \text{if } a \text{ and } b \text{ are sets.} \end{cases}$

Definition 4 *An* n*-tuple* $(a_1, \cdots, a_{\mathrm{n}})$ *is* $((a_1, \cdots, a_{\mathrm{n}-1}), a_{\mathrm{n}})$, $\mathrm{n} > 2$.

Definition 5 *The set product of two sets* $\mathscr{A}$ *and* $\mathscr{B}$ *is the set*

$$\mathscr{A} \times \mathscr{B} \stackrel{\text{def}}{=} \{(a,b) |\ a \in \mathscr{A} \ \wedge\ b \in \mathscr{B}\}. \tag{17}$$

The set product has the properties

$$\mathscr{A} \times \emptyset = \emptyset, \quad \mathscr{A} \times \{\emptyset\} = \mathscr{A}, \tag{18}$$

$$\mathscr{A} \times \mathscr{B} = \mathscr{B} \times \mathscr{A}, \tag{19}$$

$$(\mathscr{A} \times \mathscr{B}) \times \mathscr{C} = \mathscr{A} \times (\mathscr{B} \times \mathscr{C}), \tag{20}$$

which follow directly from Definition 3.

Example. Let $a \not\equiv b$, $a \in_{\mathrm{v}} \mathscr{A}_{\mathrm{a}} =_{\mathrm{v}} \{\mathrm{a}^1_{\mathrm{a}}, \mathrm{a}^2_{\mathrm{a}}\} \equiv_{\mathrm{v}} \{\mathrm{a}^1, \mathrm{a}^2\}_{\mathrm{a}}$, $b \in_{\mathrm{v}} \mathscr{A}_{\mathrm{b}} =_{\mathrm{v}} \{\mathrm{a}^1_{\mathrm{b}}, \mathrm{a}^2_{\mathrm{b}}\} \equiv_{\mathrm{v}} \{\mathrm{a}^1, \mathrm{a}^2\}_{\mathrm{b}}$, and $\mathscr{A}_{\mathrm{a}} \equiv \mathscr{A}_{\mathrm{b}} \equiv \mathscr{A} = \{\mathrm{a}^1, \mathrm{a}^2\}$. Then,

$$\begin{aligned} &\mathscr{A}_{\mathrm{a}} \times \mathscr{A}_{\mathrm{b}} = \mathscr{A} \times \mathscr{A} = \{\{\mathrm{a}^1\}, \{\mathrm{a}^1, \mathrm{a}^2\}, \{\mathrm{a}^2\}\}, \\ &\mathscr{A}_{\mathrm{a}} \times_{\mathrm{v}} \mathscr{A}_{\mathrm{b}} = \{\{\mathrm{a}^1_{\mathrm{a}}, \mathrm{a}^1_{\mathrm{b}}\}, \{\mathrm{a}^1_{\mathrm{a}}, \mathrm{a}^2_{\mathrm{b}}\}, \{\mathrm{a}^2_{\mathrm{a}}, \mathrm{a}^1_{\mathrm{b}}\}, \{\mathrm{a}^2_{\mathrm{a}}, \mathrm{a}^2_{\mathrm{b}}\}\}. \end{aligned} \tag{21}$$

Consequently, there is a bijection between $\mathscr{A}_{\mathrm{a}} \times_{\mathrm{v}} \mathscr{A}_{\mathrm{b}}$ and the Cartesian product $\mathscr{A} \times_{\mathrm{C}} \mathscr{A}$ [8, pp. 17-23], but the Cartesian product does not have properties (19) and (20), which are required for notation of functions. The set product shall be used (17) only for sets disjoint in variable, so that "$\times_{\mathrm{v}}$" is assumed when "$\times$" is written.

Let $a \in_{\mathrm{v}} \mathscr{A}$, $b \in_{\mathrm{v}} \mathscr{B}$ and $a \not\equiv b$. Then:

$b(\cdot) : \mathscr{A} \to \mathscr{B}$ is a function from $\mathscr{A}$ into $\mathscr{B}$. For some $a \in \mathscr{A}$, $b(a) \in \mathscr{B}$ is the value of the function $b(\cdot) : \mathscr{A} \to \mathscr{B}$ at a.

$b(\cdot)_{\mathscr{A}} \subset \mathscr{A} \times \mathscr{B}$ is the graph of a function $b(\cdot) : \mathscr{A} \to \mathscr{B}$. From this point on, a function will be identified with its graph. If $\mathscr{A}' \subset \mathscr{A}$ then $b(\cdot)_{\mathscr{A}'}$ is the restriction of the function $b(\cdot)_{\mathscr{A}}$ to a set $\mathscr{A}'$.
$b(\cdot)_{\mathscr{A}\times\mathscr{C}} \equiv b(\cdot)_{\mathscr{C}\times\mathscr{A}} = b(\cdot)_{\mathscr{A}} \times \mathscr{C} \subset \mathscr{A} \times \mathscr{B} \times \mathscr{C}$ is the extruded function from a function $b(\cdot)_{\mathscr{A}}$ on a set $\mathscr{C}$.
$b(\cdot)_{a(\cdot)_{\mathscr{C}}} \subset \mathscr{A} \times \mathscr{B} \times \mathscr{C}$ is a function $b(\cdot)_{\mathscr{A}\times\mathscr{C}}$ along a function $a(\cdot)_{\mathscr{C}} \subset \mathscr{A} \times \mathscr{C}$.

Definition 6 *The projection of a function* $b(\cdot)_{\mathscr{A}_1\times\cdots\times\mathscr{A}_n} \subset \mathscr{A}_1 \times \cdots \times \mathscr{A}_n \times \mathscr{B}$ *onto the set* $\mathscr{A}' \times \mathscr{B}$, $\mathscr{A}' \subseteq \mathscr{A}_1 \times \cdots \times \mathscr{A}_k$, $k \in \{0, 1, \ldots, n-1\}$, *where* $\mathscr{A}_1 \times \cdots \times \mathscr{A}_k = \{\emptyset\}$ *for* $k = 0$, *is the set*

$$b(\mathscr{A}_{k+1} \times \cdots \times \mathscr{A}_n)_{\mathscr{A}'} \stackrel{\text{def}}{=} \left\{(a_1, ..., a_k, b) \in \mathscr{A}' \times \mathscr{B} |\ \ (a_1, ..., a_n, b) \in b(\cdot)_{\mathscr{A}_1\times\cdots\times\mathscr{A}_n}\right\} \subset \mathscr{A}' \times \mathscr{B}.$$

If $\mathscr{A}' = \{\emptyset\}$, *the index* $\mathscr{A}'$ *is omitted. Note that in this case, for* $k = 0$, $(a_1, \ldots, a_k) = \emptyset \in \mathscr{A}'$.

Example. The projection $b(\mathscr{A})$ of a function $b(\cdot)_{\mathscr{A}} \subset \mathscr{A} \times \mathscr{B}$ onto the set $\mathscr{B}$ represents its range. Projection of a function $b(\cdot)_{\mathscr{A}\times\mathscr{C}} \subset \mathscr{A} \times \mathscr{B} \times \mathscr{C}$ onto the set $\mathscr{B} \times \mathscr{C}$ is $b(\mathscr{A})_{\mathscr{C}}$. $\mathscr{A}$ in $b(\mathscr{A})_{\mathscr{C}}$ is needed only to indicate along which set the projection is done. Hence, the projection of a function $b(\cdot)_{a(\cdot)_{\mathscr{C}}}$ onto the set $\mathscr{B} \times \mathscr{C}$ is rather denoted as $b(a(\cdot))_{\mathscr{C}}$ than $b(a(\mathscr{C}))_{\mathscr{C}}$, as this projection is also a function. The projection of this function onto the set $\mathscr{A} \times \mathscr{B}$ is $b(\mathscr{C})_{a(\mathscr{C})}$ and it need not be a function. Note that "the domain of the projection of a function" must be determined exactly, as is $a(\mathscr{C})$ in $b(\mathscr{C})_{a(\mathscr{C})}$ or $\mathscr{C}$ in $b(a(\cdot))_{\mathscr{C}}$.
$\underline{0} = [0, 0, \ldots, 0]^{\mathrm{T}}$.
$\mathrm{b}(\cdot)_{\mathscr{A}} = \mathscr{A} \times \{\mathrm{b}\}$ is a constant function. A constant function is different from a function that is a constant such as the sine function§ $s_{\mathrm{in}}(\cdot)_{(0,\pi)_{\mathrm{x}}} \subset \Re_{\mathrm{x}} \times \Re_{\mathrm{s_{in}}}$, which is a fixed function in the set of all continuous functions on the interval $(0, \pi)_{\mathrm{x}}$.
$i_{\mathrm{d}}(\cdot)_{\mathscr{A}} = \{(a, i_{\mathrm{d}}) |\ a \in \mathscr{A},\ i_{\mathrm{d}} = a\}$ is the identity function on the set $\mathscr{A}$, but $i_{\mathrm{d}} \not\equiv a$.
$b^{\leftarrow}(\cdot)_{b(\mathscr{A})} = \{(b, b^{\leftarrow}) |\ b = b(a),\ b^{\leftarrow} = a,\ a \in \mathscr{A}\}$ is the inverse function [4] of an injection $b(\cdot)_{\mathscr{A}}$. Note that $b^{\leftarrow}(\cdot)_{b(\mathscr{A})} = b(\cdot)_{\mathscr{A}}$, but $b^{\leftarrow}(\cdot)_{b(\mathscr{A})} \neq_{\mathrm{v}} b(\cdot)_{\mathscr{A}}$ since $\Re^{\mathrm{n}}_{\mathrm{b}^{\leftarrow}} \not\equiv_{\mathrm{v}} \Re^{\mathrm{n}}_{\mathrm{a}}$.

$$\begin{array}{l}\underline{f}(\underline{a}) = [f(a^1)\ \ \cdots\ \ f(a^n)]^{\mathrm{T}} \\ \underline{f} \in \{\underline{s}_{\mathrm{ign}}, \underline{s}_{\mathrm{gn}}\}\end{array}, \quad s_{\mathrm{ign}}(a^i) = \begin{cases} 1, & a^i{>}0 \\ 0, & a^i{=}0 \\ -1, & a^i{<}0 \end{cases}, \quad s_{\mathrm{gn}}(a^i) = \begin{cases} 1, & a^i{>}0 \\ \in[-1,1], & a^i{=}0 \\ -1, & a^i{<}0 \end{cases}.$$

$\|\underline{a}\| = \sqrt{\sum_{i=1}^{\mathrm{n}} (a^i)^2}$ is the Euclidean vector norm.
$\|\underline{A}\| = m_{\mathrm{ax}}(\{\|\underline{A}\underline{a}\| \mid \|\underline{a}\| = 1\})$ is the matrix 2-Norm [9, p. 281] induced by the Euclidean vector norm.
$\|b(\cdot)_{\mathscr{A}}\| = s_{\mathrm{up}}(\{\|b(a)\| \mid a \in \mathscr{A}\})$ is the norm of a function $b(\cdot)_{\mathscr{A}}$.
$d_{\mathrm{ist}}(\mathscr{A}, \mathscr{B}) = i_{\mathrm{nf}}(\{\|a - b\| \mid a \in \mathscr{A} \wedge b \in \mathscr{B}\})$ is the distance between sets $\mathscr{A}$ and $\mathscr{B}$. For one-element sets $\mathscr{A} = \{a\}$ or $\mathscr{B} = \{b\}$, $d_{\mathrm{ist}}(a, \mathscr{B})$, $d_{\mathrm{ist}}(\mathscr{A}, b)$ or $d_{\mathrm{ist}}(a, b)$, shall be written correspondingly.
$\mathscr{B}^{\mathscr{X}}_{\varepsilon}(a)$ is the ball open in a metric space $\mathscr{X}$, centered at $a \in \mathscr{X}$, and with radius $\varepsilon > 0$.

References

[1] Aizerman M A and Pyatnitskiy E S (1974) Foundamentals of the theory of discontinuous systems. i & ii. *Automation and Remote Control*, **(7 & 8)**, pp. 33–47,39–61. (in Russian).

[2] Boothby M W (1986)*An Introduction to Differentiable Manifolds and Riemannian Geometry*, Academic Press, New York, London.

§ Standard notations for some function have been slightly modified for the purpose of this paper. It will be clear from the context which those functions are.

[3] Bullo F and Lewis A (2005) *Geometric Control of Mechanical Systems: Modeling, Analysis and Design for Simple Mechanical Systems*, Springer Science+Business Media, New York.
[4] Dodson C T J and Poston T (1991) *Tensor Geometry - The Geometric Viewpoint and its Uses*, Springer, Berlin.
[5] Filipov A (1985) *Differential Equations with Discontinuous Right Part*, Nauka, Moscow. (in Russian).
[6] Gantmaher F R (1966) *Lectures on Analytical Mechanics*, Nauka, Moscow. (in Russian).
[7] Gelig A H, Leonov G A, and Yakubovich V A (1978) *Stability of Nonlinear Systems with Non-Unique Equilibrium State*, Nauka, Moscow. (in Russian).
[8] Hrbacek K and Jech T (1999) *Introduction to Set Theory*, Marcel Dekker, Inc., New York.
[9] Meyer C D (2000) *Matrix Analysis and Applied Linear Algebra*, Society for Industrial and Applied Mathematics, Philadelphia, PA, USA.
[10] Spivak M (1999)*A Comprehensive Introduction to Differential Geometry*, Publish or Perish, Houston.
[11] Utkin V I (1971) Equations of motion of sliding mode in discontinuous systems, *Automation and Remote Control*, **(12)**, pp.42–54. (in Russian).
[12] Živanović M. (2009) Scleronomic mechanical systems in decomposition mode, In *Proceedings of the 2nd International Congress of Serbian Society of Mechanics*, pp. A–06:1–13, Palić(Subotica).